# Hex-Urban: Investigating the adoption of hexagonal grids to represent the total urban water cycle within a distributed water balance model

Shu-Chen Hsu

TU Delft eawag aquatic research

November, 2020

# Hex-Urban: Investigating the adoption of hexagonal grids to represent the total urban water cycle within a distributed water balance model

by

Shu-Chen Hsu

to obtain the degree of Master of Science
at the Delft University of Technology,
to be defended publicly on Thursday, November 12, 2020 at 3:00 PM.

Student number: 4897323
Project duration: Feb 1, 2020 – Nov 12, 2020
Thesis committee: Dr. ir. Frans van de Ven TU Delft
Dr. Peter M. Bach Eawag
Dr. Joao P. Leitão Eawag
Dr. Markus Hrachowitz TU Delft
Dr. Fransje L. Hooimeijer TU Delft

*This thesis is confidential and cannot be made public until November 12, 2020.*

An electronic version of this thesis is available at http://repository.tudelft.nl/.
Picture cover page: Gemeinde Fehraltorf

## Abstract

With urbanization and climate change, the reliable water supply by centralized system is facing challenges. Research on the (re)use of the outflow from an urban area as an alternative water resource is increasing in recent years. This research requires spatial and temporal information on the status of components of urban water cycle. Several hydrological models exist for the purpose of urban water management. However, none of them considers modeling the total urban water cycle by a water balance approach in a spatial explicit manner. Distributed Urban Water Cycle Model (DUWCM) is developed in this thesis to investigate the benefit of a scalable and efficient water balance model that simulates the rainfall-runoff system and water supply-wastewater system in urban areas. Two case studies were carried out to verify the model and demonstrate the capability of modeling a large hydrological catchment respectively. DUWCM is developed as adaptable to a planning-support tool UrbanBEATS. Spatial representation of the second case study will be provided by it in squared and hexagonal tessellation. Hexagons have been applied in many spatial modeling fields, while rare applications can be found in water balance modeling. A comparison of model results from squared and hexagonal grids is done in this study. The comparison demonstrates that the difference in flow direction and sampling of the land cover ratio between square and hexagon blocks results in obvious differences in the location and the magnitude of peak flows. Since hexagonal grids perform better in flow path simulation (de Sousa et al.,2006), it is expected to be preferred over squared grids in distributed hydrological models. Thus, DUWCM, being scalable in the number of blocks and shapes, has the potential to be widely applied in sustainable water management.

## Acknowledgements

Foremost, I would like to express my deep and sincere gratitude to my research supervisor, Dr. ir. Frans van de Ven, Dr. Peter M. Bach, and Dr. Jaoa Paolo Leitão. Thanks Dr. ir. Frans van de Ven for being very supportive when I proposed the cooperation with Eawag. Also, thanks for providing lots of valuable advice regarding the conceptual model. Thanks Dr. Peter M. Bach and Dr. Joao Paolo Leitão for the kind hosting when I worked in Eawag, and the rigorous training. Dr. Peter M. Bach demonstrated a wonderful presentation skill and asked me to learn how to express my work without copying his presentation directly. In particularly, he led me into the project by introducing me to the model UrbanBEATS and generated the calibrated urban form data which is applied in my case study. Thanks Dr. Joao Paolo Leitão for raising critical questions , connecting me with the people having data of Fehraltorf catchment, and most important controlling the direction and domain of the whole project.

Besides my advisors, I would like to thank the other members of my thesis committee: Dr. Markus Hrachowitz and Dr. Fransje L. Hooimeijer, for their encouragement, insightful comment, and inspiring questions.

My sincere thanks also go to Max Ramgraber from Eawag, and Toine Vergroesen and Martijn Visser from Deltares. Thanks Max Ramgraber for sharing climate forcing data that has been processed and applied in other projects and sharing the groundwater modeling experience (possible challenge) in the study area Fehraltorf. Thanks Toine Vergroesen for answering the questions regarding concepts in Urbanwb model and providing suggestions for the parameters of subsurface processes. Thanks Martijn Visser for sharing the source code of Urbanwb model.

I thank my classmates in MSc. Water management, TU Delft: Diana, Tatiana, Shiyang, Ilias, Nathan, Clifford, Giorgio, Henry, Shiyu, XinChu, Elina, Rogelio and Sarah, for sharing the happiness and sadness in life, and for all the fun we have had in the past two years.

Last but not least, I would like to thank my parents for giving me the opportunities studying abroad in the topest university, TU Delft and supporting me mentally throughout my life. Thanks to my little sister taking care of me while I was quarantining in Taiwan. Thanks to my boyfriend for the discussion, practicing presentation, and mental support.

# Table of Contents

## Table of Figures

## Table of Tables

# 1. Introduction

## 1.1 Problem statement

When it comes to water resource management, there are some large challenges that many countries worldwide are facing. The rapid urbanization changes the principal hydrology processes in urban areas. Climate change effects, such as the increase of precipitation intensity (Kothavala 1997) and long dry spells (Gregory et al. 1997), bring pressure on the current water resource collection and supply. In addition to the movement toward sustainable development goals, new strategies are required for the supply of satisfying quantity and quality of water. Therefore, we need modeling to analyze the water system and its interactions with human activities. For example, land use, agriculture and consumption practice. After investigating the effect of the human activities on water system, we would like to use modeling to run scenarios to study the feasibility of alternative water resource management strategies.

Modeling is expected to provide information on the dynamics of the total water system over time and space in both urban and rural area. Especially in the urban areas, the fluxes that are important to research include the five types of water: surface water, stormwater, groundwater, drinking water and wastewater. The total urban water cycle can be defined as the water "supply, treatment, distribution, consumption, collection, provision, and reuse" in urban areas (Peña-Guzmán et al., 2017). Models that cover these processes are classified as "Integrated Urban Water Cycle Models (IUWCMs)" among the integrated urban water models discussed in Bach's review (Bach et al., 2014). Among these models, a wide range of temporal and spatial resolutions are applied. Water balance of an area is the first step, which is usually working as a lumped model with simplified mass balance equations and larger time step such as 1 day. On the other end of the spectrum, hydrodynamic modeling usually simulates a gridded domain in smaller time step for example 5 minutes. The choose of the $\Delta x$ and $\Delta t$ has always been an issue to every analysis.

Instead of the two types of model, a spatially distributed water balance model would have been an interesting alternative. The status of the five types of water at a specific block in the model domain will be available, while not too much calculation effort is required for the water balance approach within each block. Since the scale and location of the alternative water resource are of great importance to the intervention results, a spatially distributed model seems to be an appropriate way to simulate and evaluate the water system with the measures. In addition, rapid development of geographic

information system (GIS) techniques has been applied in hydrological studies. There is a need to explore the water balance in a spatially explicit manner to take advantage of the power of GIS. Thus, we would like to develop a spatially distributed water balance model and compare the model result with monitoring results from the field or, if not available with modeling results, such as the results of a widely applied urban water cycle model Aquacycle (Mitchell et al., 2001).

Total urban water cycle model simulates the rainfall-runoff system and water supply-wastewater system. The integration of water services systems in a model allows the decision-makers to have a holistic view of water management. However, often, decision-makers are faced with meeting several conflicting objectives that can vary in importance from stakeholder to stakeholder (Rittel & Weber, 1973). UrbanBEATS (Bach et al., 2015a) is one example of a planning-support tool in urban water management that generates an approximation of urban and catchment characteristics of each block, and proposes optimal layouts of sustainable water infrastructure that meet the stakeholder's preference under a range of future scenarios (Bach et al., 2018). By harnessing the capabilities of GIS, it can help facilitate the discussion around different ways in which sustainable urban water management measures and policies can be implemented.

With spatially explicit models, simplification of spatial representation or discretization is often a key consideration. Geographic data is often represented in vector (i.e. points, lines and polygons) or raster (square grids). On the other hand, hexagonal tessellation is less common, but has been known for its advantage over traditional square grids due to its identical distance to neighbors and the higher spatial resolution for the same area. Hexagonal grids have been applied and compared with square grids in some research area, such as transportation (Brodsky, 2017), accessibility analysis of a public infrastructure (Islam & Aktar, 2011; Zhu, Liu, & Yeow, 2006; Wang, Kwan, 2018), and ecology research (Birch, Oom, & Beecham, 2007). When nearest neighborhood, movement paths or connectivity are important, the hexagonal grids can have better performance than rectangles (Birch, Oom, & Beecham, 2007). Recent work in digital terrain analysis tested and concluded that hexagonal tessellation is superior to square tessellations in preserving flow direction in lower resolution cells (de Sousa et al.,2006). Despite its non-intuitive coordination system (irregularities of the shapes in a cartesian grid) and irrational area calculation (i.e. using the square root of 3), deeper exploration of adopting hexagonal grids in urban water cycle modeling is warranted.

## 1.2 Research goal and research question

The overarching aim of this project is to investigate the merit of hexagonal tessellation in modelling the total urban water cycle for sustainable planning of urban water systems. To this end, we present a comparison of a catchment's spatial-temporal urban water balance when applied to a hexagonal grid and a more conventional square grid representation. This comparison will provide insight on suitability and importance of spatial representation in integrated urban water management models. To achieve this aim, we address the following research questions:

(1) For the purpose of sustainable urban water management policy planning, how would an ideal spatially distributed balance model of the total urban water cycle look like?

(2) How is the balance modelling of the total urban water cycle affected by representation of the spatial grid? What is the impact of spatial grid representation on the total urban water balance? Particularly, how do square and hexagonal grids affect the overall representation of key urban water balance elements (e.g. catchment hydrology, water supply and wastewater cycles)

A spatially distributed urban water balance model that is compatible for data in square and hexagonal blocks will be developed in this thesis. This model will build on two existing water balance model that are simple but have proven to be effective in modeling the urban water system: Aquacycle (Mitchell et al., 2001) and Urban Water Balance (Urbanwb) model (Vergroesen & Brolsma, 2020). Furthermore, to support this work, the developed model is integrated with the UrbanBEATS Planning-Support System, which will provide the underlying spatial representation of the case study catchment. Land use data in each cell are derived by UrbanBEATS. The impact of different shape of the blocks – squares or hexagons of similar size – to the simulation result will thus be explored. The impact of differences in block size is beyond the scope of this study.

This thesis will first review the literature on urban water cycle modeling and general hydrological modeling issues (Ch. 2). Research methodology then illustrated (Ch. 3) followed by a detailed overview of the developed urban water cycle model (Ch. 4). Chapter 5 tests the model on two case studies: Curtin Catchment in Australia and Fehraltorf Catchment in Switzerland. The former is a featured case study of the Aquacycle model and is used to verify some of the algorithms with a pre-determined parameter set. The latter case applies the real observed climate, urban and hydrologic

data in grids generated by UrbanBEATS. Chapter 6 performs the in-depth comparison of model results on square and hexagonal grids. This is followed by a discussion of the overall performance of the urban water cycle model and application of hexagonal grids are carried out (Ch. 7) and finally, a conclusion and vision for further work is presented (Ch. 8).

## 2. Literature Review

### 2.1 Total urban water cycle and Integrated urban water management

The total urban water cycle is generally considered to cover the following flows and the interaction between each other, which are the natural hydrological processes (precipitation, interception, evapotranspiration, runoff, infiltration) and process induced by human society (water collection, supply, distribution, treatment, consumption, regulation) (Peña-Guzmán et al., 2017).

From the perspective of the domain of available models, we can categorize the processes of the total urban water cycle into two branches: the r*ainfall-runoff drainage system* and the *potable water supply- wastewater disposal system*. The former is also commonly handled by urban hydrological models. Compared to natural catchments, urban areas are more vulnerable to floods due to the higher impervious area ratio (Konrad, 2003). Urban hydrological models were developed for a better understanding of the stormwater flow dynamic and drainage system design in the city area to avoid loss of life and money caused by flooding. Before the first INTERURBA conference (Lijklema et al., 1993), computational models were mainly developed for simulating stormwater drainage and wastewater treatment plants separately. The discussion in the conference brought together the two subsystems in the urban water cycle, explored the relation and interaction between each other, and analyzed the integrated impact to the receiving water (Bach et al., 2014; Peña-Guzmán et al., 2017). Most existing drainage system at that time were designed to collect and transport both stormwater and wastewater, namely the combined sewer system. The impact of stormwater flow to wastewater treatment efficiency was therefore addressed in the design of a combined sewer system.

Due to urban and population growth, satisfying the growing water demand in urban areas with the original water resource becomes challenging. The water supply from catchments outside urban areas faces problems such as environmental pollution, unstable supply from reservoirs due to climate change (Mitchell et al., 2006). The potential of supplying water by internal resources of the city domain is therefore started to be considered in integrated urban water models. Alternative water resources from urban areas, including rainwater harvesting and greywater reuse, are promising solutions to reduce the potable water demand. However, the intervention of these technologies to the urban water system would introduce new interaction between the components of the total urban water cycle. To thoroughly evaluate the impact of the

technologies and interactions between different sub-systems, modeling the total urban water cycle as a whole is required (Rozos and Makropoulos, 2012).

Integrated urban water management was promoted to allow the decision-makers to have a holistic understanding of typical water-related problems faced by the urban water system: drinking water shortage, flooding and stormwater drainage, water pollution. Bach et al. (2014) classified urban water models into four levels according to the model's degree of integration . Integrated Component-based Models (ICBMs) and Integrated Urban Drainage Models (IUDMs) focus on the two subsystems in the total urban water cycle. Integrated Urban Water Cycle Models (IUWCMs) covers all components in the total urban water cycle, bringing the two types of aforementioned models (ICBMs and IUDMs) together. Moreover, Integrated Urban Water Systems Models (IUWSMs) includes the consideration of other disciplines (eg. economics, climate, citizen behaviors, etc). The stakeholders and decision-makers utilize the models that integrate the fields they are interested in.

### 2.2 Water balance approach

As mentioned before, hydraulic modeling of sewers, rivers, and drainage has been a key research focus for many decades. Flow routing approaches in models range from hydrodynamic routing (shallow water equations, Saint Venant equations, and kinematic/ diffusive/ dynamic wave approximation) to conceptual models (water mass balance approach, (non-)linear reservoirs) (Elga et al., 2015). Hydrodynamic approaches provide differential views of flow (volume) evolution during the rainfall events, thus being beneficial for drainage system design and flood management in systems with a relevant gradient. However, flat drainage systems and the other components in the total urban water cycle do not necessarily require the high temporal resolution modeling result. For integrated water management, the model complexity of quantitative analysis of available water in each storage within the model domain can be drastically decreased with a simplification of the routing method. Conceptual water balance models are thus widely applied for urban water resource estimation, as a detailed description of sewer flows is less feasible in the city-catchment scale (Elga et al., 2015). Also, model complexity should be adjusted for different modeling purposes to maximize model efficiency. In these conceptual water balance models, the movement of water and change of water in the reservoirs in the model domain are accessed by the mass balance equation (Eq. 1).

$$In - Out = S_t - S_{t-1} \quad \ldots (1)$$

Urban Water Balance Model (Vergroesen & Brolsma, 2020), referred as Urbanwb model in the following context, is a lumped hydrological model applying water balance approach for the calculation. It simulates the hydrological processes, including surface and subsurface processes, in urban areas (Fig. 2-1). Four types of surface cover are considered in this model, which are paved roof (PR), closed paved (CP), open paved (OP), and unpaved (UP). The unsaturated zone (UZ) in the Urbanwb model is represented as a container in which water content may fluctuate. The change of water content in the unsaturated zone and groundwater level is simulated considering the soil type and the corresponding characteristics, e.g. storage coefficient, saturated moisture content, saturated permeability… etc. The subsurface processes are described in a more realistic manner in the Urbanwb model.

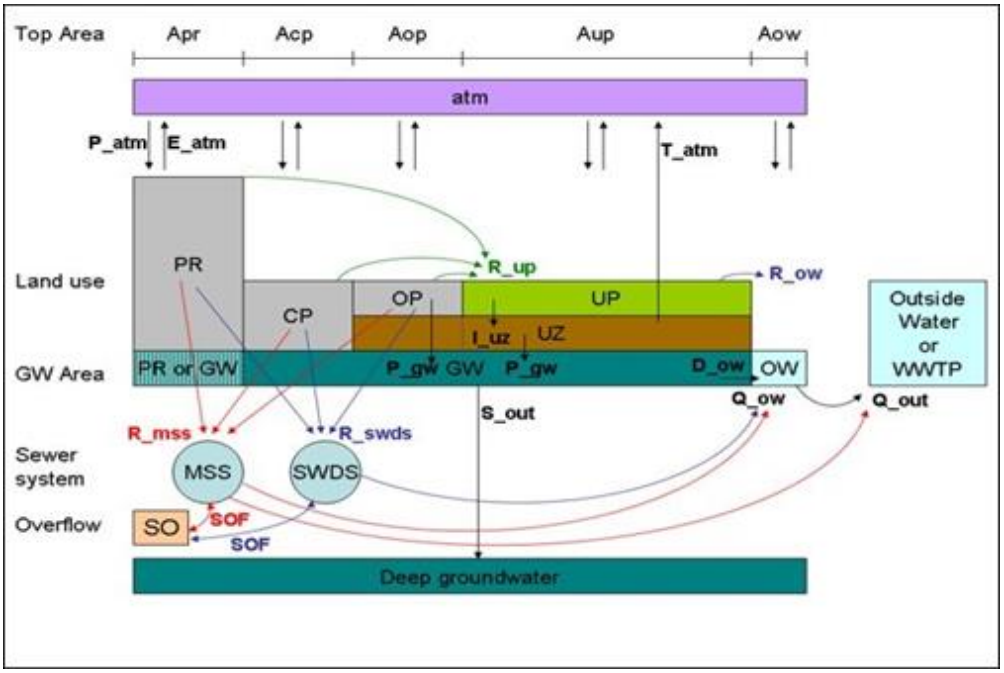


Figure 2 - 1. The conceptual representation of the urban water cycle by Urbanwb model. MSS: mixed sewer system, SWDS: stormwater drainage system, SO: sewer overflow. (Source: online documentation of Urbanwb model, https://publicwiki.deltares.nl/display/AST/Urban+Water+balance+model)

Kenway et al. (2011) implied the importance of defining the model boundary for the water balance approach. They listed the different components of the urban water cycle included in the models applying the water balance approach, concluding that those models missing some components of the total urban water cycle would result in poor estimation of the potential of alternative water supply sourced from the urban area itself. The water balance framework proposed by Kenway et. Al (2011) is described as equation 2:

$$S = C + D + P - (W + Rs + G + ET) \quad \ldots (2)$$

where S is the change of water volume in storages, including soil moisture, rain tank, surface interception, lakes … etc. The inputs C, D, P represent the centralized supply water, decentralized water from groundwater or rain tank and precipitation, respectively. The outputs W, Rs, G, ET represent wastewater discharge, stormwater runoff, groundwater, and evapotranspiration respectively. The potential of wastewater and stormwater to meet the water demand can be estimated and evaluated through this water balance framework.

However, there are still some processes in the total urban water cycle not considered for general application. The framework developed by Kenway et al. (2011) is refined and applied for a case study in a developing country (Paul et al., 2018). System losses and centralized recycled water are added to the original water balance framework to be more representative of a developing city. The refined framework helps the associated policymakers and water managers to improve integrated water resource management in the city.

### 2.3 Integrated Urban Water Cycle Models

Elga et al. (2015) divide hydrological models for urban environments into seven categories according to their model purpose and methodology. Among the seven categories, models aimed at integrated urban water balance assessment are in the "Conceptual Integrated Water Balance" group. These models mostly apply the conceptual or empirical methods to have a holistic view of water status in the urban area. Generally, they are useful as tools for water resource management and strategy evaluation. A brief introduction of these models will be discussed in the following paragraphs.

Aquacycle (Mitchell et al., 2001) is one of the pioneers of the integrated urban water cycle model. It simulates the surface rainfall-runoff process, wastewater drainage, water demand and supply in three spatial scales: block, cluster, and catchment. It is operated on a daily time step. The ability of alternative water resources to reduce the demand of imported water is estimated under different water supply scenarios. The subsurface process and hydrodynamic of sewer discharge are simplified in Aquacycle by the water balance approach of the related sub-system. Nevertheless, it is capable of simulating the water balance within the simulation unit "cluster" and the model domain.

Urban Water Quality (UVQ) enhanced Aquacycle with the simulation of contaminants (Mitchell & Diaper, 2005). The quantity and quality of components in the urban water

cycle are considered in this model package. The participation of contaminant flow provides an aspect of environmental impact for the assessment of water reuse strategies (Mitchell & Diaper, 2005). Aquacycle and UVQ model the study area with a group of "neighborhoods". The order of stormwater and wastewater flow from one neighborhood to the other can be specified to represent the real-world flow interaction.

City Water Balance (CWB) (Mackay & Last, 2010) is a scoping model simulating the dynamic balance of water, pollutants and energy in the urban areas. adopted the unit block concept and flow transfer concept from Aquacycle. Natural water bodies are allowed to be one of the options of sustainable water management. Overall, a variety of water management options is allowed in CWB, including alternative water resources from household to city scale, and the retention/detention devices.

The UrbanCycle model (Hardy et al., 2005) integrates all the components of the total urban water cycle (water supply, consumption, reuse, waste disposal and stormwater). With the spatial hierarchical structure, mitigation measures are applied to the corresponding spatial scale. The combination of graphical user interface (GUI) and the embedded network enable the user to explore the interaction of flows within and between the spatial scales. UrbanCycle is also characterized by the use of a stochastic rainfall model as climate input.

Urban Water Optioneering Tool (UWOT) (Makropoulos et al. 2008) is a planning support tool that simulates urban water demand with a demand-oriented approach. A database containing characteristics of available local and central water-saving techniques is applied in UWOT. Users select the corresponding appliance, for example, a certain type of shower, and enter the frequency of use. The modeling scale ranges from the appliances, the household, the neighborhood, to a city. The interaction between stormwater, wastewater, and water supply in the model domain is simulated to acquire the optimal alternative water technologies' intervention for the whole urban water system(Makropoulos et al. 2008). In addition to the optimization of internal water supply, a new version of UWOT is proposed to include the simulation of total urban water cycle from the operation of the external water supply system (Rozos & Makropoulos, 2013).

The Dynamic Urban Water Simulation Model (DUWSiM) is developed against the stress of urban water management under the effect of climate change and urban population growth (Willuweit, O'Sullivan & Shahumyan, 2013). It links the LARS-WG weather generator (Racsko, Szeidl, & Semenov, 1991; Semenov & Barrow, 1997) and the MOLAND land use dynamics model (e.g. Engelen et al., 2007; Shahumyan et

al., 2009) to a water balance model. By coupling the land use model and climate generator, water supply management options can be assessed for different scenarios. The model makes it possible to predict possible change of water demand, stormwater runoff and wastewater flow in different climate change or urban growth scenarios.

Sapkota and colleagues (2016) proposed an integrated framework that simulates the interaction between centralized and decentralized water supply systems, also known as "hybrid water supply systems". The flow rate and volume are both variables in the simulation. This framework comprises water balance modelling, contaminant balance modelling, multi-criteria decision analysis (MCDA), and future scenario analysis. The impact of different hybrid water supply scenarios on stormwater runoff, wastewater discharge and potable water demand is evaluated. The impact of population change and climate change can be assessed by the framework.

These integrated urban water cycle models simulate the total urban water cycle at a conceptually distributed scale. The application of alternative water resources are accessed from the perspective of flood peak reduction, water quality and even the economic benefits. The characteristics of the model domain are described in the unit of groups of neighborhoods. However, the data preparation could have been simplified if the model is compatible with GIS tools. This situation is one of the motivation of this study.

### 2.4 The spatial scale of models

Hydrological models are often characterized by their temporal and spatial resolution. In spatial scale, three different ways are often used to describe the study area. They are different from the degree of disaggregation for the study area.

In hydrological studies, lumped models treat the study area as a large unit. The parameters of lumped models describe the averaged characteristic over this study area. Therefore, it benefits from the calculation efficiency and comprehensive structure. It is more suitable to apply in rather homogeneous areas, when we are interested in the overall result of the system rather than the local results in the study area. For instance, river flood forecasting, impact study for climate change, … and so on.

For urban water studies, many models are based on Urban Hydrological Element (UHE). The definition of UHE varies slightly for each model. The general idea of UHE is a unit of calculation that corresponds to the urban topology. It can be unit blocks, e.g. in Aquacycle (Mitchell et al., 2001) and UVQ (Mitchell & Diaper, 2005), or single neighborhoods, e.g. in CWB (Mackay & Last, 2010). UHE is specially designed for

urban water systems simulation and is capable of preserving spatial information compared to lumped models. However, it is less compatible when remote sensing data is available for land use data input.

Distributed models are developed with the development of remote sensing techniques. The spatial variability provided by remote sensing data allows the hydrological models to perform simulation in every cell in the desiring resolutions (Elga et al., 2015). The most crucial spatial characteristics in urban water cycle models is the impervious surface ratio (Shuster et al., 2005). Although it is not easy to get the spatially detailed input data for distributed models, the output is beneficial when it comes to spatial scenarios, such as agricultural and ecological impact studies (Tran, Niel, & Willems, 2018).

Calibration difficulties, such as equifinality, has been a well-known challenge to distributed models. Equifinality in hydrological modeling is describing that different models and/ or parameter sets are capable of producing similar simulation results (Khatami et al., 2019). Tran et al. (2018) proposed a framework to build spatially distributed models from lumped models. Unlike the traditional calibration, this top-down approach first calibrates the parameters for the lumped model, then disaggregates the parameters to higher spatial resolution in their framework. This approach implies that constraints on the spatially variable model parameter values have to match the coarser resolution after aggregation. Three lumped conceptual hydrological models were tested with this approach to become a spatially distributed version. These spatially distributed models are proved to be able to generate results of similar accuracy to the original lumped model at the catchment outlet. Therefore, a spatially distributed model has the advantage over the ability to provide simulation results of internal location. The evaluation of distributed hydrological models should not be expected to be the ability to reproduce the flow rate, but the spatially detailed simulation results in the study area.

### 2.5 Models spatial representation

There are only three possible shapes to divide a plane regularly with only one type of polygons: squared, triangular, and hexagonal grids. Spatial representation is usually done in square grids as they have a few advantages, mainly the simple x-y coordinate system. For triangular grids, the two orientations add complexity to the coordinate system, therefore it is not the preferable tessellation for representing spatial information. Hexagons have been used in spatial modeling since the mid-1900's "Central Place Theory" (Christaller, 1966). In addition, hexagonal grids have been used on the map of

military games in cardboard and computer form since it was introduced (Palmer, 1977; Dunnigan, 1992).

Two main advantages of regular hexagonal grids over regular square grids have been investigated (de Sousa et al., 2017). Firstly, the higher achievable spatial resolution: hexagons are more compact leaving less vacant area when accommodating a circle of the same diameter. Secondly, the neighborhood regularity: neighbors of hexagons all share the same edge length and are equidistant, whereas for triangles and squares, neighbors are the ones sharing the same edges and the same vertex. Therefore, connectivity and nearest-neighbor concept become more straightforward for hexagonal grids (de Sousa & Leitão, 2018).

Hexagon patterns can be seen in many natural creatures, e.g. honeycomb and branching of young leaves etc. Mersereau (1979) demonstrates the advantage of hexagons in the application of frequency domain. Hexagonal grid is able to cover the circular band-limited signal with smaller area of Fourier spectrum (Figure 2-2). As sampling area is proportional to average sampling density, less samples are required for hexagonal sampling scheme. Thus, fewer computational cycles and less memory storage are required when applying hexagonal sampling scheme. Birch et al.(2017) explored the advantages of using hexagonal grids in ecological modeling. They recommend applying hexagonal grids when the research topic is about the construction or representation of the nearest neighborhood, movement and connectivity.

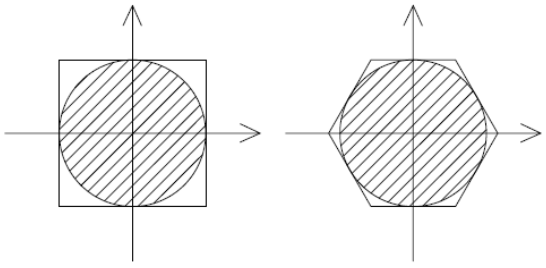

Figure 2 - 2. The sampling area of a circular band-limited signal by square and hexagon.

Although hexagonal grids show several advantages, a critical weakness of hexagonal tessellation is the flexibility of scaling. The composition and decomposition of grids is a challenge for hexagons because large hexagons cannot be divided into several entire smaller hexagons (Fig. 2-3). When it comes to modifying resolution or hybrid grids, square grids are more straight-forward.

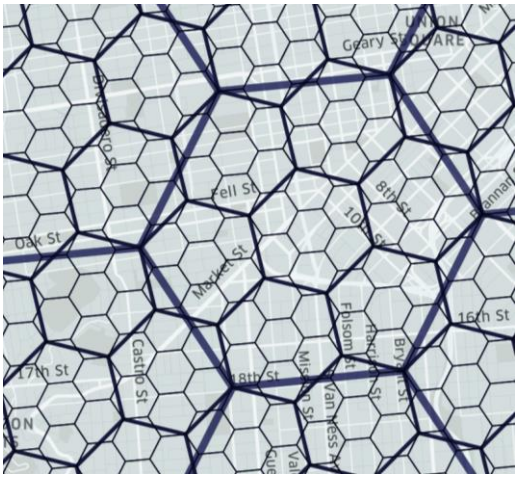


Figure 2 - 3. The large hexagon cannot be decomposition to complete smaller hexagons. Source: Uber Engineering, https://eng.uber.com/h3/)

There are not many hydrological or hydraulic applications that have explored hexagonal grids. Frisch, Hasslacher, and Pomeu (1986) applied the simulation of fluid flow on hexagonal meshes. The six velocity vectors linking to the neighboring cells are feasible to approach the Navier-Stokes equations as four velocity vectors do. de Sousa et al. (2006) tested the capacity of preserving flow direction of hexagonal and square grids from a higher to lower resolution map. Their work showed that hexagonal grids perform better than squares. The comparison of hexagonal and square tessellation in drainage network extraction from DEM data shows consistent results with de Sousa's work that hexagons are superior to squares (Wang and Ai, 2018). Tholen et al. (2017) examined and discussed the impact of different definitions of neighborhoods and cell shapes to the behavior of cellular automaton. Hexagonal cells require less iteration to reach a stable state. A recent work by de Sousa et al. (2017) demonstrates a significant difference in results for flood modeling when using hexagonal and square cells. The flood velocity estimated by hexagonal cells is higher than that derived by square cells. Therefore, the flood risk could be under-estimated in previous studies that are based on square grids.

A file format HexASCII (de Sousa & Leitão, 2018) has been proposed to enable the use of hexagonal rasters in GIS tools. The tool-kit "Hex-Utils" (de Sousa & Leitão, 2017) was also developed for creating and allowing the visualization of the hexagon rasters. As the tools for manipulating hexagonal cells are available, hexagonal grids could be tasted and adapted in spatially distributed models.

## 2.6 Conclusion

In the literature review, the emergence of the concept of total urban water cycle and integrated urban water management, the frequently used water balance approach, the available integrated urban water cycle models, the issues of spatial scale of models, and the up-to-date development of hexagonal grids application are discussed. Some key findings include:

1. Several models are available for integrated urban water management. Users should apply the one which fulfilled the desired model purpose without unnecessary complexity.

2. As the decentralized water supply policy requires the public's cooperation, the simulation result of the water management policy proposal is expected to be demonstrated as comprehensive as possible. Distributed models, from this point of view, is the preferable option as it can visualize the model result over the study area by gridded maps. In addition, computational efficiency is not the priority for water resource management modeling.

3. Aquacycle pioneered the idea of integrated urban water balance modeling and has become the basis for many integrated water cycle models hereafter. Other models expand the possible application by coupling it with the contaminant modeling module, GUI of the network system, and climate generators.

**4.** Hexagons are known for their advantage over the connectivity with neighbors and network modeling as well as better spatial and computation efficiency. Within urban water cycle modeling, the interaction with neighboring cells happens when stormwater runoff and sewer discharge outflow to downstream cells. Also, the population and infrastructure distribution in the urban topology may follow the central place theory, which can be illustrated in hexagon grids. Currently, hexagonal tessellation has not been investigated in urban water balance modeling but exhibits notable difference to square grids in urban hydrologic and hydraulic studies.

## 3. Methodology

In this section, an overview of the research approach is provided. To investigate the potential advantage of a spatially distributed urban water cycle model and the difference of model result brought by hexagonal grids, the following tasks are planned:

**Task 1.** Create a new spatially distributed total urban water cycle model.

The development of the model in this thesis will be based on improvement of existing urban water cycle models such as Aquacycle (Mitchell et al., 2001) and Urbanwb model (Vergroesen & Brolsma, 2020). The developed total urban water balance model should be compatible with the UrbanBEATS environment so that spatially explicit information for test cases can be easily generated and transferred into the developed model.

Sub-task 1.1. Define the cell-based total water cycle model.

In the literature review, Aquacycle was identified as a suitable starting point for this task given that its strong theoretical foundation and framework as an integrated total urban water balance model (Figure 3-1). It simulates the rainfall-runoff process on different surface types in the urban area, estimates the available greywater for reuse, and derives the potable water demand from the centralized water supply system. Similar to most models for urban water resource management, the subsurface process such as baseflow from groundwater to rivers, and percolation from the unsaturated zone to groundwater are simplified. Therefore, Urbanwb model is introduced.

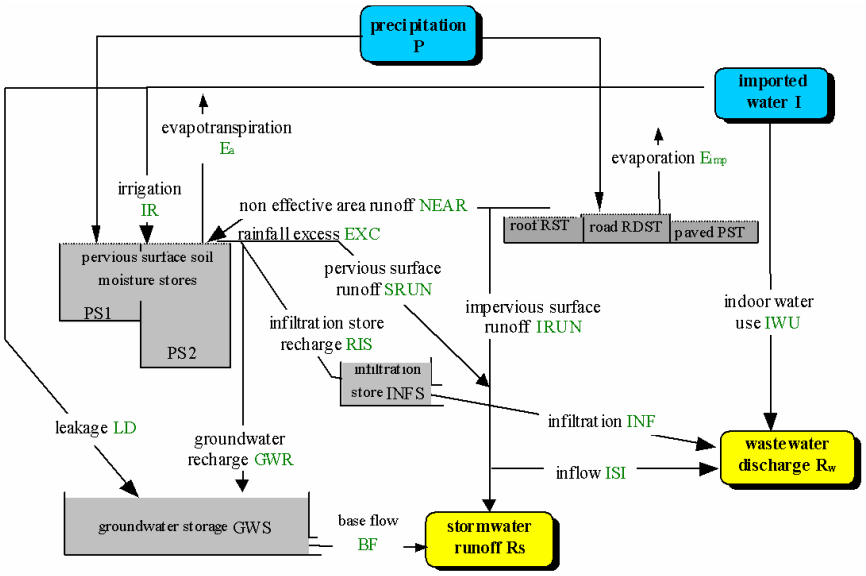


Figure 3- 1. The conceptual representation of the urban water cycle by Aquacycle (source: Aquacycle User Guide (Mitchell, 2005))

Since the goal of this study is to investigate each component in the total urban water cycle in a spatially explicit manner, we would like to improve the estimation of subsurface flows in Aquacycle by integrating the concept from the Urbanwb model (Vergroesen & Brolsma, 2020). A significant difference between Aquacycle and Urbanwb model is that the interaction between the subsurface, water supply systems, and wastewater drainage systems, which are generally neglected in urban hydrological models, are included in Aquacycle. Being more informative, dynamic and superior to Aquacycle and Urbanwb model, these processes will be integrated in the model developed in this study.

Sub-task 1.2 Define the interaction between cells.

It is assumed that stormwater runoff and wastewater discharge generated in each block are transported through the model domain within one time step (daily in our model). The stormwater runoff and wastewater sewer discharge at the outlet cells should be taken as the outflow of the whole model domain. To derive the flow at the outlet cell, we assume the stormwater runoff and wastewater sewer discharge of the upstream cell are transported to its unique downstream cell. The simulation order starts from the upstream-most cells to last downstream cells. A function is required to be developed to find this calculation order based on the list of downstream cell IDs provided by UrbanBEATS. However, there are outflows of the model that are not transferred between blocks, which are evapotranspiration, baseflow from groundwater to open water and deep percolation from groundwater to the deep groundwater reservoir. Different from stormwater runoff and wastewater discharge, for theses fluxes, the sum of outflow from every block represent the total outflow from the model domain. Further detail is explained in the next chapter.

Sub-task 1.3 Develop an interface with UrbanBEATS Planning-Support Model.

UrbanBEATS provides much a rich geospatial database of urban and catchment characteristics, including the ratio of land use types, arranged in either a square or hexagonal grid representation. This sub-task aims to develop an interface for extracting and setting up theurban water balance model from UrbanBEATS spatial output maps.

**Task 2.** Verify the model with an idealized case study.

To demonstrate that the model is able to generate stormwater runoff and wastewater discharge consistent with our conceptual model, we compare the simulation results from our model with the ones obtained using Aquacycle. In this model verification step, the purpose is to ensure that basic algorithms from Aquacycle have been properly

adapted. As such, a case study used as Aquacycle's tutorial was simulated in the newly developed model. Parameter settings are available in Aquacycle's user guide. In this case study, a small catchment Curtin in Australia is modeled as two cells. Two scenarios are done to examine the model performance when the water supply relies on centralized system and when rain tanks are applied as alternative water resource. The simulation results, except for the processes which are replaced by the Urbanwb model's modules (transpiration, deep percolation, and baseflow), should be similar to a certain level and would ensure that model algorithms were correctly adapted. A parameter sensitivity analysis is carried out to explore the effect of the parameters to the model results. In addition, the land use sensitivity is analyzed to provide a general idea of the change in urban water cycle components under different urban development scenarios.

**Task 3.** Test model performance on a real-world case study.

The proposed model is then tested with a real-world case study in Fehraltorf, Switzerland, for its ability to simulate a large spatial area. Climate data and the open water level time series as the boundary condition need to be processed for the application in a spatially distributed model. As a spatially distributed model, the model is developed to be able to take the precipitation, potential evapotranspiration data and open water level data from a single observation gauge or in a raster form. In this study, data is only available from a single gauge. Therefore, every block has the same climate input and open water level as boundary condition. Not only the climate data, the spatial characteristic and alternative water resource strategies allow both identical or different input values among blocks. The water balance of the model domain over the simulation period is discussed. The stormwater runoff and wastewater sewer discharge transfer between blocks are visualized in maps. In addition, the parameter sensitivity analysis is also done in this case study to explore the effect of parameters to the model with hundreds of blocks.

**Task 4.** Investigate the use of hexagonal grids in total urban water cycle modelling.

Since the flow interaction between cells in our model is encoded to allow any possible number of directions, the simulation can be done with either the D8 algorithm (O'Ccallaghan & Mark, 1984) for squares or the D6 algorithm for hexagons. In both D8 and D6 algorithms, it is assumed that each block has only one downstream block, which is the neighboring block with the lowest elevation. A comparison of the total water cycle model result over the Fehraltorf case study from typical square cells and the hexagonal cells will be conducted. Firstly, the terms in water balance equation will be discussed, followed by the annual outflows visualized on maps. Then, we inspect the

time series of the stormwater runoff and wastewater sewer discharge of four sampled blocks along the flow path. Finally, the inflow and outflows time series from a group of blocks covering the urban area are compared.

After completing the four tasks, we will be able to answer the research questions raised in chapter 1 and make recommendation to future research.

# 4. Modeling the Total Urban Water Cycle

## 4.1 General Overview

The aim of our model is to simulate the total urban water cycle of the study area in a spatially distributed manner. The rainfall-runoff drainage system and the water supply-wastewater system are expected to be included in our model. As a pilot of modeling the total urban water cycle, Aquacycle (Mitchell et al., 2001) was used as the basis. Aquacycle allows the evaluation of water reuse strategies by simulating the collection and consumption of alternative water resources in the total urban water cycle. The main disadvantage of Aquacycle is the simplified representation of evapotranspiration and subsurface processes. The concept of the unsaturated zone and the estimation of transpiration from plants are integrated into the previous surface storage by assigning two storage capacities much larger than possible interception capacity. Evapotranspiration is derived as the production of a built-in parameter "plant controlled maximum evapotranspiration" and the ratio of water content in the pervious area storage to the storage capacity. This simplification ignores the effect of plant type and soil characteristics on the water content in the unsaturated zone available for transpiration.

Urbanwb model (Vergroesen & Brolsma, 2020) is a lumped hydrological model applied in the Adaption Support Tool (AST) and urban water system analysis. The simulation includes the infiltration from the surface to the subsurface, water content fluctuation in the unsaturated zone, groundwater storage, and open water. Soil type and crop type can be chosen from the database, and the corresponding soil characteristics will be applied in the simulation. A variety of climate adaptation measures can be assigned in the model, which could affect the surface runoff and subsurface flows. The calculation of subsurface processes and transpiration are based on head difference and water content in storages, which grants more physical meaning than Aquacycle. Therefore, we utilize the main structure of the Urbanwb model for a better simulation of hydrological processes and then integrate the water supply-wastewater modules to complete the conceptual model of the total urban water cycle. New flows, such as leakage from the pressurized water supply mains and infiltration from groundwater to wastewater sewer, are introduced to the hydrological systems when considering the water supply and wastewater sewers to the model.

To explore the evolution of flows and available alternative water resources in the study area, we developed the (spatially) Distributed Urban Water Cycle Model (DUWCM).

The land use data of the study area is provided in a square or hexagonal mesh. The conceptual model of the total urban water cycle mentioned above is carried out in each cell in the model. These processes are simulated with the water balance approach in a daily time step. Since the time of concentration of stormwater and wastewater for an urban catchment area is on an hourly scale, stormwater runoff and wastewater sewer discharge derived in the upstream cells are assumed to be transferred to the downstream cells within the same time step (one day). In modeling the collection and consumption of alternative water resources and water demand, the daily time step is also often applied. Under these premises, the water balance approach is chosen for our model instead of complete routing methods. The hydrodynamic of sewer discharge or surface runoff in a detailed time scale is not expected for an integrated water cycle model. Instead, we would like to have a holistic view of the distribution of alternative water resources over the study area and the approximation of the inflow and outflow to the study area.

### 4.2 From Lumped to Spatially Distributed Model

The conceptual DUWSM model that is implemented on each cell is shown in figure 4-1. Stormwater runoff (Rs) and wastewater runoff (Rw) from upstream become one of inflow to the downstream Rs and Rw. To conduct the water transfer in the correct order, the execution of the model in the cells should follow the order from upstream to downstream.

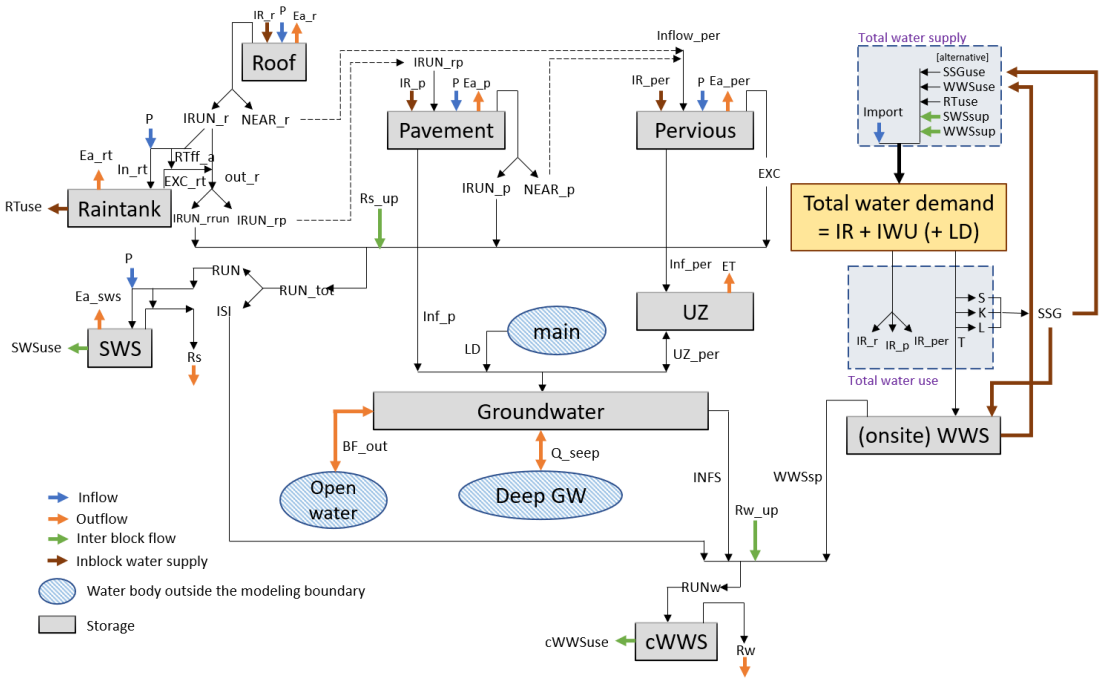


Figure 4 - 1. The conceptual DUWCM model of the total urban water cycle in each cell.

**Storages**: Roof, Pavement, Pervious area, Unsaturated zone (UZ), Groundwater, Raintank, Stormwater storage (SWS), onsite wastewater treatment and storage (onsite WWS), cluster-scale wastewater treatment and storage (cWWS). **Water body outside the modeling boundary**: pressurized water supply main (main), open water, deep groundwater (deep GW). **Inflow**: precipitation (P), imported water (Import). **Outflow**: actual evaporation (Ea), transpiration (ET), stormwater runoff (Rs), wastewater sewer discharge (Rw), baseflow (BF_out), deep seepage (Q_seep). **Inter block flow**: stormwater runoff from upstream (Rs_up), wastewater sewer discharge from upstream (Rw_up), consumption from stormwater storage (SWSuse), consumption from cluster-scale wastewater treatment and storage (cWWSuse). **Inblock water supply**: consumption of subsurface grey water irrigation (SSGuse), consumption of onsite wastewater treatment and storage (WWSuse), consumption of water in raintank (RTuse), supply from cluster-scale stormwater storage (SWSsup), supply from cluster-scale wastewater treatment and storage (WWSsup). **Total water demand** is used for irrigation (IR) and indoor water use (IWU), including kitchen (K), shower (S), laundry (L), and toilet (T).

A function “findorder” is developed to find this calculation order. In this function, the index of the upstream blocks of each block will first be derived from the downstream block index. Then, the calculation order will be determined. The downstream block index of each cell is given by the spatial delineation result from UrbanBEATS as a part of input data. However, the information of the upstream block indexes is more important for determining the calculation order among the blocks in each time step and the stormwater runoff and wastewater sewer discharge inflow from upstream blocks. By checking whether the downstream block index of each neighboring block of a block is the block itself , we can easily summarize the upstream blocks information of each block (Figure 4-2). The calculation order starts from the blocks that do not have any upstream block (group 0). The downstream blocks of group 0 (group 1) will be appended to the next group of calculation order if they have single upstream block. If the blocks in group 1 have more than one upstream block, it will be appended to the calculation order list only if its multiple upstream blocks are all available in the calculation order list. The same determination is carried out along the flow path until all the blocks are appended to the calculation order list. The number of neighboring blocks is different for squares and hexagons. Therefore, special care is taken for the two kinds of spatial representation.

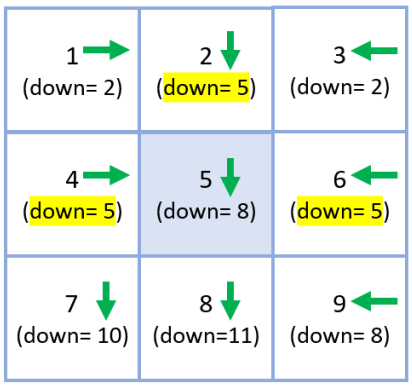


Figure 4 - 2. Example of determining the upstream block index. Each block has a single downstream block, and the upstream block can be summarized by checking its neighboring blocks. For example, the upstream blocks of block 5 are block 2, 4, 6.

The outflows that are not transferred between blocks are evapotranspiration, baseflow from groundwater to open water, and deep seepage from groundwater to deep groundwater storage. Evapotranspiration includes the evaporation from surface interception and transpiration from root zone (modeled as the unsaturated zone). The baseflow is determined by the drainage resistance and head difference between groundwater storage and open water. When groundwater level is higher than open water level, a positive value of baseflow will be derived to represent the groundwater outflow to open water. If groundwater level is lower, then a negative baseflow will be derived to represent the river feeding to groundwater storage. The deep seepage can be derived either as a calibrated constant value or depending on the vertical drainage resistance and the head difference between groundwater storage and a predefined hydraulic head of deep groundwater storage.

In DUWCM, two types of alternative water resource in terms of the supply range are included. Local-scale alternative water resource, which are subsurface greywater irrigation, onsite-wastewater treatment and storage, and rain tank, supply the water demand of the block it is located in. Cluster-scale alternative water, including the stormwater storage and cluster-scale wastewater treatment and storage, supply the cluster of blocks defined in the supply strategy. In the current development, there is only one option of supply strategy: randomly chosen blocks from the whole model domain.

Therefore, the simulation of the total urban water cycle in each time step can be subdivided into two stages. In the first stage, the models within the blocks are executed in the order we derived from the function “findorder”. The rainfall-runoff processes, subsurface processes, fill and spill of the alternative water resources, and the

consumption of local-scale alternative water resources are included in this stage. After this stage, the five important outflows, Rs, Rw, baseflow, deep seepage, and total evapotranspiration, from each block are available. The required potable water is derived temporarily because it can be updated after the distribution of cluster-scale alternative water resources. In the second stage, the consumption of cluster-scale alternative water resources is carried out. The available water in stormwater storage and cluster-scale wastewater storage are distributed to support the water demand of other cells. The required potable water of the receiving cells can, therefore, be reduced. The complete simulation including these two stages is illustrated in figure 4-3.

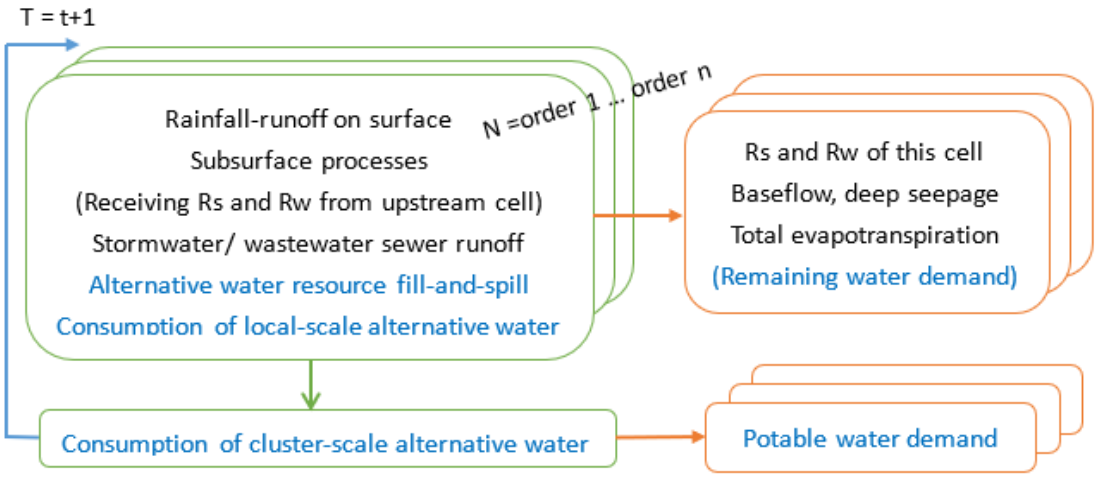


Figure 4 - 3. Simulation procedure happens within each time step. The upper green blocks show the execution of the processes in DUWCM model in each cell following the order from upstream to downstream. N is the array of cells id in the calculation order. Orange blocks represent the simulation result of each cell derived from that stage. After every cell is done in the first stage, the model goes through the cells having cluster-scale alternative water resource to distribute the collected water. Potable water demand of the cells receiving the supply from cluster-scale alternative water resource will be updated.

### 4.3 Input data of DUWCM

For a spatially distributed model as DUWCM, the resolution of the input data and parameters determine the degree of complexity and the calculation efficiency of the model. UrbanBEATS, as the provider of the land use and water demand data of the cells, generates the spatial data with the user-defined resolution and shape of the grid. The three surface types considered in our model are: *roof, partially pervious pavement, and pervious area*. If the input land use map has more land use categories, they will be grouped into the three types in our model under the condition of not changing the total

impervious area. The water demand for different water use is provided considering the population within the cells (ch 6.3 in Aquacycle user guide (Mitchell, 2005)).

The other input data required to run the model are climate forcing data, annual irrigation data, open water level time series, initial groundwater level, and the system configuration data.

a. ***Climate forcing data*** includes daily precipitation and potential evaporation time series over the simulation period. In most cases, uniform data for the cells in the whole study area applied. If observation data from multiple gauge stations or remote sensing measured data is available, DUWCM also allows the application of spatially distributed input data.

b. ***Annual irrigation*** is required as the daily irrigation data is rarely available. We assumed the yearly irrigation is distributed over the year following the pattern of potential evaporation. The down-scaled irrigation data is applied to the model as one of the inflows to the surface storages.

c. The ***open water level time series*** is applied as the boundary condition for this model. In the current version, we applied the open water level measured by a gauge station and transfer the unit from meters above sea level to meters below surface level. With the open water level data, our model estimates the baseflow from groundwater to open water by the hydraulic head difference. The unit of climate forcing data, annual irrigation and open water level time series are listes in Table 4-1.

d. The ***initial groundwater level*** is required as the initial status of groundwater storage. In addition, the initial water content in the unsaturated zone is derived by checking the equivalent moisture content in the database correspond to the groundwater level, soil type, and crop type we assigned. Similar to the climate forcing data, we can apply either identical value for the whole study area or the spatially distributed data. For a mountainous area, it is recommended to apply spatial data considering the variation of elevation.

e. ***System configuration data*** includes the input parameters determined by user (Table 4-2), measured parameters (Table 4-3), calibrated parameters (Table 4-4), the dimension of the alternative water resources (Table 4-5), and the water reuse plan (Table 4-6). Measured parameters are provided by the spatial delineation result from UrbanBEATS, which has to be spatial data. Calibrated parameters are the parameters we applied in the simulation. Manual adjustment

to the calibrated parameters is made during calibration to improve the model performance. The dimension of alternative water resources documents the characteristics, such as storage capacity, initial water content, first flush, and open for precipitation and evaporation or not. Finally, the water reuse plan is defined by users under fit-for-purpose consideration. For example, whether the rain tank is allowed to support the water demand from the laundry. Except for the measured parameters are determined by UrbanBEATS, user can choose to apply uniform value or different values for each cell of the other input data.

Table 4 - 1. List of input variables

| **Input variable** | **symbol** | **Unit** |
|---|---|---|
| Precipitation | P | mm/day |
| Potential evaporation | Ep | mm/day |
| Open water level | OWt | Average m a.s.l. (meter above sea level)/day |
| Yearly irrigation | IR | kL/yr |

Table 4 - 2. Input parameters determined by user

| **Input parameters** | **symbol** | **Unit** |
|---|---|---|
| Time step | dt | day |
| Soil type * | soil type | - |
| Crop type * | crop type | - |
| Cell size (side length) | size | m |
| Definition of seepage | seep_def | 0 for constant flux, 1 for head difference method |
| Leakage rate * | LR | % |

* Based on investigation of the study area.

Table 4 - 3. Measured parameters provided by UrbanBEATS.

| **Measured parameters** | **symbol** | **Unit** |
|---|---|---|
| Roof area | AR | $m^2$ |
| Paved area | AP | $m^2$ |
| Pervious area | APer | $m^2$ |
| Percentage of roof connected to rain tank | pRT | % |
| Average occupancy | Aoccu | People/house |
| Number of houses | NH | - |
| Downstream cell id | DownID | - |

Table 4 - 4. Calibrated parameters.

| **Calibrated parameters** | **symbol** | **Unit** |
|---|---|---|
| Effective roof area | ERA | % |
| Roof area maximum initial loss | RIL | mm |

| | | |
|---|---|---|
| Effective roof area flow to drainage | ERA_out | % |
| Effective paved area | EPA | % |
| Paved area maximum initial loss | PIL | mm |
| Infiltration capacity of the paved area | Infilc_p | mm/day |
| Pervious area maximum initial loss | PerIL | mm |
| Infiltration capacity of the pervious area | Infilc_per | mm/day |
| infiltration store recession constant ratio | IRC | - |
| horizontal flow resistance from shallow groundwater to open water | w | Day |
| vertical flow resistance from shallow groundwater to deep groundwater | vc | Day |
| constant downward flux from shallow groundwater to deep groundwater | down_seep | mm/d |
| Percentage of runoff become inflow to wastewater | perI | % |
| Hydraulic head of deep groundwater | h_dgw | m-SL |

Table 4 - 5. Dimension of alternative water resources

| **Alternative water resources parameters** | **symbol** | **Unit** |
|---|---|---|
| Index of cell | id | - |
| Is the rain tank open for P and E? | RTop | - (0: False/1: True) |
| Area of Rain tank | ART | $m^2$ |
| Rain tank storage capacity | RTc | L |
| Predefined first flush of rain tank | RTff | L |
| Initial storage in the rain tank | RT0 | L |
| % of houses(AR) installing Rain tank (NH * pRT = number of rain tank) | pRT | % |
| Area of stormwater storage (SWS) | ASWS | $m^2$ |
| Is the SWS open for P and E? | SWSop | - (0: False/1: True) |
| SWS storage capacity | SWSc | L |
| Initial storage of SWS | SWS0 | L |
| Predefined first flush of SWS | SWSff | L |
| Area of on-site wastewater storage (WWS) | AWWS | $m^2$ |
| On-site WWS storage capacity | WWSc | L |
| Initial storage in the on-site WWS | WWS0 | L |
| Area of cluster-scale WWS | AcWWS | $m^2$ |
| Cluster scale WWS storage capacity | cWWSc | L |
| Initial storage in the cluster scale WWS | cWWS0 | L |

Table 4 - 6. Water reuse plan

| Water reuse plan | symbol | Unit (0: True/1: False) |
|---|---|---|
| Wastewater from kitchen inflows to SSG or not (SSG: subsurface greywater irrigation) | KforSSG | - (0/ 1) |
| Wastewater from Shower inflows to SSG or not | SforSSG | - (0/1) |
| Wastewater from laundry inflows to SSG or not | LforSSG | - (0/1) |
| On-site WWS supply irrigation demand or not | WWSforIR | - (0/1) |
| On-site WWS supply Toilet demand or not | WWSforT | - (0/1) |
| Rain tank supply kitchen demand or not | RTforK | - (0/1) |
| Rain tank supply shower demand or not | RTforS | - (0/1) |
| Rain tank supply laundry demand or not | RTforL | - (0/1) |
| Rain tank supply toilet demand or not | RTforT | - (0/1) |
| Rain tank supply irrigation demand or not | RTforIR | - (0/1) |
| Cluster scale WWS supply toilet demand or not | cWWSforT | - (0/1) |
| Cluster scale WWS supply irrigation demand or not | cWWSforIR | - (0/1) |
| SWS supply toilet demand or not | SWSforT | - (0/1) |

## 4.4 Modules and important processes

In this section, the main algorithms and important processes of the model will be discussed. Various complex calculation procedures are elaborated in-depth in Appendix 1.

### 4.4.1 Roof area and Rain Tank water collection

The roof storage takes precipitation and irrigation as input. The interception of the roof area is limited by the storage capacity (denoted as *RIL*, roof maximum initial loss), overflow happens when the storage is full. The evaporation from roof interception is then calculated as the minimum between available water in the roof storage and potential evaporation. The part of overflow that is collected by gutter is represented by the “effective roof area” (*ERA*). The remaining overflow becomes inflow to pervious area. The parameter *pRT* indicates the ratio of the roof area that is connected to a rain tank. This percentage of collected overflow from roof interception becomes inflow to rain tank. The area, initial water content, storage capacity, and predefined first-flush volume of rain tanks in the study area can be the same or differs between the cells. The user can define if the rain tank is open for precipitation and evaporation. The overflow from rain tank adding to the first flush and the part of collected roof interception overflow that is not connected to rain tank are separated to

inflow to the stormwater sewer system and the paved area depends on whether the rain tank overflow is connected to the stormwater sewer or not.

### 4.4.2 Paved area

The paved area includes all the surfaces that are neither building nor pervious area. For example, the sidewalk, parking lots, streets, driveways… etc. In addition to precipitation and irrigation as input, the paved area has inflow from the roof and rain tank system (spills). The overflow from pavement interception will be separated into effective surface runoff and non-effective surface runoff. The former is collected to the stormwater sewer system, while the latter flows to pervious area. The water intercepted by the paved area will be lost by evaporation and percolation to groundwater because we assume that the paved area is partially pervious. The infiltration capacity of the paved area is smaller than which of pervious area. The value is to be calibrated to simulate the slow percolation from pavement to groundwater storage.

### 4.4.3 Pervious area

In our model, the pervious area algorithm is mainly based on the unpaved algorithm in Urbanwb model (Vergroesen & Brolsma, 2020). The pervious area takes the non-effective surface runoff from roof and pavement, irrigation and precipitation as inflow, but it is assumed to not be limited by the interception capacity. The water remains from the previous time step plus the sum of the inflows becomes the initial interception storage in pervious area. The saturated permeability and soil profile data corresponding to the soil type and crop type we assigned are applied for the estimation of infiltration from pervious area to the unsaturated zone. The initial interception storage in pervious area will be depleted by evaporation and infiltration proportionally to a time factor, the ratio of available water to the sum of potential evaporation and actual infiltration capacity (Eq. 3). The time factor represents the percentage of time in a time step that intercepted water retained in the surface, therefore its maximum is limited to 1.

$$Time\ factor = \min\left(1, \frac{initial\ interception\ storage}{\left(E_p + Infiltration\ capacity_{actual}\right)}\right) \quad \ldots(3)$$

$$E_a = E_p \times time\ factor \quad \ldots(4)$$

$$Inf\_per_a = actual\ infiltration\ capacity\ \times time\ factor \quad \ldots(5)$$

Although there is a parameter “infiltration capacity of pervious area”, the actual infiltration capacity is also limited by the available free space in the root zone for infiltration. The free space in the unsaturated zone is the difference between maximum moisture content and the actual soil moisture content at the same time step, but this

space can be expanded by anticipated percolation from unsaturated zone to groundwater storage. The anticipated percolation is limited by the saturated soil permeability and available water content for percolation. If the water in the pervious area interception storage after the evaporation and infiltration is still more than the interception capacity, the overflow occurs and is assumed to be collected to the sewer system. The transpiration from plants is estimated in the unsaturated zone algorithm.

### 4.4.4 Unsaturated zone and transpiration

The unsaturated zone in our model is represents the root zone. Therefore, the area of unsaturated zone is assumed to be the same as pervious area. Applying the concept of Urbanwb model, transpiration from plants in pervious areas is estimated as the product of reference crop evapotranspiration (*Eref*) and transpiration reduction coefficient ($\alpha$). Reference crop evapotranspiration is the evapotranspiration from a reference surface, a hypothetical grass reference crop with specific characteristic (Allen et al., 1998). A transpiration reduction factor is derived from the concept of Feddes plant water stress factor(Feddes et al, 1978).

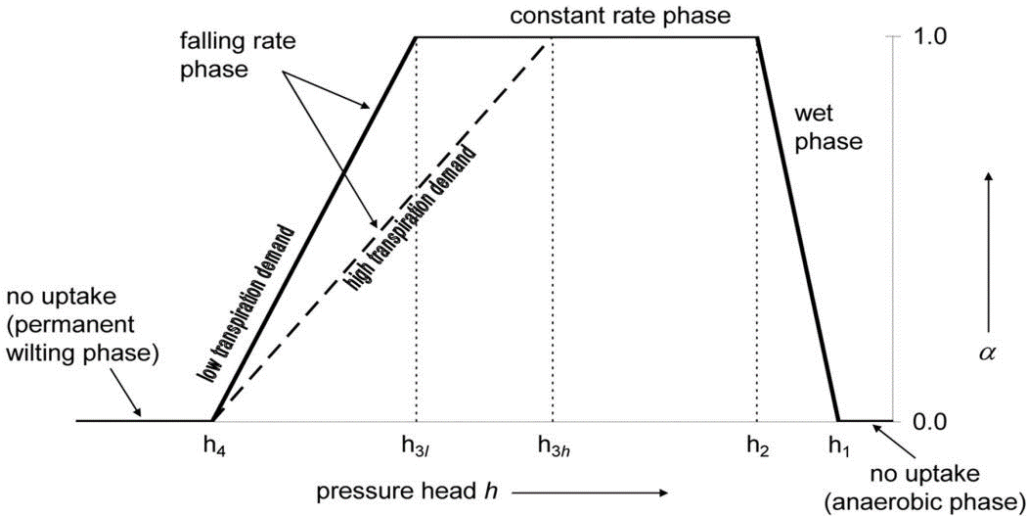


Figure 4 - 4. Transpiration reduction coefficient in Urbanwb model and our model in relation to root zone water potential (Source: de Jong van Lier et al, 2008).

Figure 4-4 shows the relationship between the transpiration reduction coefficient ($\alpha$) and root zone water potential. For each combination of soil type and crop type, the different values of *h1*, *h2*, *h3l*, *h3h*, and *h4* will be used. The *h1* in figure 4-4 is the pressure head when the soil is saturated. The *h2* represents the field capacity, defined as the amount of water the soil can hold against gravity. The pressure head *h3* is the transpiration reduction point, whose value differs with the reference crop evapotranspiration. The values of *h3l* and *h3h* are the transpiration reduction point when

the reference crop evapotranspiration is smaller than 1 mm/day or larger than 5 mm/day respectively. The actual *h3* is derived by interpolation of *h3l* and *h3h* when reference crop evapotranspiration is in the range of 1 mm/day and 5 mm/day (Eq. 6).

$$h3 = \begin{cases} h3l, E_{ref} \leq 1\ mm/day \\ h3l + \frac{E_{ref} - 1}{5 - 1} \times (h3h - h3l), 1 < E_{ref} \leq 5\ mm/day \\ h3h, E_{ref} > 5\ mm/day \end{cases} \quad \ldots(6)$$

The *h4* is the wilting point where crops are no longer be able to extract water from the soil. When the pressure head is lower than *h3*, there is drought stress, thus the $\alpha$ linearly reduces to zero at *h4*. When the pressure head is larger than *h2*, the $\alpha$ reduces linearly to zero at *h1* because of the anoxic moisture condition (Vergroesen & Brolsma, 2020).

In our model, infiltration from pervious space is the only inflow to the unsaturated zone. The transpiration and percolation from unsaturated zone to groundwater storage are the outflows. The moisture content of the unsaturated zone after accepting the inflow and extracting the transpiration is compared with the equivalent moisture content. If it is larger than the equivalent soil moisture content, percolation happens downward to groundwater storage as outflow. On the contrary, the percolation goes upward from groundwater storage, denoted as a negative value. For this situation, groundwater feeds the unsaturated zone, known as capillary rise. Equivalent soil moisture content fluctuates with the groundwater level and depends on the combination of the soil type and crop type. The percolation is limited by available water in the unsaturated zone and saturated soil permeability. While the amount of capillary rise is limited by available water in the unsaturated zone and the maximum capillary rise rate. Both the saturated soil permeability and maximum capillary rise rate are characteristic of the combination of soil and crop type and vary with the groundwater level at the previous time step.

### 4.4.5 Groundwater, leakage, and baseflow

The groundwater storage simulates the subsurface of the whole study area. The inflow to groundwater storage is the sum of infiltration from the paved area, percolation (or capillary rise) from the unsaturated zone, and leakage from pressurized water supply main. Leakage from pressurized water mains happens mostly because of the aging or cracking infrastructures. Normally, water utility has an estimation of the amount of leakage as a percentage of water demand of the system. Therefore, leakage is estimated as the product of the total water demand and the user-determined parameter *leakage rate (LR)* in our model. Total water demand includes indoor water use (IWU), outdoor irrigation demand, and the anticipated leakage (Eq. 7). Therefore, leakage is calculated as Eq. 8.

$$\text{Leakage} = \text{Leakage rate (LR)} \times \text{total water demand (total irrigation} + \text{IWU} + \text{leakage)) } \quad \ldots(7)$$

$$\text{leakage} = (((\text{total irrigation} + \text{IWU}) \times \text{LR})/(1 - \text{LR})) \quad \ldots(8)$$

The outflow from groundwater storage are infiltration to wastewater pipe (INFS), baseflow (drainage to open water), and deep seepage (to deep groundwater). The estimation of the outflows is driven by the hydraulic head difference between groundwater and the destination (Eq. 9, 10, 11). For the INFS, we assumed the pipes are generally located 3 meters below surface. If the groundwater head is lower than 3 m-SL, there will be no INFS.

$$INFS = \max(0.0, (h_{gw}(t) - 3)) \times IRC \quad \ldots(9)$$

The shallow saturated groundwater drains to the open surface water and to the more or less confined deep groundwater in linear relation to its head difference from the destination and drainage resistance. See Eq. (10) and (11).

$$Baseflow = \frac{h_{gw}(t) - h_{open\ water}(t)}{w} \quad \ldots(10)$$

$$Deep\ seepage = \frac{h_{gw}(t) - h_{deep\ gw}}{c} \quad \ldots(11)$$

Where $w, c$ : drainage resistance of baseflow and deep seepage(day)

The head difference between groundwater level and open water level is applied for deriving baseflow. Ideally, each block should have their own corresponding open water level data. For the blocks that having river pass through, the observed water level in the block will be applied. For the blocks not having river, the idea is to apply the water level of which the nearest downstream block having river (Fig 4-5). The resistance of no-river blocks is estimated with the distance to their nearest downstream block having river. The distance in the equation is not the shortest distance between the center of the block and its nearest downstream block having river, which can be derived by the coordinate of their centers. Instead, the distance along the flow path is applied in the estimation, which can be calculated easily by the number of blocks it passes through. For squares, there are two possible distance of the block's center to its downstream block's center depending on the flow direction. On the other hand, hexagon has the identical distance to all the neighbors. The relationship of the distance and the block size (L) of square and hexagonal grids is summarized in table 4-7.

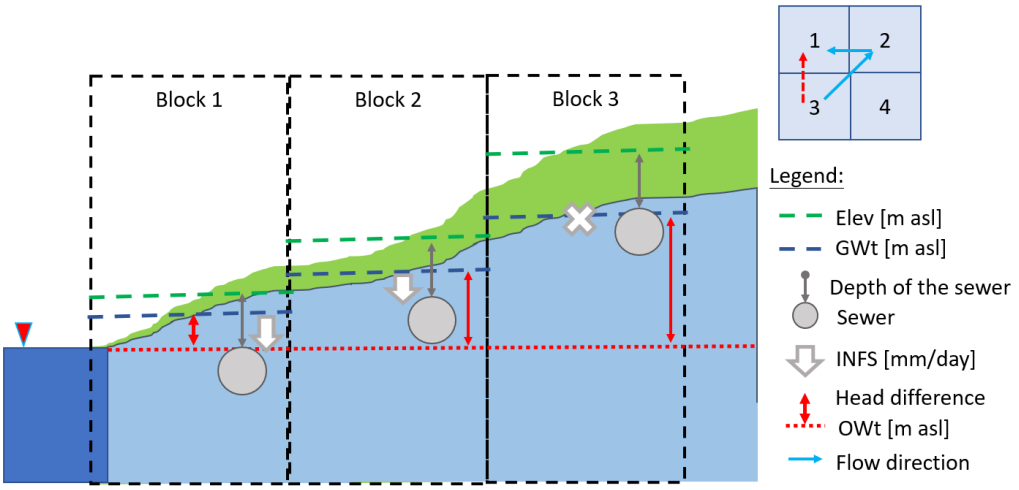


Figure 4 - 5. The water levels and head difference applied in the calculation of outflow from groundwater storage. Block 1 in the figure contains river in the surface land use. Therefore, the drainage resistance w of block 1 would be the value we calibrated. Block 2 and 3 have no open water in their surface land use. We estimate the drainage resistance by their distance along its flow path (the blue arrows in the right upper figure) to the nearest downstream block with open water (block 1). The grey arrows indicate the fixed depth of sewer pipes we assumed. For Block 3, the groundwater level at time t is lower than the depth of pipe, therefore no INFS is going to happen. The red dotted line implies the value of open water level each block apply to estimate the baseflow, which is the open water level of its nearest downstream block with open water.

Table 4 - 7. The distance of the centers of neighboring blocks.

| Square: $D = \sqrt{2} \times L$ or $D = L$ | Hexagon: $D = \sqrt{3} \times L$ |
|---|---|
| 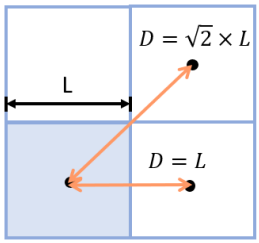 | 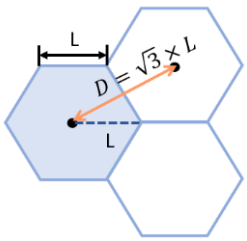 |





Since the flow direction is different for the two outflows, the drainage resistances are calibrated respectively. The groundwater level at each time step can be derived by solving an ordinary differential equation Eq. 12.

$$\frac{dh(t)}{dt} = \frac{Inflow\ (In) - baseflow - deep\ seepage - INFS}{storage\ coefficient\ (\mu)} \quad \ldots(12)$$

With initial condition $h(t = 0) = h_0$, the solution is shown in equation 13. The complete calculation process from Eq. 12 to Eq. 13 is elaborated in Appendix 1-d.

$$h(t) = -\left[\left[h_0 - \frac{w \times vc \times In - h_{deep\ gw} \times w - h_{open\ water}(t) \times vc - 3 \times IRC \times w \times vc}{w + vc + IRC \times w \times cv}\right] \times e^{\frac{w+vc+IRC\times w\times vc}{\mu\times w\times vc}\times t} + \frac{w \times vc \times In - h_{deep\ gw} \times w - h_{open\ water}(t) \times vc - 3 \times IRC \times w \times vc}{w + vc + IRC \times w \times vc}\right] \quad \ldots (13)$$

In each time step, the $h_0$ in Eq. 13 is the groundwater level at the end of previous time step, and t is the time step we defined. The solution $h(t)$ will be the groundwater level at the end of this time step.

The groundwater level, the assumed location of wastewater pipe, hydraulic head of deep groundwater, and open water in this equation are in the unit of meters-below-surface level (m-SL). We applied this unit for the convenience of comparison between blocks. The storage coefficient is the ratio of volume change to hydraulic head change in the soil. The value depends on the groundwater level, soil type, and crop type. The baseflow and deep seepage are both possible to be negative, meaning the opposite flow direction (river water feeding groundwater and groundwater recharge from deep groundwater). In Urbanwb and our model, deep seepage is also allowed to be approximated as a constant daily flow.

### 4.4.6 Local-scale water reuse

With rapid technology development, there are more and more new water reuse techniques. For the purpose of modeling, we categorize these techniques into five types: subsurface greywater irrigation (SSG), on-site wastewater treatment and storage (WWS), rain tank (RT), cluster-scale wastewater treatment and storage (cWWS), and cluster-scale stormwater storage (SWS). The supply, demand, consumption, and deficit of the first two local types are included in this module. The fill and spill of water in the rain tank are simulated in the rain tank module. But the consumption and the water content of rain tank at the end of this time step are simulated in this module. The use of water in the two cluster-scale alternative water sources is calculated at the end of each time step, after the calculation of every cell.

This module is adapted from the water reuse scheme of Aquacycle (Mitchell et al., 2001), using a lot of the similar terminology and table structure as Mitchell et al. The water reuse setting, indoor water demand, and irrigation demand are required as input. In the input file “water reuse plan”, information about whether each type of alternative water is assigned to support the water demand under the fit-for-purpose (FFP) water quality is noted respectively (Table 4-6). The water demand for different water use is

provided by the spatial mapping module of UrbanBEATS. The water demand types in UrbanBEATS are residential (kitchen (K)/ shower (S)/ laundry (L)/ toilet (T)/ irrigation (IR) demand of total houses/allotments respectively), non-residential (commercial, light industrial, heavy industrial), and public open space irrigation demand. In the current development stage of DUWCM, the consumption of alternative water resources for residential water demand can be simulated.

In UrbanBEATS, the five FFP water quality level from the lowest to highest are greywater (GW), non-potable (NP, i.e. treated water to non-potable level) , stormwater (SW), rainwater (RW), and potable water (PO). The minimum FFP source in UrbanBEATS are defined by users according to the input file "water reuse plan". The options for different water use are different. The minimum acceptable water quality for indoor usage except for toilets is stormwater. While the toilet and irrigation can accept all the water quality level from GW to PO. In addition, the use of alternative water resources from the local resources (SSG, WWS, RT) is prior to the larger scale supply (cWWS, SWS). As for public IR demand, the available resources are the large-scale ones, which are cWWS and SWS. Table 4-8 shows the priority of the alternative water resource for each water use. For example, if we set the minimum FFP level of toilets is NP, that means the toilet demand will not be supplied by SSG, but supplied by the other resources in the following order: WWS, RT, cWWS, SWS, and PO.

In each time step, the available amount of the alternative water resources of every cell will be calculated. After deriving the consumption of local resources (SSG, WWS, and RT) in each cell depending on the water reuse plan, the model distributes the water collected in cWWS and SWS by different strategies. The output from this module are the remaining water demand for each water use, a temporary value of required potable water and the amount of water spilled from WWS. The latter is an input for the cluster-scale wastewater storage and sewer discharge module.

Table 4 - 8. Priority of the alternative water resource allowed for each water demand (1: most preferable). Water quality level from lowest to highest: grey water (GW), non-potable water (NP), stormwater (SW), rainwater (RW), and potable water (PO). Types of water demand: kitchen (K), shower (S), laundry (L), toilet (T), and irrigation (IR).

| Water resource and water quality level\ demand | K | S | L | T | Residential IR | Public IR |
|---|---|---|---|---|---|---|
| SSG ∈ GW | | | | 1 | 1 | |
| WWS ∈ NP | | | | 2 | 2 | |
| RT ∈ RW | 1 | 1 | 1 | 3 | 3 | |

| | | | | | | |
|---|---|---|---|---|---|---|
| cWWS ∈ NP | | | | 4 | 4 | 1 |
| SWS ∈ SW | 2 | 2 | 2 | 5 | 5 | 2 |
| (PO) | 3 | 3 | 3 | 6 | 6 | 3 |

### 4.4.7 Stormwater Runoff and Storage

In this module, the total stormwater runoff (RUN_tot) will be calculated first by summing the overflow from pervious area (EXC), effective runoff from roof (IRUN_rrun) and paved area (IRUN_p), and the stormwater runoff from upstream cells (Rs_up) (Eq. 14).

$$RUN\_tot = IRUN\_rrun + IRUN\_p + EXC + Rs\_up \quad \ldots(14)$$

A part of this total runoff becomes inflow to the wastewater sewer system (ISI) because of misconnection or representing the percentage of the combined sewer system in the modeling domain. The other part of runoff (RUN) becomes inflow to the stormwater storage (SWS) if there is one.

$$ISI = perI * RUN\_tot \quad \ldots (15)$$

$$RUN = (1\text{-}perI) * RUN\_tot \quad \ldots (16)$$

A predefined amount of first flush is excluded before the runoff enters the SWS. Users can define whether the SWS is open for precipitation and evaporation. When the SWS is full, the overflow from SWS (EXC_sws) in addition to the first flush becomes the final stormwater runoff of this cell (Rs). If there is no stormwater storage in the cell, the part of stormwater runoff not going to the wastewater system directly becomes the Rs (Eq.17).

$$Rs = EXC\_sws + SWSff \quad \text{or} \quad Rs = RUN \quad \ldots (17)$$

The stormwater runoff will either be transferred to the downstream cell or becomes the outflow stormwater runoff of the study area if the cell is the outlet cell.

### 4.4.8 Wastewater storage and sewer runoff (cWWS)

The flows related to wastewater sewer are calculated from previous modules and accumulated in this module: overflow from onsite-wastewater storage (WWSsp), infiltration from groundwater storage (INFS), inflow from stormwater runoff (ISI). In addition, the wastewater sewer discharge from the upstream cells (Rw_up) is also added to the wastewater sewer discharge (RUNw) (Eq. 18).

$$RUNw = WWSsp + INFS + ISI + Rw\_up \quad \ldots(18)$$

$$Rw = EXC\_cWWS \quad or \quad Rw = RUNw \quad \ldots(19)$$

If there is a wastewater storage in this cell, the wastewater sewer discharge is the inflow to this storage (Eq. 19). The overflow from the storage will be the final wastewater sewer discharge (Rw) of this cell, which will be transferred to the downstream cWWS module or become the outflow wastewater discharge of this study area.

### 4.4.9 Cluster-scale alternative water resource distribution

As described in section 4.2, the distribution of water in the cluster-scale alternative water resource happens at the end of each time step after every cell goes through the above modules. After the simulation of the hydrological processes and local-scale alternative water consumption of every cell, the remaining demand for each water use and the available water in cluster-scale alternative water becomes the input to this module. In this module, the water content in the cluster-scale alternative water resources will be distributed to the cells allowing the supply from these sources. The distribution strategies could be for example supplying the upstream blocks, supplying the neighboring blocks within a certain distance, … etc. In the current development stage of DUWCM, only the option "supplying the randomly chosen blocks in the study area" is available. This distribution strategy is an idealized planning without considering the energy efficiency of transporting the water. The distribution will proceed until either all water demand is satisfied or the water content in the cluster-scale water resources is emptied.

## 4.5 Water balance of the whole model domain

The stormwater runoff and wastewater sewer discharge of the study area, which is comparable with the result of lumped models, are defined to be the value of the outlet cell or the cell where the gauge located in. While for the total potable water demand, baseflow, deep seepage, and total evapotranspiration of the study area, the sum of these outflows from each cell should be used to represent the study area.

The water balance of the system is examined for each time step. When taking the whole model area as one, the terms we applied in the water balance formula (Eq. 20) are described below:

$$WB = In - Out - dS = In - Out - (S_t - S_{t-1}) \quad \ldots(20)$$

- The "WB" term is expected to be zero at each time step.
- Inflow (In) = precipitation + Imported water

- Outflow (Out) = total evapotranspiration + baseflow + seepage + stormwater runoff at outlet + wastewater sewer discharge at outlet
- dS (change in storages) = dS of (roof interception + pavement interception + pervious surface interception + unsaturation zone + groundwater storage + rain tank storage + wastewater storage + cluster-scale stormwater storage + cluster-scale wastewater storage), dS = water level at current time step – water level at previous time step

The leakage from pressurized water main to groundwater and irrigation might be considered to be inflow to the total urban water cycle system. However, the amount of irrigation and leakage are supplied by alternative water resources and imported water. Therefore, it is more proper to put imported water in the water balance formula to avoid counting the same amount twice.

## 5. Model Verification and Calibration

To test the performance of our model, two case studies simulated for model verification and calibration respectively. Verification is done after the development of a model to check if the model behaves the same as the conceptual model it is based on. Since our model is developed mainly based on Aquacycle, we compared the model result of Aquacycle and our model from the same climate data and catchment characteristics. A tutorial case study of Curtin Catchment, Australia, is available in the user guide of Aquacycle (Mitchell, 2005). Although the algorithm of estimating evapotranspiration and subsurface flows are different in the two models, the other process can be verified, and the water balance of the whole model area can be checked. The case study where we test the model performance was the Fehraltorf Hydrologic Catchment in the Canton of Zurich, Switzerland, which is well-monitored. Input data for our model in this catchment was readily available. Fehraltorf was also a good opportunity to demonstrate the integration with spatial data generated by UrbanBEATS as a model setup for the area was already undertaken independently. Parameter sensitivity evaluation was carried out for both case studies.

### 5.1 Verifying the Model: Case Curtin

#### 5.1.1 Curtin catchment and model setting

To verify that our model was able to produce reasonable results, we compared it to results from Aquacycle. The study area, Curtin catchment, is located south-west of the city of Canberra, Australia. Ten years of precipitation and potential evaporation data (1980-1990) were available as the input climate data. In the tutorial case study of Aquacycle, the study area was separated into two model units. Therefore, we applied the same setting in our model so the model result is comparable.

In Aquacycle, the model unit is called a "*cluster*", which is composed of a group of unit blocks having the same area of the land-use types, surrounding road area, and open space area. A unit block represents a household unit, including roof area, paved area, and garden area. In Aquacycle, the total area of a cluster does not have to be the same with the other clusters. On the other hand, there is no spatial hierarchy in the land use delineation in DUWCM. The many surface land-use types in each cell are summarized into three types: roof, pavement, and pervious area. The transformation of land-use data from Aquacycle to DUWCM is shown in Eq. 21. Land-use data of the two cells representing the Curtin catchment are shown in table 5-1.

$$Roof_{my} = Roof_{Aquacycle} \times number\ of\ blocks$$
$$Pavement_{my} = Paved_{Aquacycle} \times number\ of\ blocks + Road_{Aquacycle} \quad \ldots(21)$$
$$Pervious_{my} = Garden_{Aquacycle} \times number\ of\ blocks + Open\ space_{Aquacycle}$$

Table 5 - 1. Land-use data of the two cells

| **Cell id** | **1** | **2** |
|---|---|---|
| Roof area (AR) [m2] | 1800 | 3750 |
| Paved area (AP) [m2] | 2000 | 2700 |
| Pervious area (APer) [m2] | 12700 | 11550 |
| Occupancy (Aoccu) [pp/household] | 2.7 | 3 |
| Number of houses (NH) [-] | 10 | 15 |
| Outflow to | Cell 2 | - |

In our model, annual irrigation data was required as an input to the model, while in Aquacycle, irrigation is a simulation result modeled based on a behavior parameter and soil moisture conditions. The irrigation in Aquacycle is estimated by a user-defined "*trigger-to-irrigate level*". If the water level in pervious storage is lower than the irrigation trigger level, the deficit becomes the irrigation demand which can be satisfied by potable water or alternative water resources (Fig. 5-1). The different implementation of irrigation (demand) will result in the discrepancy in imported water and total evapotranspiration, which will be discussed in section 5.1.2. In this case study, the observed yearly irrigation data is not available as input to our model. We applied the yearly irrigation estimated by Aquacycle to our model so that we have the same irrigation inflow to Aquacycle and our model.

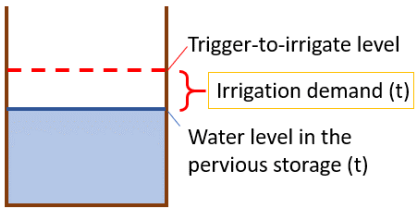


Figure 5 - 1. The irrigation estimation in Aquacycle. If the water level in the pervious storage at time t is higher than trigger-to irrigate level, then the irrigation demand is zero.

The optimal parameter sets are designed to be derived by manual calibration in both Aquacycle and DUWCM. The parameters related to the surface runoff in DUWCM is transferable with Aquacycle. Since the tutorial provided the calibrated parameter for Aquacycle (Table 5-2 (a)), we applied the same value of all transferable parameters to allow the comparison of the model results. Parameters in DUWCM related to

subsurface processes and transpiration, however, cannot be derived from the tutorial of Aquacycle because of the different algorithms. For instance, the infiltration capacity, the lateral and vertical drainage resistance, the soil type, and crop type. A manual, trial and error approach was carried out to find the optimal parameter set. Nash-Sutcliffe efficiency (Nash and Sutcliff, 1970) of the stormwater runoff (Rs), wastewater sewer discharge (Rw), imported water, and the total change in storage are the indicators to evaluate the performance of DUWCM in terms of producing the same result as Aquacycle in this case.

The Nash-Sutcliffe efficiency coefficient (Eq. 22) is a widely used objective function for hydrological model calibration. It is derived to quantify how well the model can predict the observed flows, here the model result of Aquacycle. The Nash-Sutcliffe efficiency coefficient ranges from 1 to -∞. The closer to 1 it is, the better the model performs. Note that the value is sensitive to extreme flows.

$$NSE(\theta) = 1 - \frac{\sum_{t=1}^{T}[Q_{obs} - Q_{sim}]^2}{\sum_{t=1}^{T}[Q_{obs} - \overline{Q_{obs}}]^2} \quad \ldots(22)$$

Two scenarios for case Curtin are considered in this study: the base case (no alternative water reuse) and the scenario that rain tanks exist in cell 1. The model results of the scenarios and comparison of the two models are discussed in section 5.1.2 and 5.1.3.

### 5.1.2 Model result of scenario 0: no alternative water resource

In the base case, we applied the values in Table 5-2 (b) for the user determined parameters (Table 4-2) and calibrated parameters (Table 4-4). The soil type and crop type are chosen based on the most representative type in the cell. The actual soil type and crop type that the numbers correspond to are listed in Appendix 2. In this case study, we apply soil type =17 and crop type=1, representing the heavy clay and grass respectively. Among the parameters, *ERA, EPA, RIL, PIL, LR, perI* are transferable with Aquacycle. Therefore, the values are not considered to be calibrated in this comparison with Aquacycle.

Table 5 - 2. Parameters applied in Aquacycle and DUWCM for scenario 0. (a) Parameters in Aquacycle provided by the user manual. (b) User determined parameters and calibrated parameters in DUWCM. The parameters colored in blue are the ones to be calibrated in this case to compare with the model result of Aquacycle.

| Calibrated Parameter | |
|---|---|
| Percentage area of store (%) | 22 |
| Pervious storage 1 capacity (mm) | 32 |
| Pervious storage 2 capacity (mm) | 240 |
| Roof area initial loss (RIL) (mm) | 0 |
| Effective roof area (ERA) (%) | 100 |
| Paved area initial loss (PIL) (mm) | 0 |
| Effective paved area (EPA) (%) | 100 |
| Road area initial loss (RDIL) (mm) | 0 |
| Effective road area (ERDA) (%) | 100 |
| Base flow index (-) | 0.55 |
| Base flow recession constant (-) | 0.0025 |
| % of surface runoff as inflow (perI) (%) | 3 |
| Infiltration index (-) | 0.095 |
| Infiltration store recession constant (-) | 0.12 |
| Garden trigger-to-irrigate (-) | 0.5 |
| Public open space trigger-to-irrigate (-) | 0.46 |

(a)

| User determined parameters | | Calibrated parameters | |
|---|---|---|---|
| Time step (day) | 1 | ERA (%) | 100 |
| Soil type (-) | 17 | RIL (mm) | 0 |
| Crop type (-) | 1 | ERA_out (%) | 100 |
| seep_def (0/1) | 1 | EPA (%) | 100 |
| LR (%) | 3 | PIL (mm) | 0 |
| | | Infilc_p (mm/day) | 2 |
| | | PerIL (mm) | 20 |
| | | Infilc_per (mm/day) | 80 |
| | | IRC (-) | 1.50E-06 |
| | | w (day) | 50 |
| | | vc (day) | 1000 |
| | | perI (%) | 3 |
| | | h_dgw (m-SL) | 1.28 |

(b)

Table 5 - 3. The Nash-Sutcliffe efficiency coefficients of scenario 0 (8 years).

| | |
|---|---|
| NSE_Import | 0.4048 |
| NSE_Rs | 0.9715 |
| NSE_Rw | 0.6736 |
| NSE_dS | 0.8999 |

The simulated hydrographs of imported water, total evapotranspiration, Rs, Rw, and total change of storage are presented in figure 5-2. The Nash-Sutcliffe efficiency coefficient of Rs, Rw and dS are above 0.6, while the modeling result for imported water is not considered an acceptable simulation (NSE < 0.6, (Freer et al., 2004)). The difference in imported water and total evapotranspiration between DUWCM and Aquacycle are obvious from the hydrograph (Fig. 5-2 (a) and (b)). The change of imported water is dominated by irrigation demand because the indoor water use is constant over time. In addition, there is no (dynamic) alternative water resource that can substitute the imported water. The irrigation demand of DUWCM is assumed to be the same pattern as the potential evaporation. Therefore, the peaks are in summer while the low values happen in winter. It is worth noting that this catchment is located in the southern hemisphere, the months of season is opposite to what we are used to. The upper limit of import water from Aquacycle can be a result of the estimation of irrigation demand, which is to satisfy the water content in the pervious storages to the trigger-to-irrigate level.

A closer inspection to the hydrograph of total evapotranspiration (Fig. 5-2 (b)) shows that the lowest value is still larger than zero. It is obvious that the total

evapotranspiration is dominated by transpiration, and the transpiration is larger than zero during the simulation period. This situation demonstrates the function of the capillary rise. Capillary rise allows the water feeding from the groundwater storage to the unsaturated zone, avoids the unsaturated zone from drying out completely. DUWCM allows the simulation of this process in a way with more physical meaning than Aquacycle.

Figure 5-2 (c) to Figure 5-2 (e) demonstrate the similar simulation result of stormwater runoff (Rs), wastewater sewer discharge (Rw) and changes in storages (dS). Although the hydrographs of Rs and Rw demonstrate a constant underestimation of Rs and overestimate of Rw, the value of perI, the parameter controlling the proportion of inflow from stormwater to the wastewater sewer system, is not going to be modified. Because it is one of the transferable calibrated parameters adapted from Aquacycle (Table 5-2). The other possible reason for the discrepancy can be the small difference in the design of the Rs and Rw transportation between cells in Aquacycle and DUWCM. Although we tried to build our model based on the concept model of Aquacycle as much as possible, there could still be some settings not listed in the user manual and Mitchell's article (Mitchell et al., 2001).

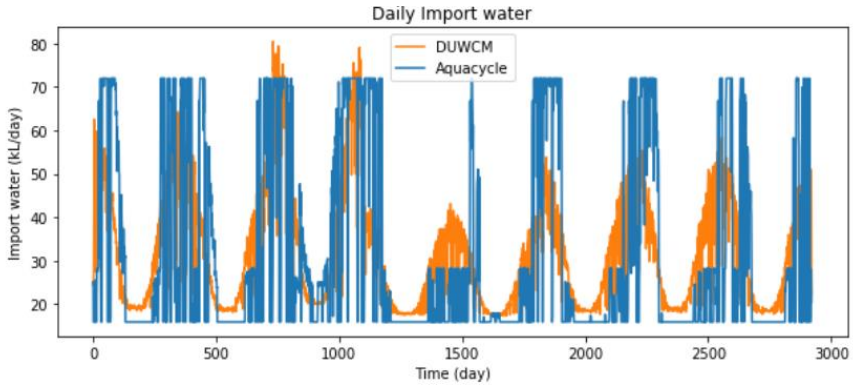


(a)

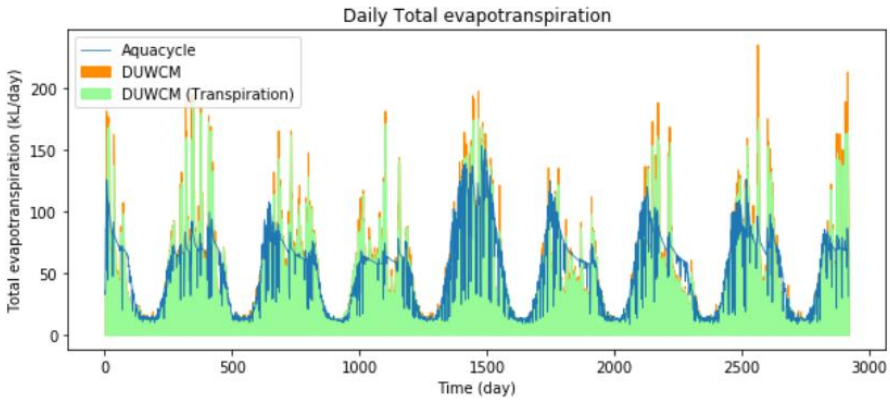


(b)

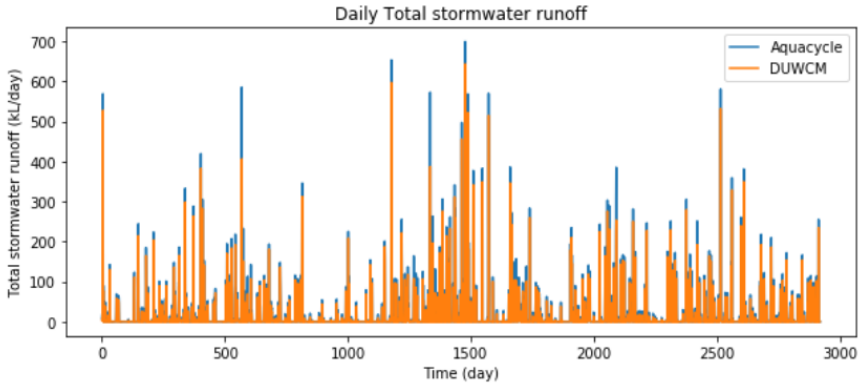


(c)

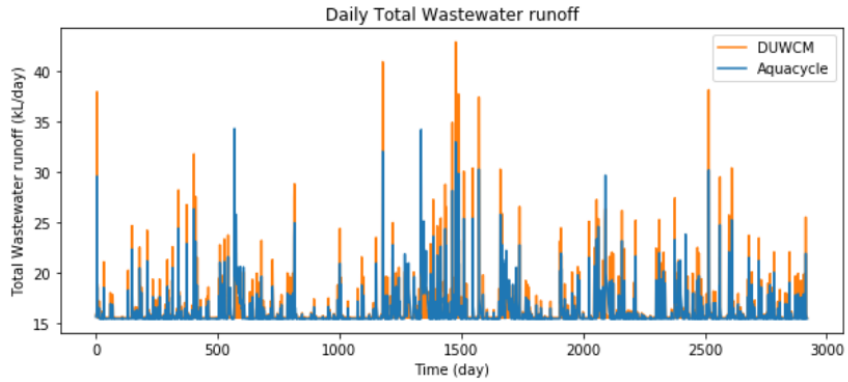


(d)

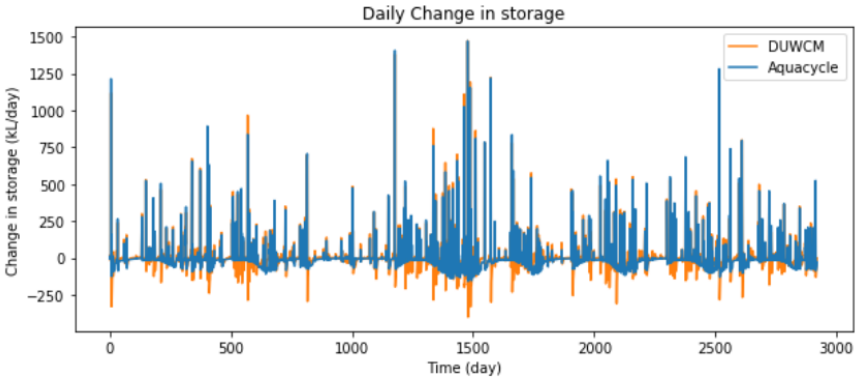


(e)

Figure 5 - 2. The simulated hydrograph for the catchment by DUWCM and Aquacycle: (a) Imported water demand (b) daily total evapotranspiration (c) daily total stormwater runoff (d) daily total wastewater sewer discharge (e) daily total change in storages.

### 5.1.3 Model result of scenario 1: rain tanks exist in Cell 1

The storage capacity of each rain tank installed at the households is 7000 liters. The first flush, 45 liters, is discarded from rain tank to the stormwater sewer for the purpose of promising water quality. The same calibrated parameters with case 0 are applied in this case, yielding the Nash-Sutcliffe efficiency coefficients against the simulation result of Aquacycle as table 5-4.

Table 5 - 4. The Nash-Sutcliffe efficiency coefficients of Scenario 1

| | |
|---|---|
| NSE_Import | 0.4583 |
| NSE_Rs | 0.9653 |
| NSE_Rw | 0.6794 |
| NSE_dS | 0.91 |

The NSE of Rs, Rw, and dS remain almost the same as scenario 0. The NSE values point out that the rain tank module is working as designed. The hydrograph of the model results can be seen in figure. 5-3.

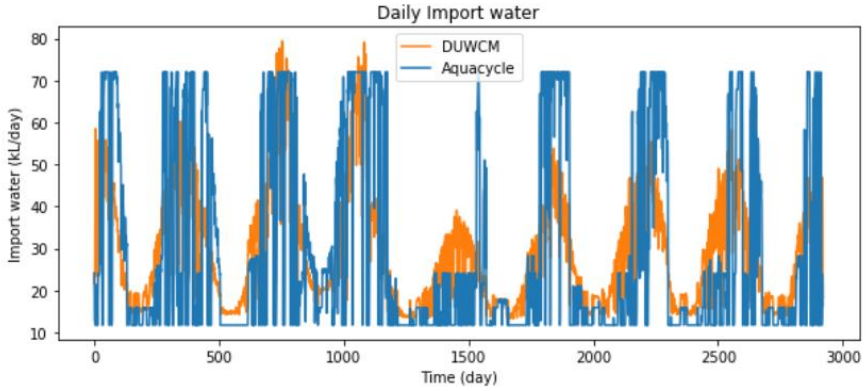


(a)

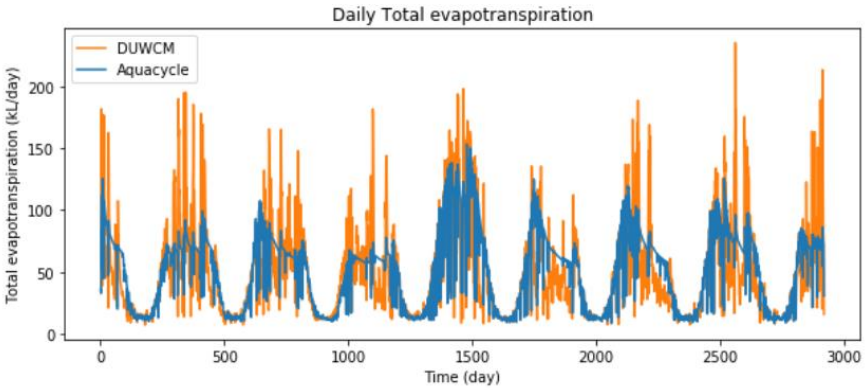


(b)

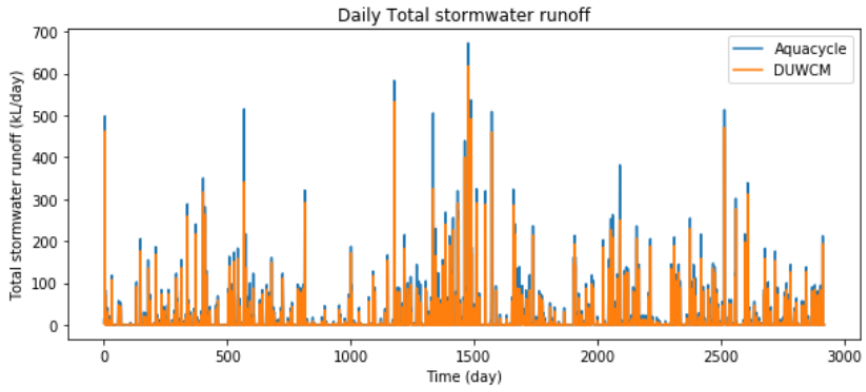


(c)

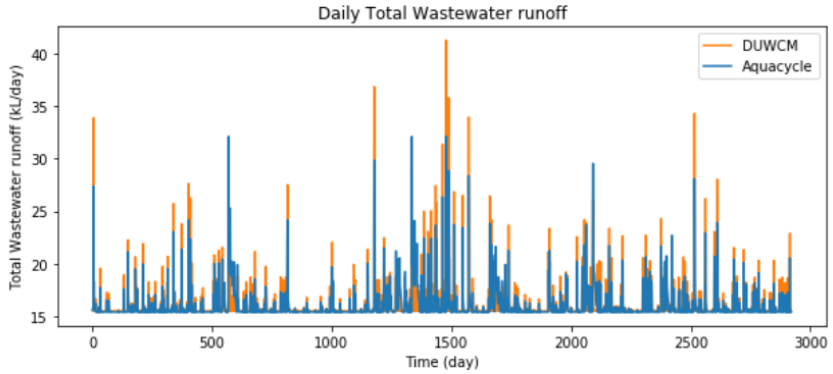


(d)

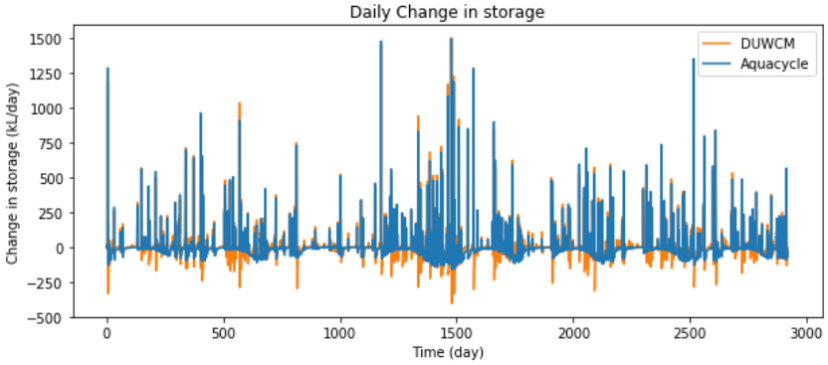


(e)

Figure 5 - 3. The simulated hydrograph by DUWCM and Aquacycle (Scenario 1): (a) Imported water demand (b) daily total evapotranspiration (c) daily total stormwater runoff (d) daily total wastewater sewer discharge (e) daily total change in storages.

By comparing the imported water simulated in the two scenarios, we can evaluate the effect of the rain tank implementation on the required imported water. Taking a closer look at the simulated imported water of the second year (Fig. 5-4), it can be said that the simulated total imported water of scenario 1 was lower than that of scenario 0 by the amount of water consumption from the rain tank.

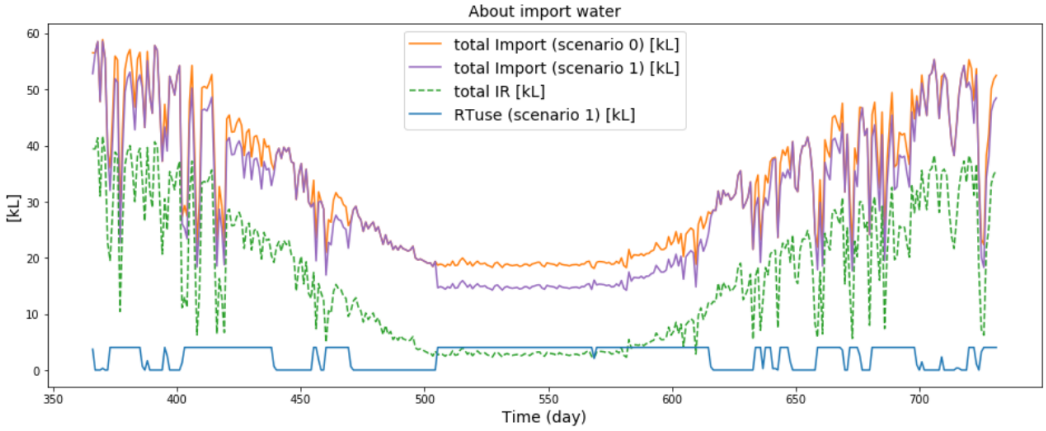


Figure 5 - 4. The import water of scenario 0 and scenario 1.

### 5.1.4 Parameter Sensitivity

There are several parameters (Table 5-2) have to be calibrated for a better result in the proposed model. For the purpose of a fair comparison with Aquacycle's result, we applied the same leakage rate (*LR*) and percentage of surface runoff inflows to wastewater sewer system (*perI*) in section 5.1.2 and 5.1.3. In this section, a sensitivity test of the two parameters and the other parameters newly implemented compared to Aquacycle is carried out. We compared the outflows under changes in parameters with the outflows of our main parameter sets. For each parameter, we compare the six important simulation output, which are baseflow, deep seepage, stormwater runoff, wastewater sewer discharge, evapotranspiration and import water demand.

Figure 5-5 and figure 5-6 shows the boxplot of standardized daily difference (Eq. 23) to demonstrate the trend under change of parameters. In Appendix 3, the boxplots together with tables of the mean square "error" (difference between the result from test parameter set and main parameter set result) (Eq. 24) and the hydrographs of the outflows during a low flow period (day 625 to day 800) are shown.

$$Standardized\ daily\ difference(t) = \frac{outflow_{test}(t) - outflow_{main}(t)}{outflow_{test}(t)} \quad \dots (23)$$

$$Mean\ square\ error = \frac{\sum_{t=625}^{800}(Standardize\ daily\ difference(t))^2}{len(t = 625{\sim}800)} \quad \dots (24)$$

The parameter sensitivity can be summarized as following:

a. Baseflow (BFout_all) and deep seepage (Qseep_all) are most sensitive to the change in the head of deep groundwater. Lower value of *h_dgw* implies the head is closer to the surface as the unit of *h_dgw* is "meters below surface level". Less seepage would happen in this case which results in a decrease of water feeding from open water to groundwater storage (negative baseflow). The change in vertical drainage resistance (*vc*) also results in obvious difference in deep seepage and baseflow. Lower *vc* allows higher seepage to the deep groundwater. Thus, the negative baseflow increase.

b. Imported water demand is only sensitive to the leakage rate. Lower leakage rate results in lower import water demand.

c. Stormwater runoff (Rs) is sensitive to infiltration capacity of paved area (*Infilc_p*), which is shown in the higher 75$^{th}$ percentile. Lower value of *Infilc_p* implies less water losing from surface water to subsurface system. The difference mainly happens when there is precipitation.

d. Wastewater sewer discharge (Rw) is more sensitive to the changes in the parameters regarding subsurface processes than stormwater runoff. Because one of the components of wastewater sewer discharge is the infiltration from groundwater to wastewater sewer pipes. Parameters regarding subsurface processes include leakage rate (*LR*), infiltration recession constant (*IRC*), drainage resistance ***w*** and ***vc***, and head of deep groundwater (*h_dgw*). In addition, lower *perI* would result in a lower 25$^{th}$ percentile of Rw.

e. Total evapotranspiration is more sensitive to the head of deep groundwater than the other parameters. However, the difference in totalE results from 40% lower *h_dgw* is not even 1% compare to the main simulation. This implies the value of total evapotranspiration is not sensitive to the value changes in parameters. Infiltration capacity of pervious area (*Infilc_per*)only affects total evapotranspiration. We should be aware that this analysis is based on the values of the main parameter set we applied in this case study.

Overall, *Infilc_p* and *perI* are the two parameters that should be taken care when calibrating the model with observed stormwater runoff or wastewater sewer discharge data. A change in *h_dgw* will results in great difference in baseflow, deep seepage and the total transpiration. The effect of changes in *IRC* is relatively small compare to the other parameters.

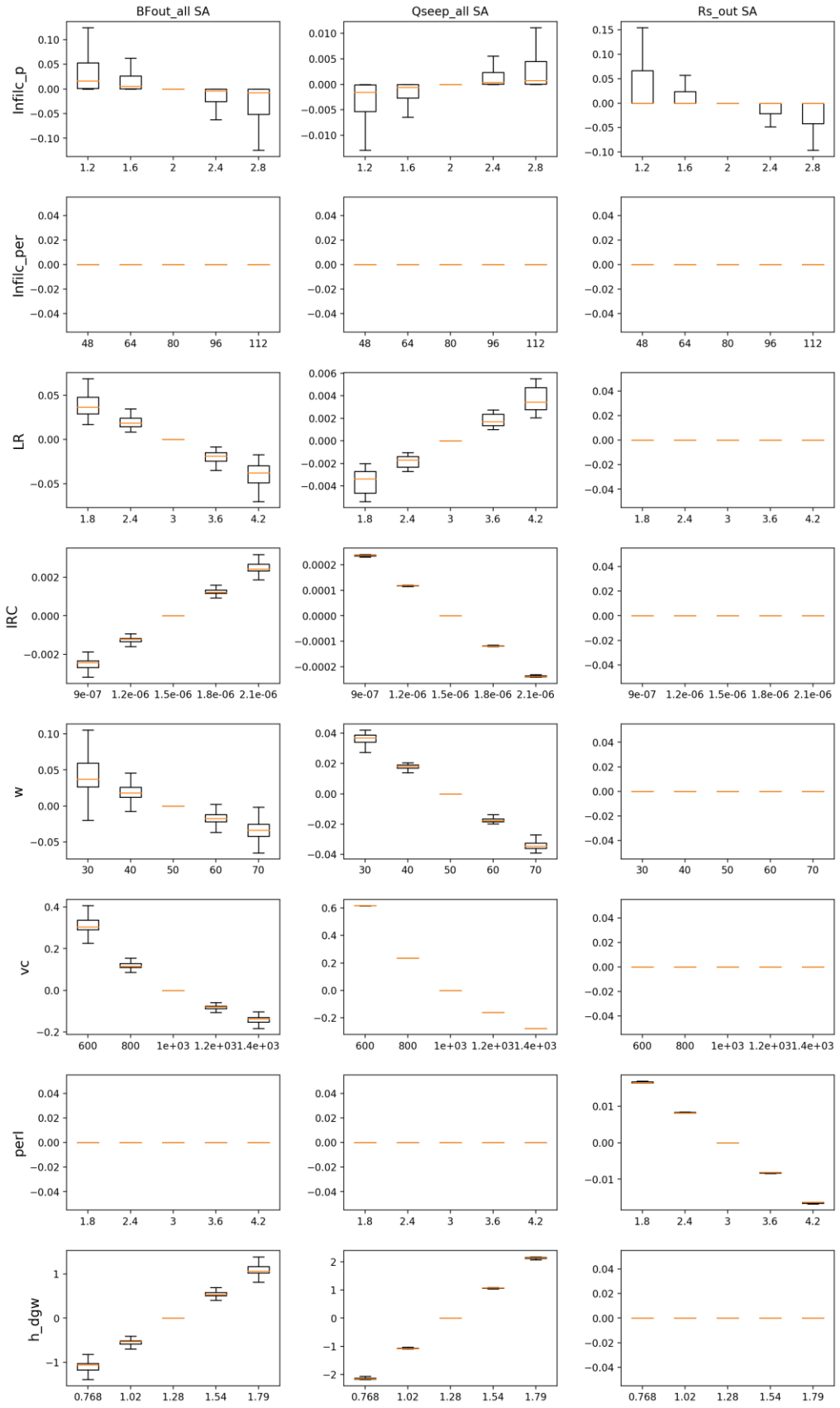


Figure 5 - 5. Boxplots of the standardized difference of the outflows (baseflow, deep seepage, and stormwater runoff) compared to main simulation of Case Curtin under changes in parameters.

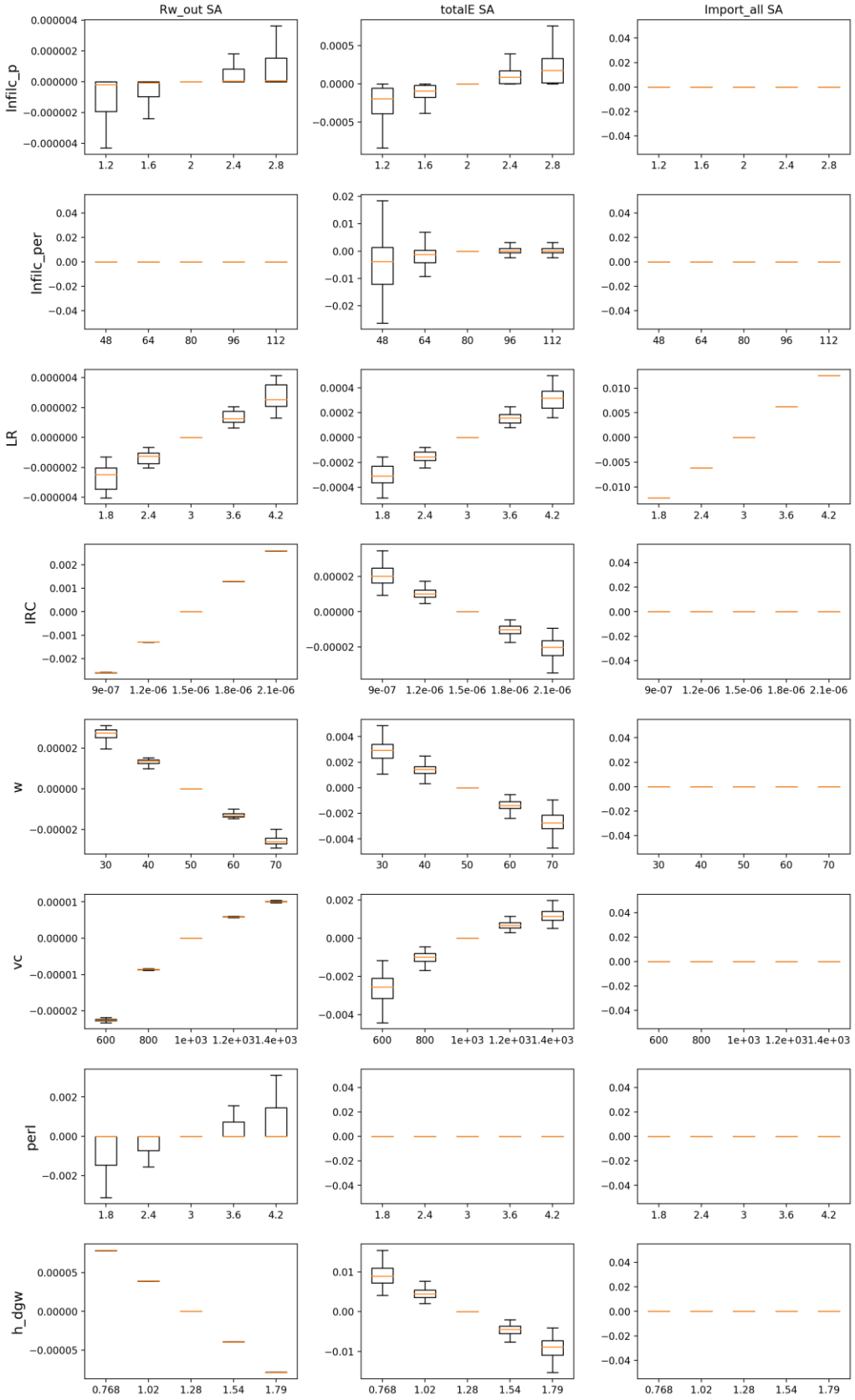


Figure 5 - 6. Boxplots of the standardized difference of the outflows (wastewater sewer discharge, total evapotranspiration, and imported water) compared to main simulation of Case Curtin under changes in parameters.

### 5.1.5 Land use sensitivity

As a water balance model developed for simulating urban water cycle, the effect of land use evolution in the study area is also worth explore. The urbanized process usually changes the pervious area to buildings or roads, the roof area and paved area in our model. Therefore, we simulated six scenarios, which are changing 10% and 20% of the total area from pervious area to roof, pavement, or the combination of roof and pavement, respectively (Table 5-5).

Table 5 - 5. The land use area in the two blocks in six urbanized scenarios.

(The first and second column in each scenario represent the first and second blocks.)

| Land use type | scenario | R | P | Pervious | Total | scenario | R | P | Pervious | total |
|---|---|---|---|---|---|---|---|---|---|---|
| Original | | 1800 | 2000 | 12700 | 16500 | | 1800 | 2000 | 12700 | 16500 |
| | | 3750 | 2700 | 11550 | 18000 | | 3750 | 2700 | 11550 | 18000 |
| | Change 10% of total area from pervious to Roof/ Paved area | | | | | Change 20% of total area from pervious to Roof/ Paved area | | | | |
| Roof (R) | LU1 | 3450 | 2000 | 11050 | 16500 | LU4 | 5100 | 2000 | 9400 | 16500 |
| | | 5500 | 2700 | 9750 | 18000 | | 7350 | 2700 | 7950 | 18000 |
| R+P | LU2 | 2625 | 2825 | 11050 | 16500 | LU5 | 3450 | 3650 | 9400 | 16500 |
| | | 4650 | 3600 | 9750 | 18000 | | 5550 | 4500 | 7950 | 18000 |
| Pavement (P) | LU3 | 1800 | 3650 | 11050 | 16500 | LU6 | 1800 | 5300 | 9400 | 16500 |
| | | 3750 | 4500 | 9750 | 18000 | | 3750 | 6300 | 7950 | 18000 |

The same indexes from section 5.1.4 are applied to analyze the effect of urbanization to the outflows. A series of the comparison of hydrographs between the scenarios are available in Appendix 4. Figure 5-7 shows the boxplots in each scenario.

To sum up, the increase in roof and paved area result in obviously rising stormwater runoff (Rs). The increase of Rs in scenario LU3 and LU6 is shown in the increase of $75^{th}$ percentile (see fig. 5-7). The effect on stormwater runoff is more obvious than which of wastewater runoff because the percentage of surface runoff inflow to wastewater sewer pipes is only 3%. Because of the less pervious area, the total evapotranspiration and irrigation water demand reduce.

The outflows react differently when the same pervious area becomes roof area and paved area. The comparison between scenario LU1, LU2, LU3 or scenario LU4, LU5, LU6 can give us the idea. For example, table 5-6 showed the flow when 20% of total area transformed to roof area (scenario LU4), paved area (scenario LU6), or the combination of both (scenario LU5). Because water intercepted on paved area are

allowed to infiltrate to groundwater, the inflow to groundwater is larger when the pervious area transforms to paved area than roof area. However, it is worth noted that the total evapotranspiration decline result from the decrease in pervious area has an important effect on the total inflow to groundwater. Total inflow to groundwater is the sum of leakage from pressurized water supply pipe, infiltration from paved area to groundwater and the percolation from unsaturated zone to groundwater. The amount of evapotranspiration in the unsaturated zone can result in a demand of capillary rise (negative percolation) from groundwater to unsaturated zone during dry days, which dominates the amount of inflow to groundwater. Because of the evapotranspiration, the capillary rise is larger before pervious area are developed to roof or paved area than which after the urbanization. Overall, the decrease of 20% total area in pervious area makes around 30% lower total evapotranspiration. Therefore, the total inflow to groundwater and deep seepage is higher after urbanization, and the feeding from river to groundwater (negative baseflow) becomes smaller.

Table 5 - 6. Sum of the important flows for day 625 to day 800 (unit: mm catchment). Total inflow to groundwater (Inflow_gw) = leakage from pressurized water supply pipe (LD) + infiltration from paved area to groundwater (Inf_p) + percolation from unsaturated zone to groundwater (UZ_per).

| | ET | UZ_per | Inf_p | LD | Inflow_gw |
|---|---|---|---|---|---|
| **main** | 329.222 | -51.4727 | 9.79132 | 7.44 | -34.2414 |
| **LU4** | 235.81 | -37.1043 | 9.79132 | 6.01124 | -21.3017 |
| **LU5** | 235.965 | -37.2509 | 16.9786 | 6.01124 | -14.2611 |
| **LU6** | 236.119 | -37.3974 | 24.1658 | 6.01124 | -7.22033 |

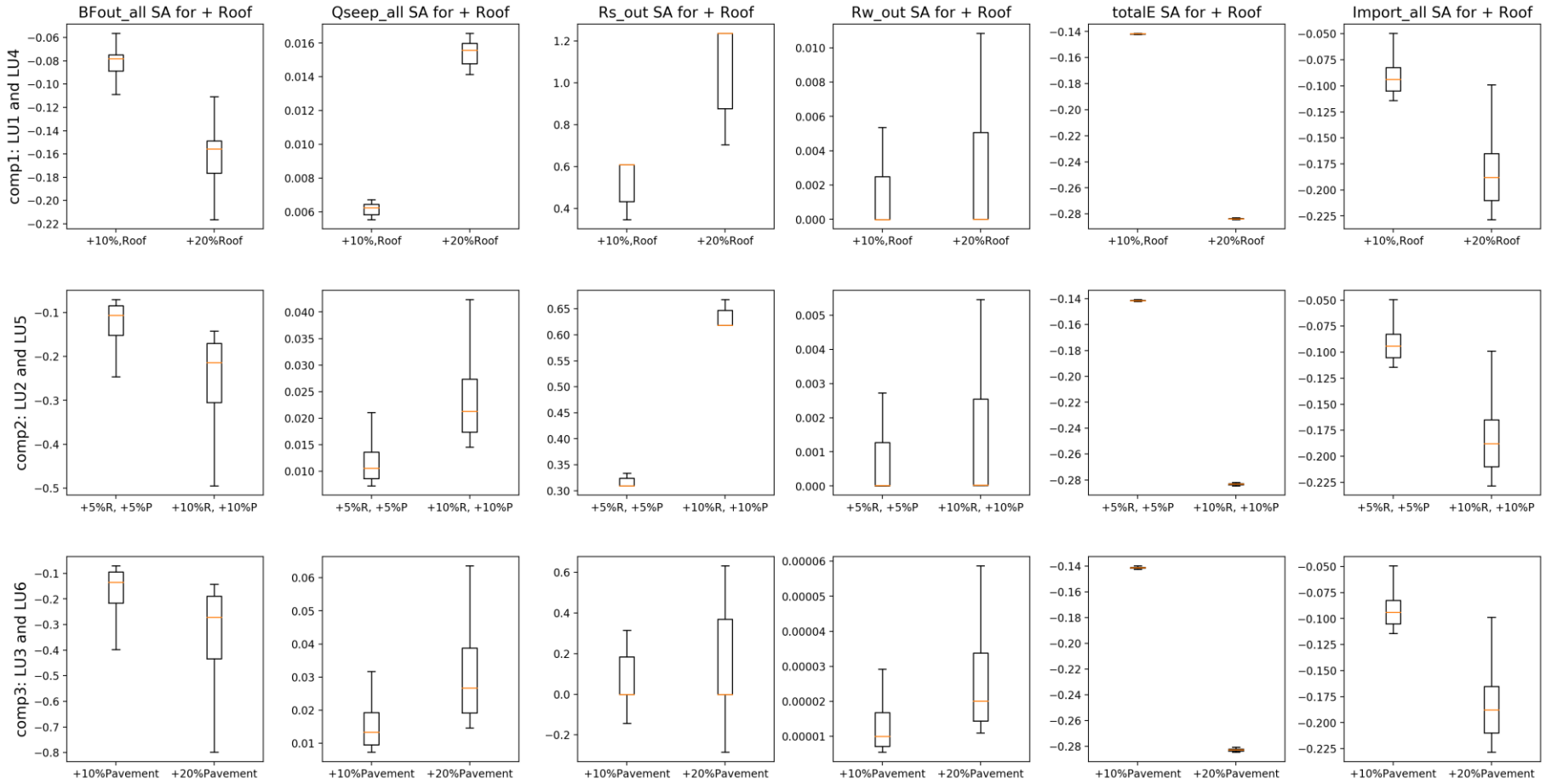


Figure 5 - 7. Boxplots of the standardized difference of the outflows compared to main simulation of Case Curtin under changes in area of land use types.

## 5.2 Modeling the real world: Fehraltorf urban water catchment

In this case study, we simulated a large catchment Fehraltorf with around 400 blocks. The spatial data in blocks is provided by the planning support tool UrbanBEATS. Fehraltorf catchment is a hydrological catchment in the upper Kempt river catchment. Around 90% of the surface area in this catchment is pervious area. The elevation in this catchment ranges from 508.17 to 905.14 meters above sea level (m a.s.l.). The average elevation is 616.69 m a.s.l. Precipitation, evapotranspiration, and river water level data in 2018 are applied for the simulation. The hourly precipitation data is from one of the gauges in Fehraltorf, while the potential evaporation data is the spatially averaged evaporation data from nearby METEOSWISS meteorological stations. The annual mean of precipitation and potential evapotranspiration are 882.45 mm/year and 811.48 mm/year.

### 5.2.1 Input data and parameters

a. Land use and water use data

The parameters regarding land use, population and water demand in each block are provided by the spatial delineation module of UrbanBEATS. The spatial input data set required by UrbanBEATS are land use, population, and elevation in a 10m×10m or finer resolution. Other input data such as waterways, planning regulation, demographic information are applied for the aid of calibration (Bach et al, 2018). In our case, the most important calibration in UrbanBEATS to our model is the imperviousness. We applied the detailed polygon map of "Bauzonen" (building zone) to calibrate the imperviousness in each block. The optimal output spatial data from UrbanBEATS we applied as input to DUWCM is with Nash-Sutcliffe Coefficient 0.75.

$$Total\ Imperviousness\ of\ the\ block\ (TIF) = \frac{A_{roof}+A_{pavement}}{A_{total}} \ldots(25)$$

The land use are distinguished into detail by UrbanBEATS, for example residential area and high density residential area, light and heavy industry, office,…etc. (Bach et al., 2015b). For each land use, the specific parameters are calibrated to describe the area according to construction laws (Bach et al., 2018). However, DUWCM currently has only three surface type: road (R), pavement (P), and pervious area (Per). Therefore, we applied the total roof area and total impervious area of each block summarized by UrbanBEATS to derive the corresponding value of area that is required as the input data to our model.

$$A_{total} = \text{Active} * \text{cell area};$$
$$AR = Blk_{RoofsA};$$
$$AP = Blk_{TIA} - AR;$$
$$APer = Atotal - AR - AP$$

The parameter "Active " from the output of UrbanBEATS is for defining the percentage of the block area that is really within our model domain. The "Active" for most blocks are 1, while the blocks located on the boundary of the model domain could have values between 0 and 1.

The indoor water demand of each end use is estimated by the usage pattern and unit flow rate (Bach et al., 2020) in UrbanBEATS. However, the data we found regarding the indoor water use of the study area are the average total daily usage, 162.0 liters per person per day, and the partition of each end use (Table 5-7). The parameters of the indoor water use in UrbanBEATS are thus calibrated to meet the daily usage data. The calibrated result yields 162.7 liters per person per day.

Table 5 - 7. The percentage of different indoor water end use.

| End use type | Toilet | Shower | Laundry | Kitchen | Total |
|---|---|---|---|---|---|
| percentage | 30.75% | 32.75% | 20.75% | 15.75% | 100% |

For the garden irrigation, we did not find corresponding data. Therefore, we assumed 1000 $m^3$/ha/yr to estimate the irrigation demand. In our simulation, the water demand from offices and industry are not considered. We estimated the water demand for the indoor use and irrigation in residential area. After the calibration, UrbanBEATS generates the estimation of indoor and irrigation water demand for each block.

b. Open water level time series and drainage resistance.

The open water level (OWt) time series is required as the boundary condition of our model. There is one surface water gauge (Kempt – Fehraltorf, ZH580) in our study area. For the current model development stage, we apply the same open water level in the unit meters above sea level (m a.s.l.) at this gauge for every block. The interaction between groundwater reservoir and open water (river) will depends on their head difference and the drainage resistance $\boldsymbol{w}$. If the groundwater level is higher than open water level, there will be outflow (positive baseflow) from groundwater to open water. In contrast, the water flows from open water to the groundwater reservoir (feeding, negative baseflow).

c. Initial groundwater level

The initial level of groundwater and deep groundwater are required as input parameters to our model. The *Water Resource and Drinking Water Department of Swiss Federal Institute of Aquatic Science & Technology (Eawag)* installed several observation wells along the river in the city of Fehraltorf. We took the observed data at these wells on the first day of the simulation period to estimate the initial groundwater level of each block. The spatial interpolation method we applied in this case is the inverse-distance-weighted interpolation (Eq. 26). The distance from the observation wells to the center of the blocks determines the weights (p =2).

$$z(x_0) = \frac{\sum_{i=1}^{n} w_i \times z(x_i)}{\sum_{i=1}^{n} w_i} \qquad \ldots(26)$$

, where $z(x_0)$ the estimated value of the block, z($x_i$) the observation of the wells, $d_i$ the distance from center of the block to the well $x_i$, and the weight $w_i = d_i^{-p}$ ( p>0, the power).

The interpolated initial groundwater level is transferred to the unit meters below surface level (m-SL), which is applied in our model. In the map (Fig. 5-8), we can tell that the interpolated initial groundwater level of the right part of the catchment are generally deeper than 20 [m-SL]. There are two potential reason for this situation.

Firstly, the elevation of the right part is mostly above 600 meters above sea level (m a.s.l.) while the area where the wells located is not higher than 550 [m a.s.l.] (Fig. 5-9). The range of the original observed groundwater level is between 513.73 to 536.35 [m a.s.l.]. Since the interpolated values are always in the range of the original observation data, these interpolated groundwater values become large when transferred to the unit meters below surface. Secondly, the quality of the interpolation is not promising because of the coverage area. The range of the observation wells is not covering our modeling area. Many of the blocks are receiving extrapolation values.

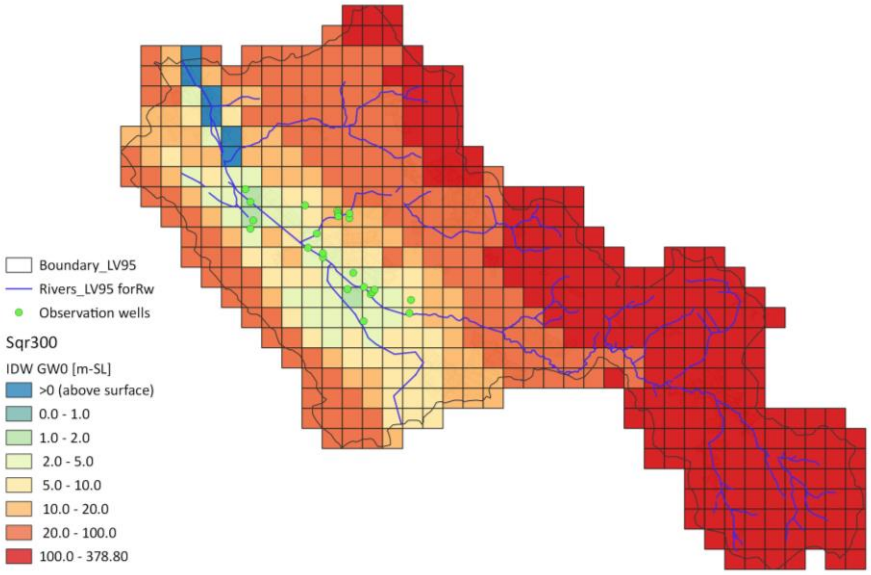


Figure 5 - 8. The initial groundwater level estimated by IDW (power 2) in the unit meters below surface (m-SL).

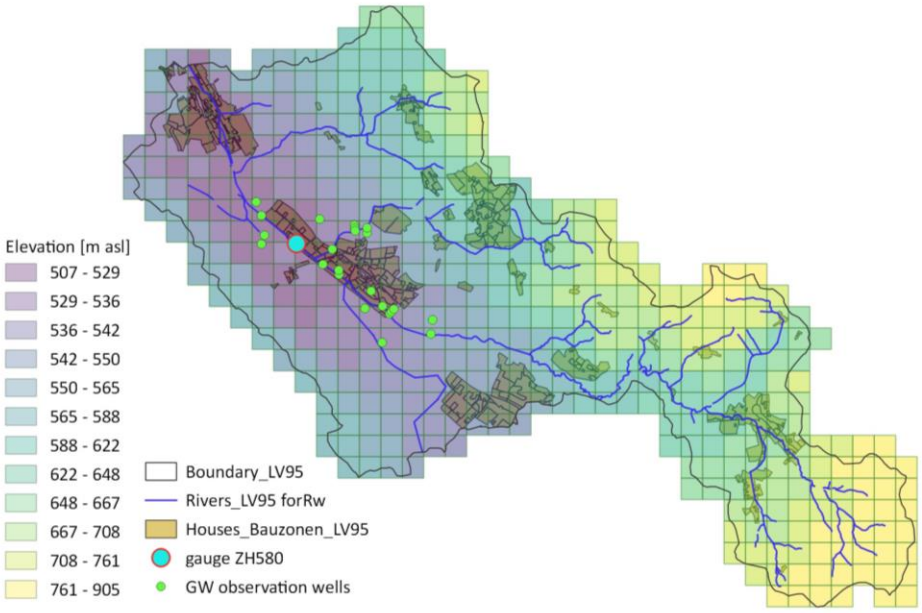


Figure 5 - 9. The average elevation of the blocks in the unit meters above sea level [m a.s.l.].

Moreover, research about the geology in Fehraltorf shows shallow groundwater reservoir exist only in the western portion of the catchment (Fig. 5-10). To simulate the water balance of this catchment with our model, we hence need to do the following assumptions:

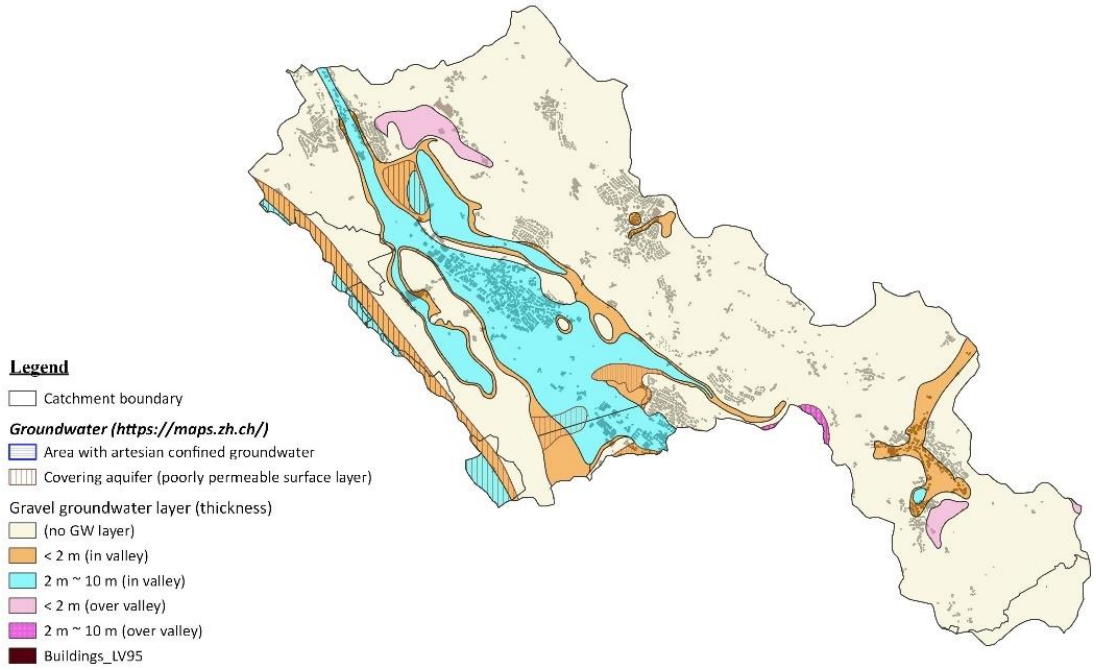


Figure 5 - 10. Geology (groundwater layer) of the Fehraltorf catchment. (Spatial data downloaded from the online cantonal groundwater map, layer: "Grundwasserkarte (Mittelwasserstand)" (http://maps.zh.ch/)).

***(1) Seepage to deep groundwater layer (Q_seep)***:In this case, we assumed a constant seepage every day in the blocks. In the areas without groundwater layer, the deep seepage should be zero. Since the area showing interpolated groundwater values larger than 20 m-SL are approximately in line with the area without groundwater layer, we assigned a constant seepage in these blocks to 0 mm/day.

**(*2) Drainage resistance to open water (w)***: For the blocks with "water" surface land use type larger than 0.05%, we took it as the blocks that river flow through. The drainage resistance of these blocks is to be the calibrated value in the range 10 to 100 days, while which of the other blocks are estimated based on the distance to its nearest downstream block having open water (Eq. 27). The values derived by this equation is generally larger than the calibrated value, implying a low flow from groundwater to river (or the opposite direction).

$$w = \frac{L^2}{8 \times k \times D} \qquad \ldots(27)$$

where L the distance along the flow path to the nearest downstream block, k the hydraulic conductivity [m/d] of the layer that is drained, and D the thickness [m] of the saturated layer that is drained. In our case, k=1.5 m/day and D = 0.2 m are applied for

the blocks in the catchment considering the hillslope is not able to keep a thick saturated groundwater layer.

***(3) Percolation from unsaturated zone to groundwater (UZ_per):*** When groundwater level GWt is smaller than 10 m-SL, capillary rise can happen as negative UZ_per if the moisture content is lower than equivalent moisture content, which is dependent on groundwater level. But when GWt > 10 m-SL, we assume the water is not able to rise against the gravity, thus no capillary rise happens.

***(4) The equivalent moisture content (heq) and storage coefficient (sc_gw):*** When GWt is larger than 10 m-SL are assumed to be the same value of which when GWt is 10 m-SL. This is the maximum depth in our soil database. Because the groundwater deeper than 10 meters is too far to affect the moisture content in the root zone, therefore it is no difference how far it is after 10 meters.

It is worth noting that the groundwater levels we applied in the model might be far too deep from the real conditions. However, with the coarse time step (1 day) we applied and the actual absence of an aquifer in the catchment, the combination of these assumptions is the optimal strategy among the ones we have tried. More discussion will be carried out in the later chapter.

With the interpolated initial groundwater level input, the model showed the tendency of the groundwater level to stabilize to the elevation of open water level. However, the large head difference between groundwater and river in the beginning results in an unreasonable high baseflow from groundwater to the river (Fig. 5-11 (a)). If we assume the long-term yearly climate forcing data is not far from the annual climate forcing data we applied, the groundwater level and the outflow should be coherent in the beginning and the end of the year. The extreme value implies the initial groundwater value we applied is not close to the reasonable range in the system. Therefore, we took the simulated groundwater level at the end of the simulation period as the initial groundwater level of the second run. The initial run was a ‘warm-up’ run for the model to derive the stabilized groundwater in the system. The second run with the stabilized groundwater level as initial value yielded a lower and smoother response to the river level change from the beginning of the simulation period. Therefore, we took the second run as the main simulation case for the following discussion.

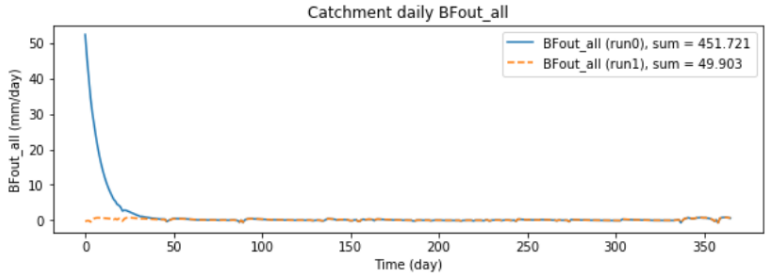


(a)

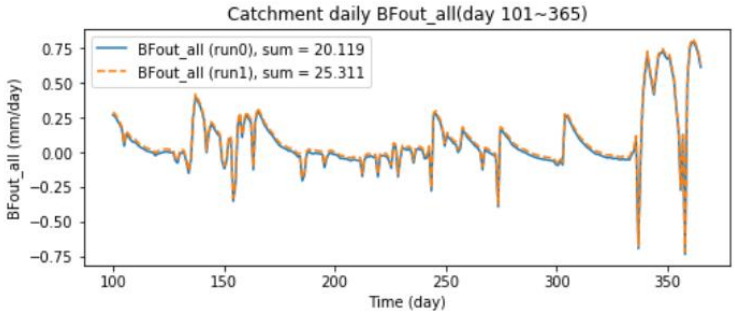


(b)

Figure 5 - 11. Daily total baseflow of the catchment. (a) The complete simulation period. (b) The 101th to 365th day in the simulation period.

### 5.2.2 Model result

The value of the calibrated parameters we applied are listed in Table 5-8.

Table 5 - 8. Parameter list of the main simulation.

| parameter | value | Comments |
|---|---|---|
| dt | 1 | |
| soiltype | 12 | weakly loamy: fine sand |
| croptype | 6 | miscellaneous |
| seep_def | 0 | Constant seepage |
| ERA [%] | 80 | |
| RIL [mm] | 0 | |
| ERA_out [%] | 100 | |
| EPA [%] | 50 | |
| PIL [mm] | 0 | |
| PerIL [mm] | 8 | |
| Infilc_p [mm/day] | 5 | |
| Infilc_per [mm/day] | 35 | |
| LR [%] | 2.5 | |
| IRC [-] | 1.5E-06 | |

| | | |
|---|---|---|
| w [day] | 25 | For blocks with No open water: Eq. 27 |
| down_seep [mm/day] | 1.4 | If GW0 >20 m-SL: 0 mm/day |
| perI [%] | 90 | Non-urbanized area: perI = 5 % |

The values of the parameters are the same in each block except for drainage resistance (*w*), constant seepage (*down_seep*), and percentage of the surface runoff inflow to sewer pipes (*perI*). The criterions are listed in Table 5-8. For blocks without open water, the drainage resistance is estimated by Eq. 27. The constant seepage in blocks having deep interpolated initial groundwater level (*GW0*) are zero. The percentage of surface runoff inflow to sewer pipes is dependent on the imperviousness of the block. In the non-urbanized area, *perI* should be close to zero to represent the absence of sewer system in these blocks. We assume the block belongs to non-urbanized area if the total imperviousness (TIF) of the block is smaller than 0.05%. We can tell from Fig. 5-12 that this criterion recognized 95% of the blocks having houses. Since around 66% of the blocks of Fehraltorf are non-urbanized area, this assumption is important to our case study.

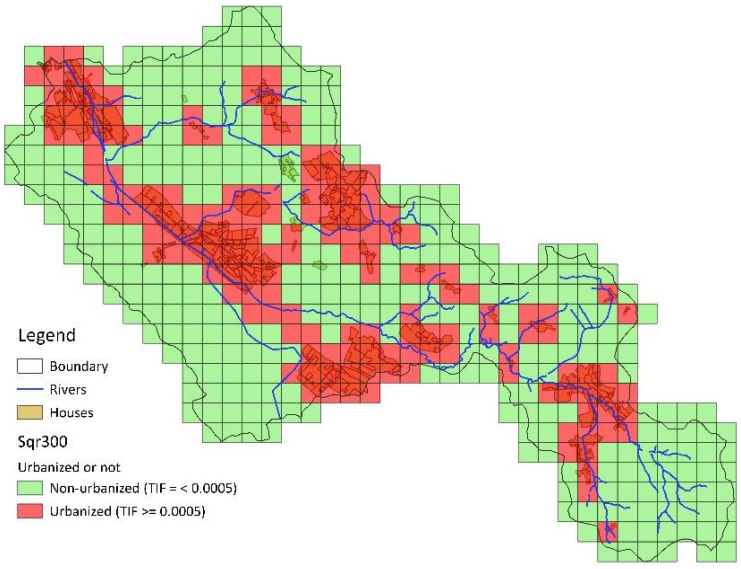


Figure 5 - 12. The urbanized blocks determined by the total impervious fraction (TIF) of the block.

The simulation result of year 2018 with the parameter set is shown in the following paragraphs. Firstly, the terms in the water balance equation of the Fehraltorf catchment are shown in figure 5-13. The amount of import water is little compared with the precipitation. Among the outflows from the catchment, total evapotranspiration takes 49.35%, while Rs only takes 0.02%. This can be the result of the large portion of

pervious area in our study area. The hydrographs of outflows can be checked in Appendix 2.

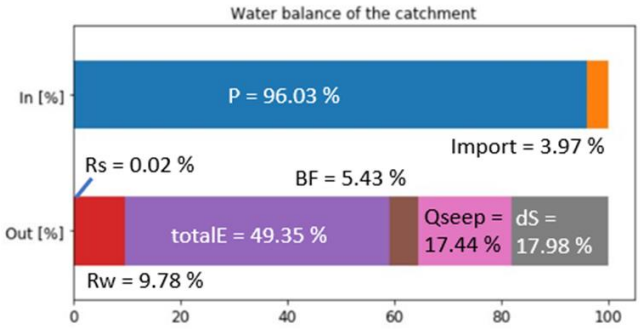


Figure 5 - 13. Percentage of each term of inflow and outflow of the catchment (unit: %).

By comparing the Rs and Rw, we can tell that most of the surface runoff becomes the (wastewater) sewer discharge. This is because we applied the *perI*= 90% in urbanized blocks to represent the combined sewer system. The stormwater runoff (Rs) and wastewater sewer discharge (Rw) are transferred between blocks. In figure 5-14 and 5-15, we represent the flow transferred to downstream blocks with the line connecting to the downstream blocks. The larger the yearly flow is, the wider the line would be.

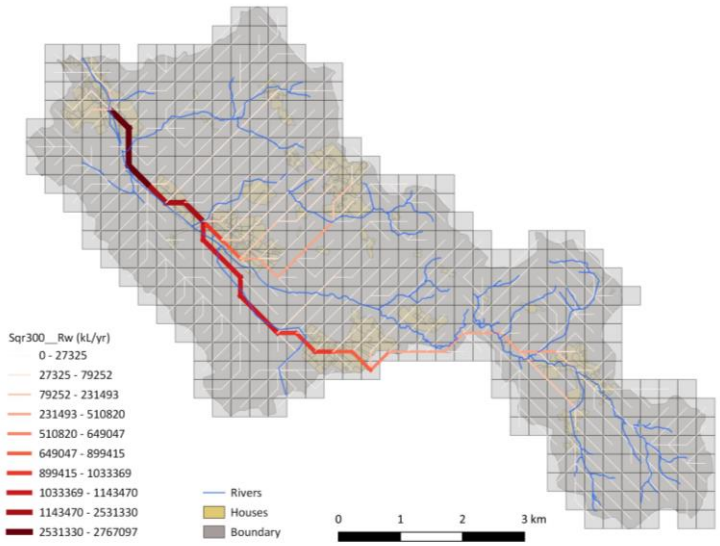


Figure 5 - 14. Yearly sewer discharge (Rw) accumulation from upstream to downstream blocks.

Figure 5-14 demonstrates the yearly sewer discharge (Rw) accumulation from upstream to downstream blocks. The blocks not covering any houses are the non-urbanized areas. The Rw start from these blocks increase slightly. On the other hand, the Rw start from the urbanized blocks begin with a moderate value and keep increase along the flow path. When Rw pass through the urbanized blocks, the values increase obviously.

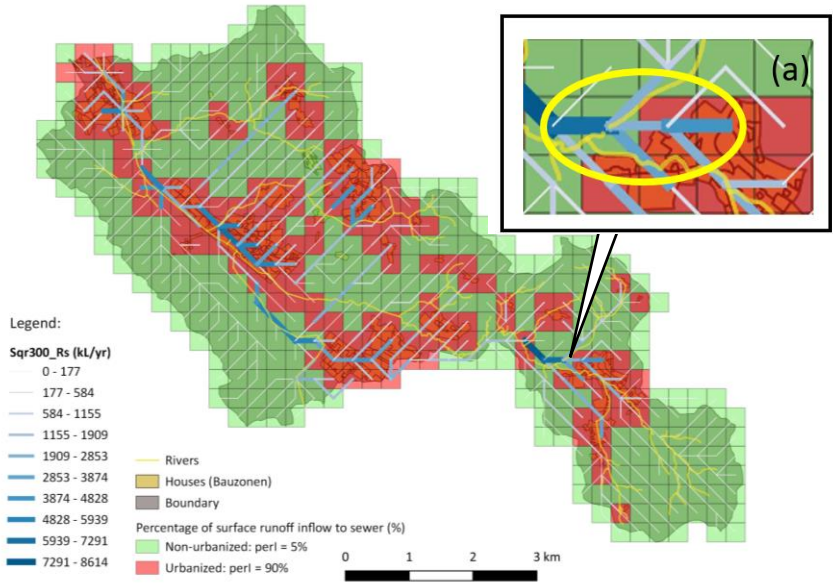


Figure 5 - 15. Yearly stormwater discharge (Rs) accumulation from upstream to downstream blocks.

Figure 5-15 shows the evolution of yearly stormwater discharge (Rs) along the flow path. Unlike the Rw, Rs is not having the accumulating behavior. The downstream blocks can have outflow smaller than inflow Rs. This is the characteristic of the area with combined sewer system. We can derive the condition of the blocks having larger Rs outflow than Rs inflow by Eq. 14 and Eq.17:

$$RUN_{tot} = RUN_{self} + Rs_{up} = \left(IRUN_{rrun} + IRUN_{p} + EXC\right) + Rs_{up} \quad \ldots(14)$$

$$Rs = RUN_{tot} \times (1 - perI) \ldots(17)$$

$Rs - Rs_{up} > 0$:

$$\begin{aligned} Rs - Rs_{up} &= RUN_{tot} \times (1 - perI) - Rs_{up} = \left(RUN_{self} + Rs_{up}\right) \times (1 - perI) - Rs_{up} \\ &= RUN_{self} \times (1 - perI) + Rs_{up} \times (1 - perI) - Rs_{up} \\ &= RUN_{self} \times (1 - perI) + Rs_{up} \times 1 - Rs_{up} \times perI - Rs_{up} \\ &= RUN_{self} \times (1 - perI) + \cancel{Rs_{up} \times 1} - Rs_{up} \times perI - \cancel{Rs_{up}} > 0 \end{aligned}$$

→ Rs outflow is larger than $Rs_{up}$ when $\frac{RUN_{self} \times (1 - perI)}{perI} > Rs_{up}$. …(28)

In our case, the condition is different for the urbanized and non-urbanized blocks.

Table 5 - 9. Conditions of the Rs larger than Rs_up

| | perI | Condition |
|---|---|---|
| Non-urbanized blocks | 5% | $\frac{RUN_{self} \times (1 - perI)}{perI} = \frac{RUN_{self} \times 0.95}{0.05} = 19 \times RUN_{self} > Rs_{up}$ |

| | | |
|---|---|---|
| Urbanized blocks | 90% | $\frac{RUN_{self} \times (1 - perI)}{perI} = \frac{RUN_{self} \times 0.1}{0.9} = \frac{1}{9} \times RUN_{self} > Rs_{up}$ |

Although the condition seems easier for the non-urbanized blocks, the $RUN_{self}$ from these blocks is generally low because of the little portion of impervious area. Therefore, most of the time the outflow from non-urbanized blocks is smaller than inflow from upstream block. When the upstream blocks are all non-urbanized blocks, the outflow is more possible to be larger, transferring the inflow from upstream to downstream and combined with the surface runoff it generates. For the urbanized blocks, the blocks having higher imperviousness would generate higher surface runoff. When the imperviousness of the downstream block is higher than the upstream block, the condition is more possible to be satisfied because of the large surface runoff generated by itself. Figure 5-15 (a) showed the opposite example. The downstream urbanized block is having lower imperviousness than the upstream block. In addition, it receives the inflow from three upstream blocks. Therefore, the Rs inflow from upstream to this block is larger than the Rs it transfers to its downstream block (the thinner lighter blue line).

### 5.2.3 Parameter sensitivity analysis

The parameters we explored for case Fehraltorf are effective area of roof (*ERA*, %), effective area of pavement (*EPA*, %), pervious area initial loss (*PerIL*, mm/day), infiltration capacity of pavement (*Infilc_p*, mm/day), infiltration capacity of pervious area (*Infilc_per*, mm/day), leakage rate (*LR*, %), parallel drainage resistance (*w*, day), constant deep seepage (*down_seep*, mm/day), and percentage of surface runoff inflow to sewer pipes (*perI*, %). By evaluating the boxplots and hydrographs in Appendix 6, we can get the following conclusions:

a. The decrease in *ERA* and *EPA* implies more inflow to the pervious area thus groundwater storage, therefore higher baseflow to river and evapotranspiration can be observed.

b. The decrease in *Infilc_p* and *Infilc_per* result in lower baseflow, and higher surface runoff.

c. Lower leakage rate implies less inflow to groundwater storage, therefore the total evapotranspiration becomes lower. The total imported water includes the amount of leakage, therefore the change of it is to the same direction as leakage rate.

d. When the deep seepage is less, the baseflow increase so the total outflow from groundwater remains the same scale. The same behavior is shown in the higher infiltration from groundwater to sewer discharge, thus higher wastewater sewer discharge.

e. The percentage of inflow from surface runoff to wastewater sewer (*perI*) only make difference to the Rs and Rw. The lower *perI* brings less inflow to Sewer discharge, thus, lower Rw.

Overall, as shown in the boxplots (Fig. 5-16), baseflow is the most sensitive outflows among the model results. the change in E*RA, Infilc_per, w* and constant daily deep seepage (*down_seep*) will results in higher change of baseflow. Stormwater runoff is also sensitive to the change in *ERA* in terms of the decrease in 75$^{th}$ percentile. Rw_out is more sensitive to parameters regarding surface runoff, *ERA* and *EPA,* as in the urbanized blocks 90% (*perI)* of the surface runoff enters to the wastewater sewer. Total evapotranspiration is sensitive to *Infilc_per* and *down_seep* as they determine the amount of infiltration and available capillary rise to unsaturated zone where transpiration happens. The boxplots of imported water and deep seepage are not shown since they are sensitive to the change of leakage rate and constant deep seepage respectively.

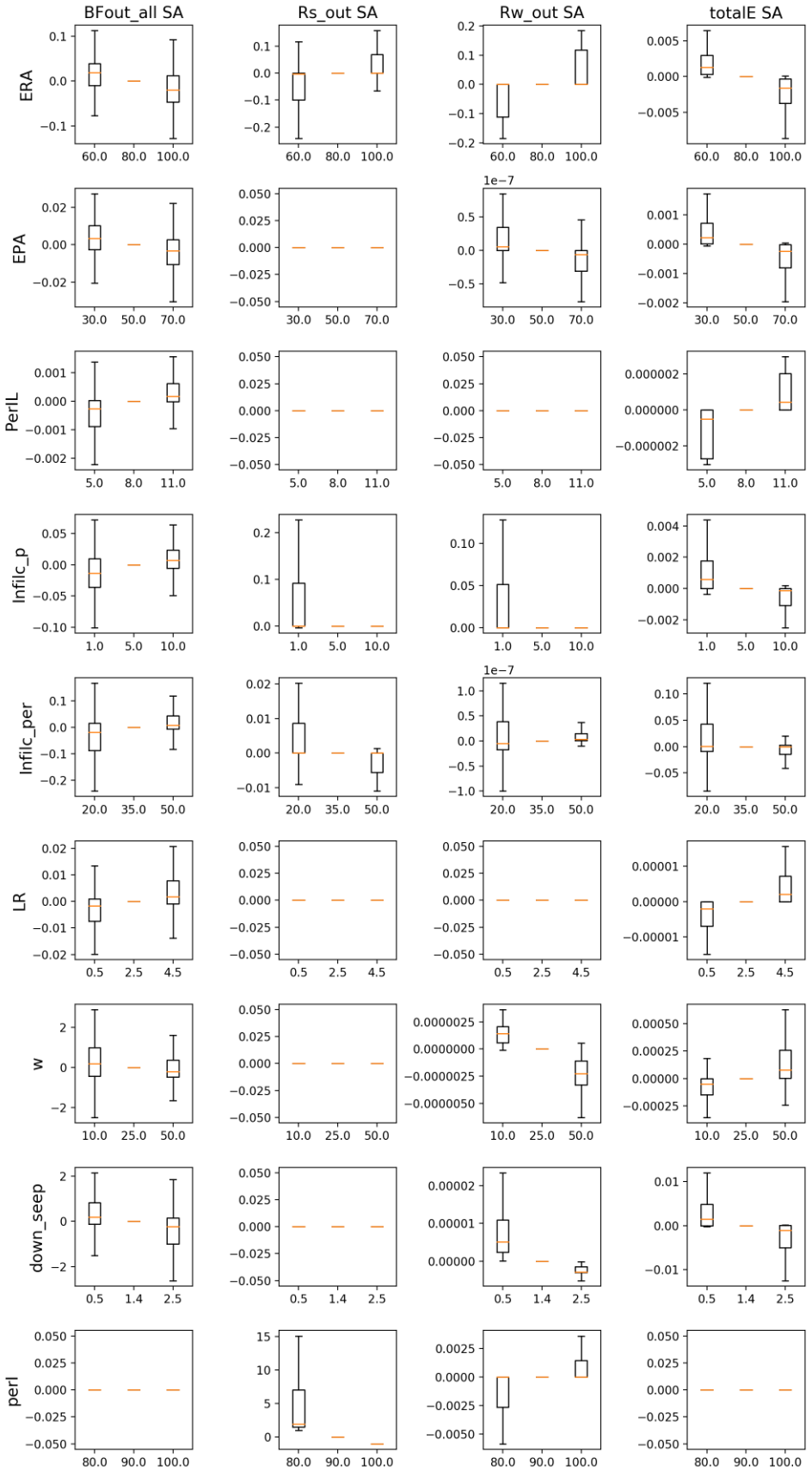


Figure 5 - 16. Boxplots of the standardized difference of the outflows compared to main simulation of Case Fehraltorf.

## 6. Investigating the effect of spatial representation

DUWCM has been developed to be able to work with square and hexagonal grids. When developing the model, different calculation must be considered regarding the interaction to neighbors, distance, and area. To be specific, three parts in the modules been adapted for hexagonal grids.

Firstly, the derivation of upstream blocks from the information of downstream block ID. The number of neighboring blocks is different for squares and hexagons. Therefore, special care is taken for the two kinds of spatial representation. Secondly, the estimation of drainage resistance ($w$) of the blocks that do not have the river surface land use type (Eq. 27). When estimating the w by the distance to its downstream block having open water, the distance along the path is applied instead of directly derive from the coordination. A square has two possible distance to its neighbor, while hexagons have identical distance to its neighbors (see table 4-7). Finally, the area of each block is derived by different equation for squares (Eq. 29) and hexagons (Eq. 30).

$$Area_{squares} = L^2 \quad \ldots(29)$$

$$Area_{hexagons} = \frac{3}{2} \times \sqrt{3} \times L^2 \quad \ldots(30)$$

With these adjustment of calculation for hexagons in DUWCM, hexagonal grids can be applied as input to DUWCM. The effect of the different spatial representation is explored in the following section.

### 6.1 Catchment water balance

To investigate the effect of different spatial representation, we simulated the water balance in Fehraltorf catchment with 300×300 m square blocks and hexagon blocks with edge length of 200 m respectively. The spatial data as input to DUWCM is provided by UrbanBEATS. The impervious areas in the two spatial representation have been calibrated as best as possible, yielding NSE = 0.75 for both 300m square and 200m hexagon girds.

Table 6 - 1. Summary of the two input maps

| | No. of blocks | Area per block [m2] | Water demand (ML/yr) | IWU (ML/yr) | IR (ML/yr) | Population | Residential population | AR [ha] | AP [ha] | APer [ha] | Atotal [ha] | average TIF (%) |
|---|---|---|---|---|---|---|---|---|---|---|---|---|
| Sqr_300 | 466 | 90000 | 1263 | 1179 | 84 | 20406 | 18851 | 223 | 120 | 3210 | 3553 | 8.81 |
| Hex_200 | 401 | 103923 | 1278 | 1193 | 85 | 20308 | 19003 | 240 | 102 | 3217 | 3558 | 8.73 |

* IWU: indoor water use, AR: Area of roof, AP: Area of pavement, APer: Area of pervious area, TIF: total impervious fraction

We can tell from Table 6-1 that the spatial information delineated with hexagon maps is slightly different from which with square maps. It is worth noted that although the total population of square blocks is higher than hexagonal blocks, the indoor water use is the contrast. Because the population includes not only the residential population but also the population in the commercial areas. Since we don't have the exact statistic data of the water demand of irrigation and the demand from industry and offices, we made the assumption of the irrigation to be 1000 $m^3$/ha/yr on the irrigated area. The water demand from industry and offices are not considered in our simulation. Therefore, the indoor water use (IWU) is estimated as the product of residential population and the personal daily water use (162.7 L/person/day).

The water balance of the urban water cycle simulation result with square grids and hexagonal grids are listed in Figure 6-1 and Table 6-2. Except for the baseflow, the other fluxes of hexagonal grids are higher than square grids because of the higher inflow it received.

Figure 6 - 1. The amount and proportion of each terms in inflow and outflow respectively.

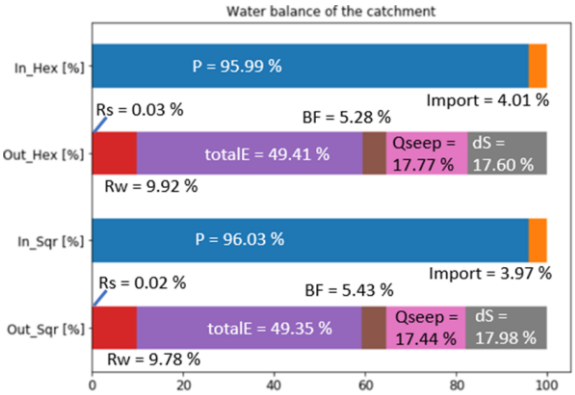


Table 6 - 2. Values of the water balance terms of square and hexagon grids. (unit: m3/ yr)

| (m3/yr) | In_Sqr | Out_Sqr | In_Hex | Out_Hex |
|---|---|---|---|---|
| P | 31352.97 | 0.00 | 31400.93 | 0.00 |
| Import | 1295.86 | 0.00 | 1310.96 | 0.00 |
| Rs | 0.00 | 7.51 | 0.00 | 10.29 |
| Rw | 0.00 | 3192.58 | 0.00 | 3243.53 |
| totalE | 0.00 | 16111.11 | 0.00 | 16162.68 |
| BF | 0.00 | 1773.03 | 0.00 | 1725.66 |
| Qseep | 0.00 | 5694.48 | 0.00 | 5811.88 |
| dS | 0.00 | 5870.12 | 0.00 | 5757.85 |

The spatial distribution of the annual simulation result will be shown for the comparison of spatial effect. The classification of the values of each flux is the same for hexagon and square maps. Since the values are in the volume unit, the values at the boundary blocks will be generally lower as only parts of the area in the block participated in the simulation.

Firstly, the maps of imported water demand (Fig. 6-2) capture the urbanized areas well. If we take a closer look at the group of blocks that covering the urban areas, hexagonal blocks are usually able to cover the area with less number of blocks. In addition, less redundant area is left in the blocks applied for sampling the urban areas. The two maps didn't show the same location of highest water demand because a small move of the sampling area can result in large difference in the land use ratios and sampled population.

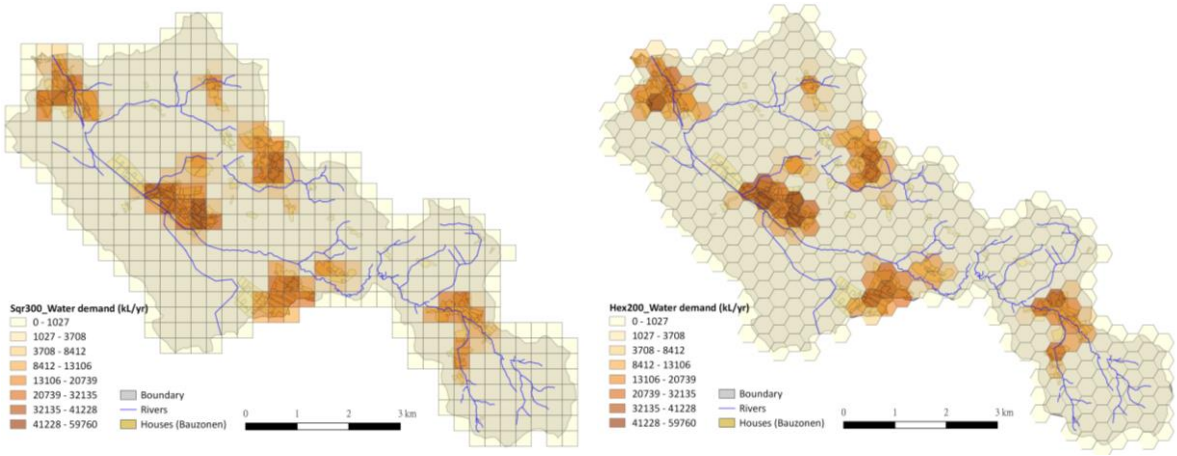


Figure 6 - 2. Yearly imported water demand (kL/yr)

The stormwater runoff (Rs) and wastewater sewer discharge (Rw) transferred among the blocks are represented with the line connecting the block to its downstream blocks. We can observe the different flow paths result from the shape of blocks. Inconsistency in flow path can leads to a diversity in the contributing area of the same location in the two maps. An exploration of this effect will be carried out in section 6-3. As mentioned in Chapter 5-2, the Rs didn't show a continuous accumulation behavior, while Rw did. When planning stormwater harvesting devices, one may consider installing the device at the location where the yearly flow is the highest. Therefore, different conclusion can be derived by using the square and hexagonal map. In Figure 6-4, the main route of the sewer discharge is showing similar trend in the amount from upstream to downstream. However, the values in the tributaries may have obvious discrepancy because of the different contributing area.

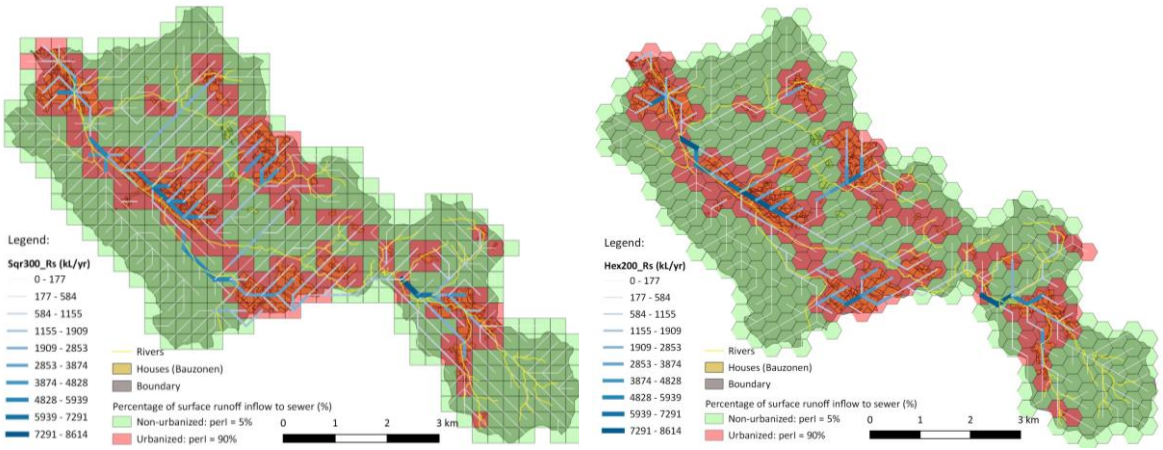


Figure 6 - 3. Yearly stormwater runoff (Rs) (kL/yr). Left: Squared grids, right: hexagonal grids.

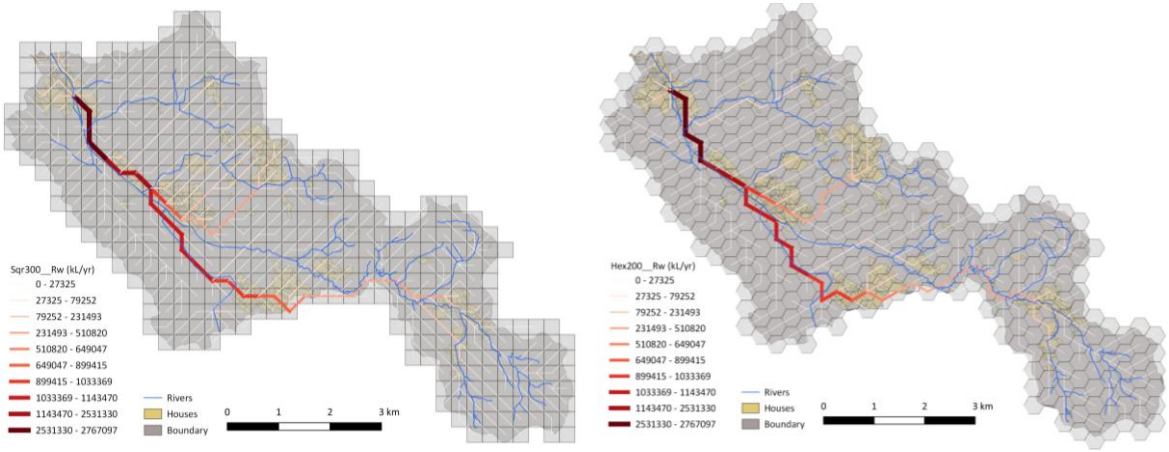


Figure 6 - 4. Yearly wastewater sewer discharge (Rw) (kL/yr). Left: Squared grids, right: hexagonal grids.

The estimation of evapotranspiration, baseflow and deep seepage are simulated as best as possible with the assumption we have made. We will compare the spatial effect of the two grid shapes on the simulation result. The square and hexagon representation both result in lower evapotranspiration in the urban areas than the blocks not covering urban areas (Fig. 6-5). The higher evapotranspiration along the downstream of the river is because of the groundwater level is closer to the surface, meaning more water is available for the plants. Figure 6-6 demonstrate the yearly baseflow from the blocks. The amount of baseflow generally declines with the distance to the river in both maps. However, because of the different flow path, the exact locations generating higher baseflow can differ a lot. The yearly deep seepage shown in Figure 6-7 shows our assumption of the constant seepage. The lower values at the boundary are because of smaller participating area.

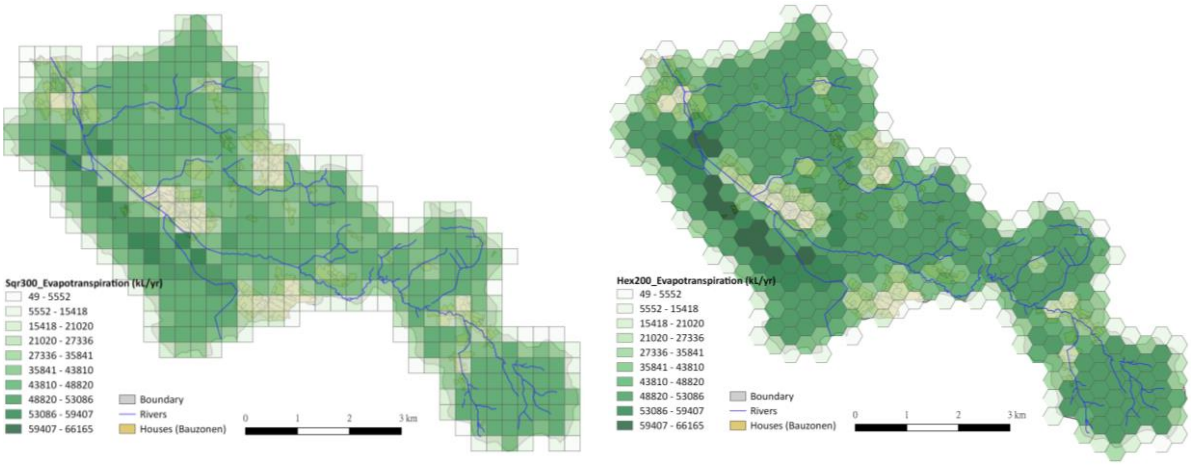


Figure 6 - 5. Yearly evapotranspiration (totalE) (kL/yr).

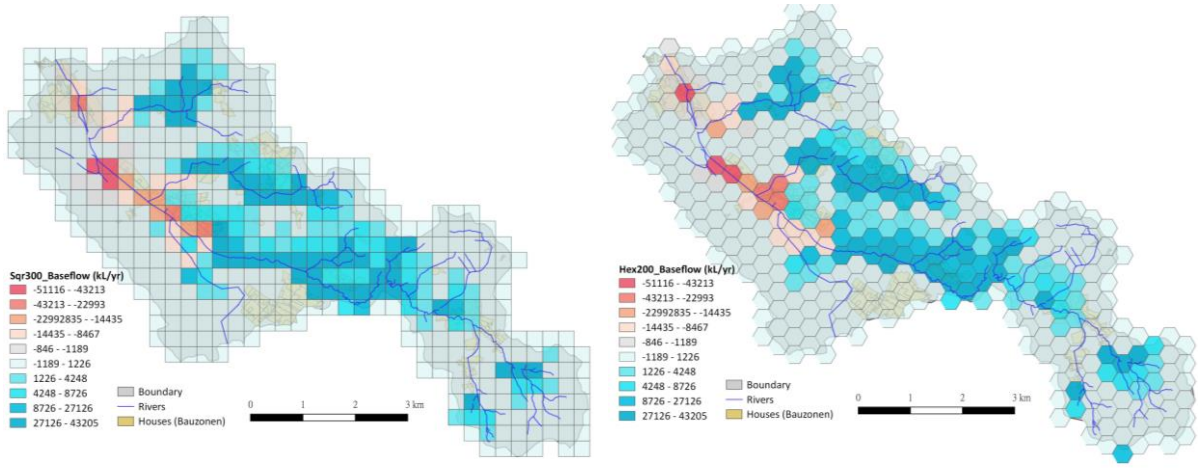


Figure 6 - 6. Yearly baseflow (BF) (kL/yr). (Positive values in blue represent the baseflow from groundwater storage to the river; negative values in red represent the feeding from river to groundwater storage.

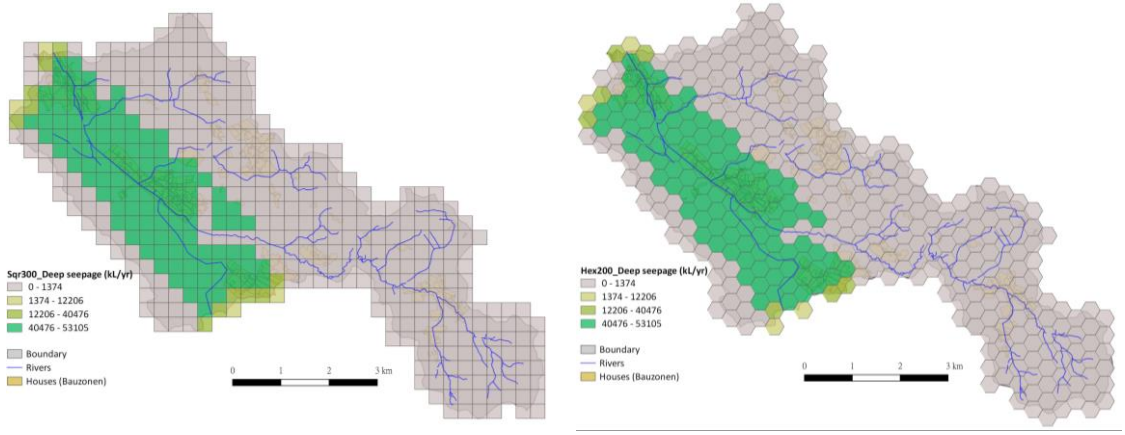


Figure 6 - 7. Yearly deep seepage (Qseep) (kL/yr).

## 6.2 Four sample blocks along the flow path

To explore the water transfer in the catchment, we chose four blocks located from the upstream to the downstream of the main riverway on the two maps respectively (Fig.

6-8). Noted that the blocks we chose in the two maps are not absolutely center at the same location in the two maps, therefore the area of each land use type might be different. The important parameters are listed in Table 6-3.

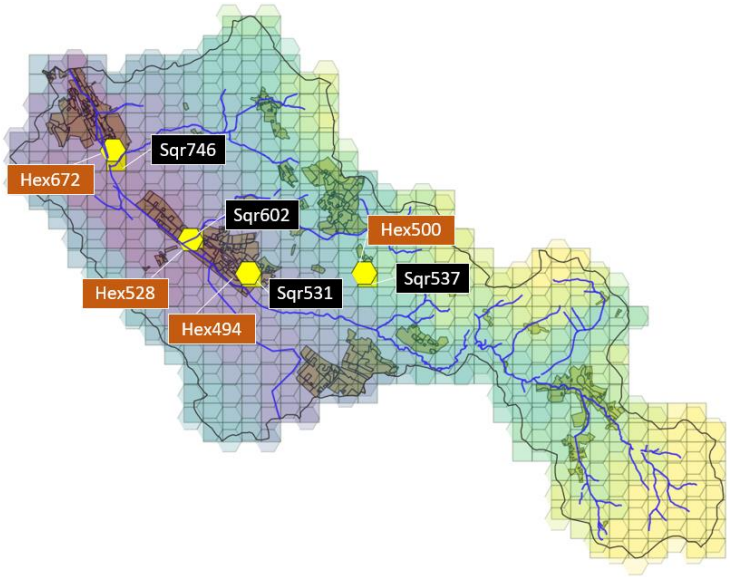


Figure 6 - 8. Sampled blocks from upstream to downstream.

Table 6 - 3. Important parameters of the sampled blocks.

| | unit | Sqr537 | Hex500 | Sqr531 | Hex494 | Sqr602 | Hex528 | Sqr746 | Hex672 |
|---|---|---|---|---|---|---|---|---|---|
| **AR** | [m2] | 6306.67 | 11602.16 | 65419.20 | 77507.64 | 56017.87 | 69701.37 | 0.00 | 9694.68 |
| **AP** | [m2] | 2098.66 | 3684.88 | 14635.85 | 18221.95 | 17109.14 | 17777.04 | 0.00 | 11135.69 |
| **APer** | [m2] | 81594.67 | 88636.01 | 9944.95 | 8193.45 | 16872.99 | 16444.64 | 90000.00 | 83092.68 |
| **TIF** | [%] | 9.34 | 14.71 | 88.95 | 92.12 | 81.25 | 84.18 | 0.00 | 20.04 |
| **AGW** | [m2] | 90000.00 | 103923.05 | 90000.00 | 103923.05 | 90000.00 | 103923.05 | 90000.00 | 103923.05 |
| **Population** | [-] | 31.00 | 48.00 | 708.00 | 806.00 | 538.00 | 602.00 | 0.00 | 24.00 |
| **IWU** | [kL/yr] | 0.00 | 0.00 | 45426.78 | 51669.37 | 34478.26 | 38607.96 | 0.00 | 1612.83 |
| **Blk_WDIrr** | [kL/yr] | 0.00 | 0.00 | 714.49 | 804.71 | 563.45 | 615.63 | 0.00 | 1037.92 |
| **w** | [day] | 549632.03 | 450000.00 | 25.00 | 200000.00 | 25.00 | 25.00 | 218566.02 | 200000.00 |
| **perI** | [%] | 90.00 | 90.00 | 90.00 | 90.00 | 90.00 | 90.00 | 5.00 | 90.00 |
| **GW0** | [m-SL] | 90.09 | 86.85 | 16.68 | 4.61 | 6.40 | 5.86 | 6.83 | 5.83 |
| **Elev** | [m a.s.l.] | 623.08 | 620.59 | 535.44 | 535.27 | 525.17 | 524.63 | 512.78 | 511.63 |

As stated in section 5.2.2, the wastewater sewer discharge is expected to accumulate the flux from upstream to downstream. On the other hand, because of the percentage of inflow is high in urbanized area, a big part of surface runoff becomes the inflow to sewer discharge. Therefore, the outflow stormwater runoff from a block is not necessarily larger than the inflow stormwater runoff it receives. Figure 6-9 demonstrates the wastewater sewer discharge of the chosen blocks in square and hexagon grids during a lower flow period. The outflow from the blocks is always larger

than the inflow from upstream in both square and hexagon grids. In addition, the more downstream the blocks located, the larger outflow it generates.

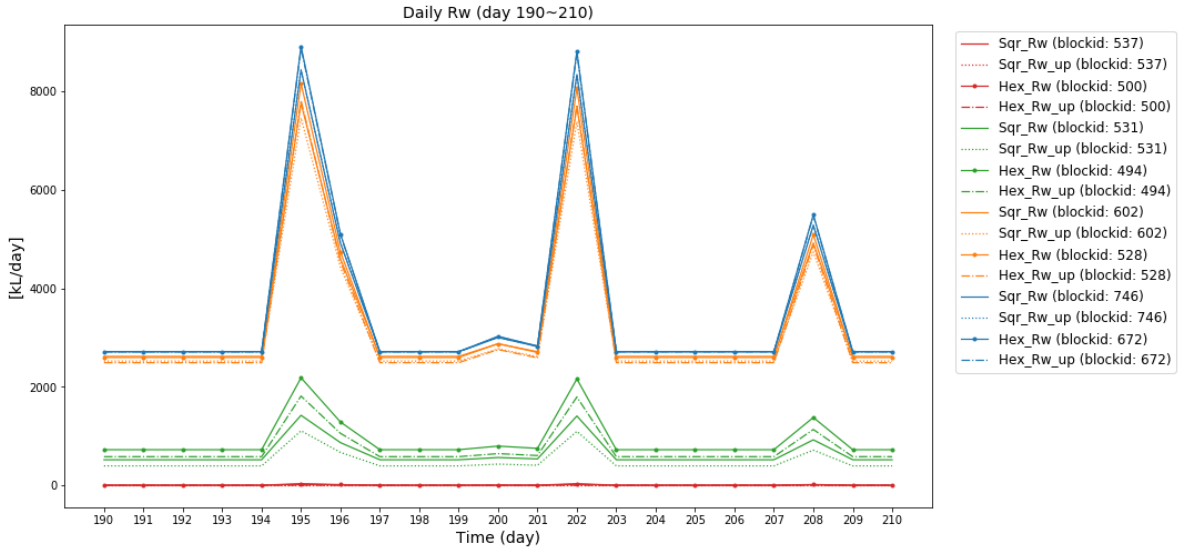


Figure 6 - 9. Wastewater sewer discharge inflow from upstream (Rw_up) and outflow (Rw)

On the other hand, the stormwater runoff from upstream (Rs_up) and the amount leaving the block are not regularly increasing. The amount of Rs depends on the parameter "*perI*" (percentage of surface runoff inflow to wastewater sewer) and "*TIF*" (total impervious fraction). The *perI* determines the ratio of surface runoff, which include the Rs inflow from upstream, becoming Rw. The TIF determines the amount of local surface runoff. The higher TIF (higher urbanized blocks) of the block, the more precipitation becomes surface runoff. Figure 6-10 demonstrates that the second blocks from upstream (block 531 in square map, block 494 in hexagon map) have higher outflow Rs than inflow Rs (Rs_up) even though the perI are 90% (Table 6-3). The high TIF allow them to generate a lot more surface runoff than the inflow. The first blocks (block 537 in square map, block 500 in hexagon map) are the starting point of the tributary, therefore the Rs from upstream is zero. The third blocks (block 537 in square map, block 500 in hexagon map) have lower outflow Rs than inflow Rs (Rs_up) even though the TIF seems high. This can be verified by the conditions listed in table 5-9. The most downstream blocks (block 746 in square map, block 672 in hexagon map) have the combination of low TIF and high perI. Therefore, the decrease in Rs outflow from the inflow is shown as expected.

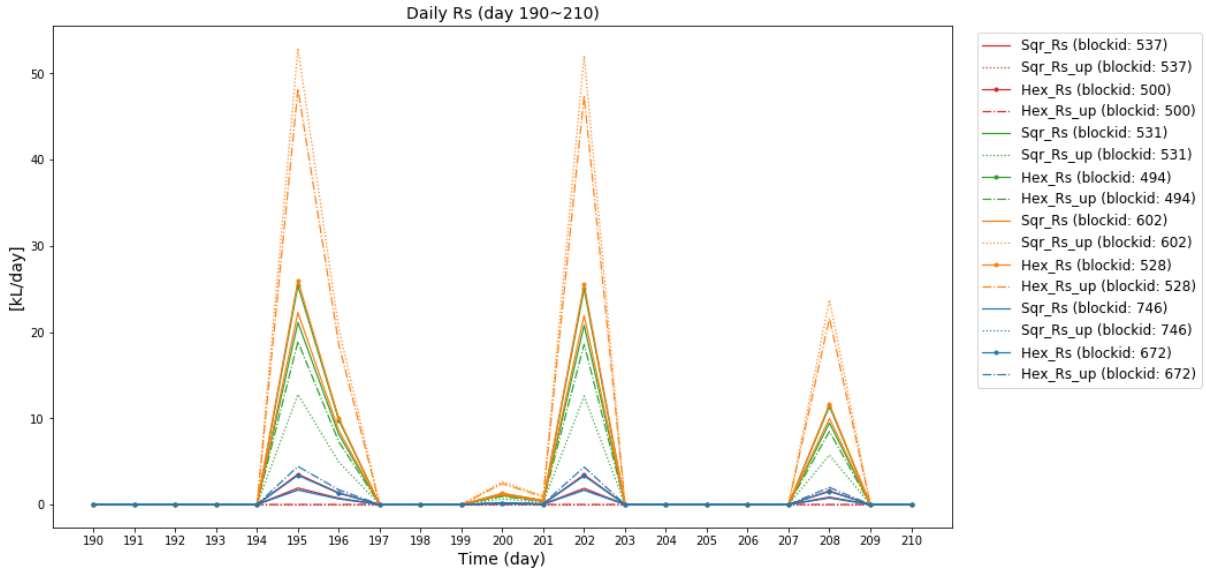


Figure 6 - 10. Stormwater runoff inflow from upstream (Rs_up) and outflow (Rs)

## 6.3 Groups of blocks covering approximate the same area

To compare the simulation result in an urbanized sub-catchment in Fehraltorf, we chose a group of blocks covering approximately the same area (Fig. 6-11). The spatial information of the combination of the blocks are listed in Table 6-4. Noted that it is difficult for the squares and hexagons to cover the exact same area. Also, a 10 meters offset may result in an obvious discrepancy in the population and land use spatial delineation result. This comparison is shown in order to give an idea about any potential difference results from different spatial representation when modeling a smaller region.

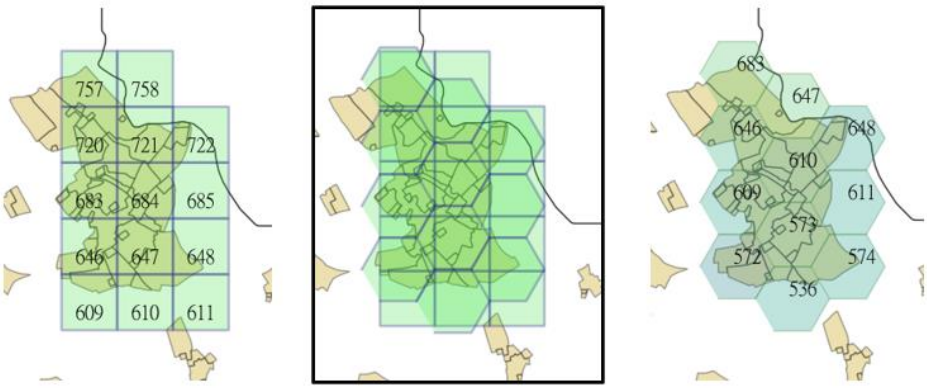


Figure 6 - 11. The group of blocks covering approximately the same area (region of interest)

Table 6 - 4. The information of the region of interest.

| | AR [ha] | AP [ha] | APer [ha] | A_total [ha] | Population [-] | IWU [kL/yr] | Blk_WDIrr [kL/yr] | TIF [-] |
|---|---|---|---|---|---|---|---|---|
| **Sqr** | 27.918 | 13.164 | 67.698 | 108.780 | 2428.0 | 153381.82 | 10386.50 | 0.377660 |
| **Hex** | 31.088 | 10.968 | 63.392 | 105.448 | 2540.0 | 160394.33 | 10911.36 | 0.398829 |

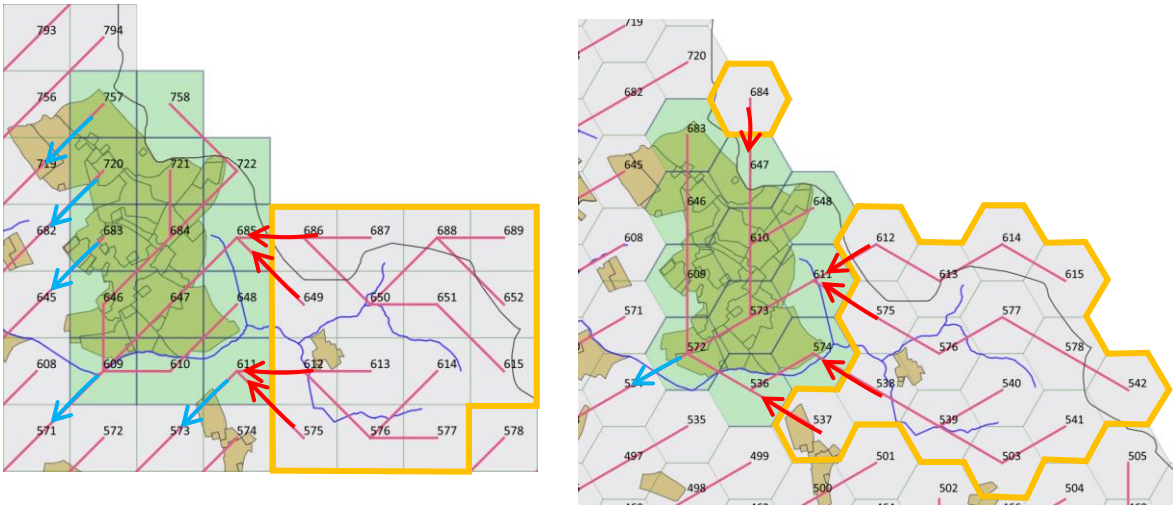

Figure 6 - 12. The water transfer across the boundary of region of interest. (Pink lines: flow path, red arrows: inflow, blue arrows: outflow, orange area: contributing area of the upstream inflow.)

The group of blocks is considered to be our region of interest for the water balance comparison. The inflow in the water balance equation of the region of interest includes not only the precipitation and imported water of the blocks, but also the stormwater runoff (Rs) and wastewater sewer discharge (Rw) from upstream blocks. Figure 6-12 demonstrated the outlet blocks and the contributing area of the upstream inflow. The outflow from the sampled area are the evapotranspiration, baseflow, deep seepage and the Rs and Rw from the outlet blocks (Figure 6-13).

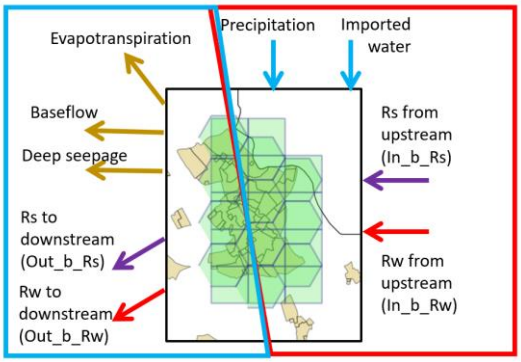


Figure 6 - 13. Water balance flux of the region of interest.

Figure 6-14 is the hydrograph of total inflow to the region of interest (ROI) and the difference between the result from hexagon and square grid map. We can tell from it that when there is rainfall event, total inflow to the ROI is larger in square map. This is

the result of the slightly larger total area in the square map, which allows it to receive 3% more precipitation input. When the precipitation is lower than a certain amount, the inflow of hexagonal map is higher because of the higher inflow from upstream (both Rs and Rw, Fig. 6-15 and Fig. 6-16). We can get the hint from upstream stormwater runoff that the contributing area of hexagon map is larger than square map because the stormwater runoff of hexagon map is larger than which of square map when there is rainfall. On the other hand, the wastewater sewer discharge of hexagon map is constantly larger than square map, because the demand of imported water in the contributing area of hexagonal map is larger than which of square map.

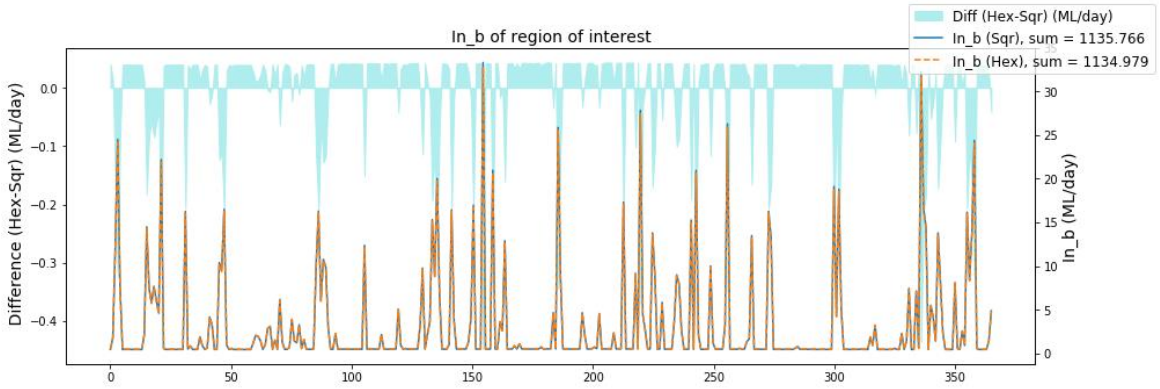


Figure 6 - 14. Total inflow to the region of interest.

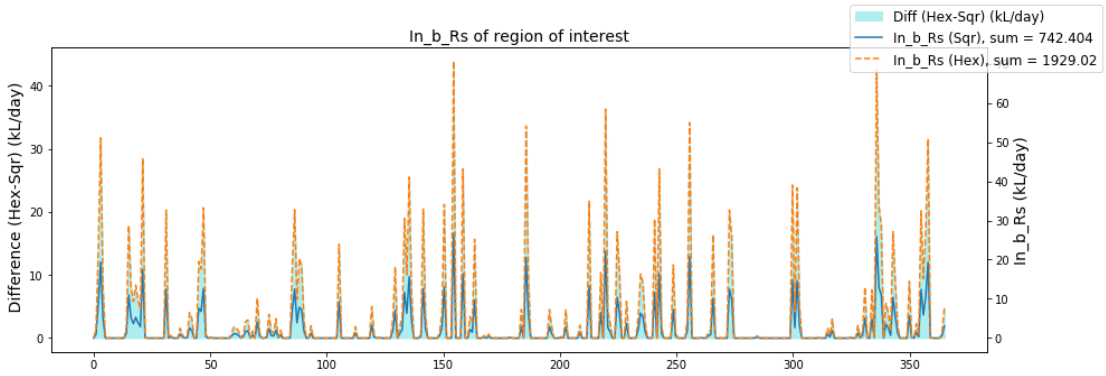


Figure 6 - 15. Inflow stormwater runoff from upstream to the region of interest.

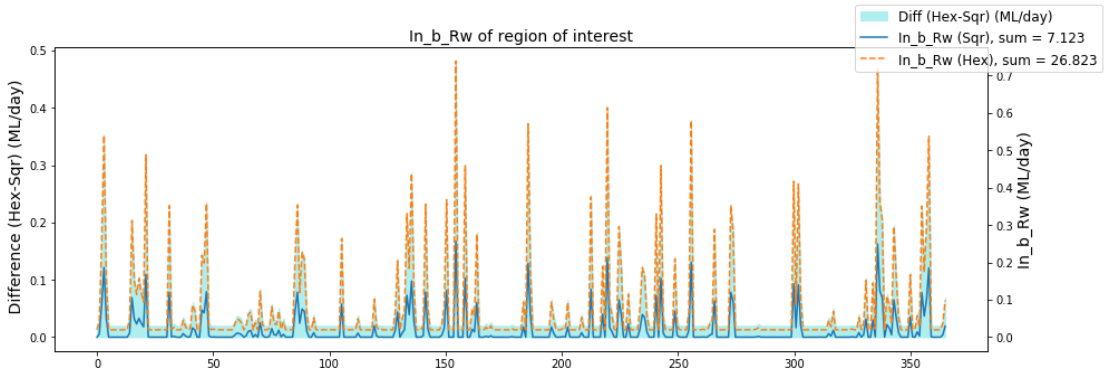


Figure 6 - 16. Inflow wastewater sewer discharge from upstream to the region of interest.

The total outflow from the region of interest shows an opposite behavior to the total inflow. The outflow of hexagonal map is larger than which of square map in the rainy days (Fig. 6-17). Although the higher stormwater runoff during rainfall days in Square maps in Figure 6-18 support our opinion of larger precipitation input to the area, the scale of wastewater sewer discharge (Fig. 6-19) is larger than the stormwater runoff. In addition, the other outflow components, such as baseflow (Fig. 6-20) and evapotranspiration (Fig. 6-21), of the square maps are larger than which of hexagonal map. Therefore, the total outflow of square map is larger than hexagon map. Only when during heavy rainfall events, the amount of wastewater from hexagon map becomes larger than square map.

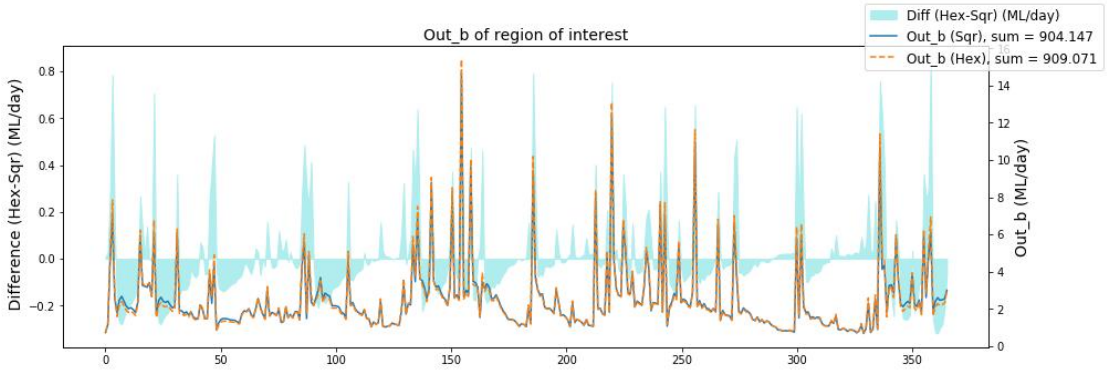


Figure 6 - 17. Total outflow from the region of interest.

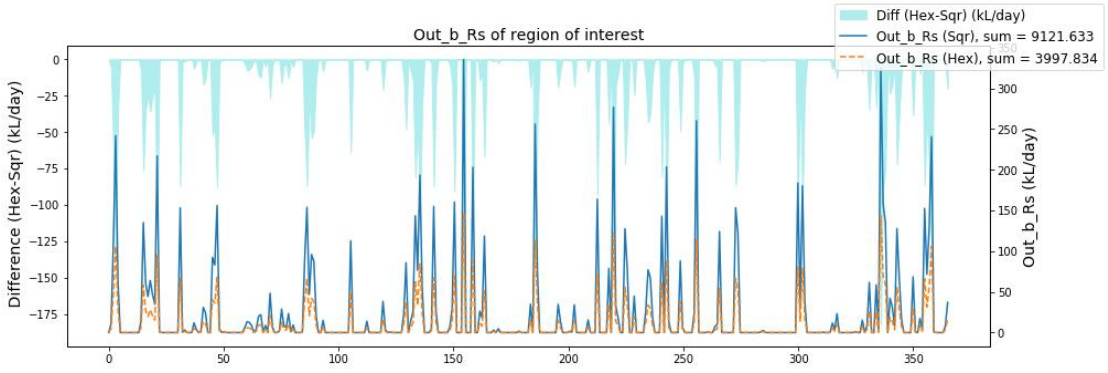


Figure 6 - 18. Outflow stormwater runoff from the region of interest.

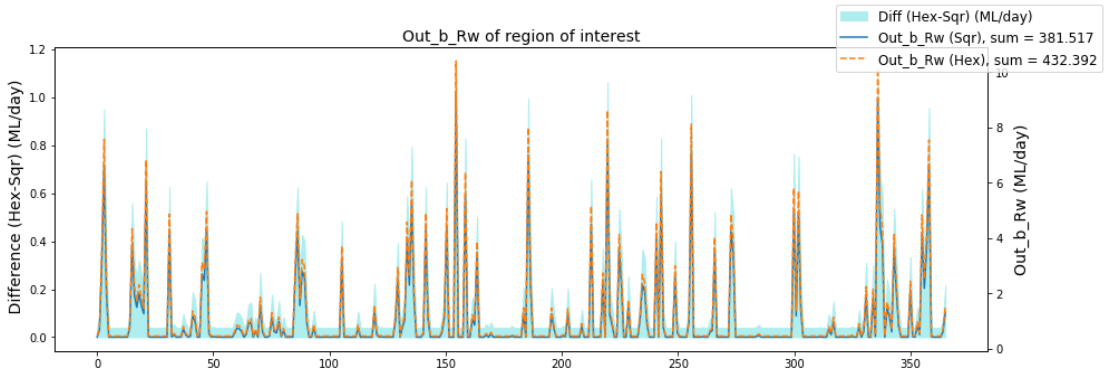


Figure 6 - 19. Outflow wastewater sewer discharge from the region of interest to downstream area.

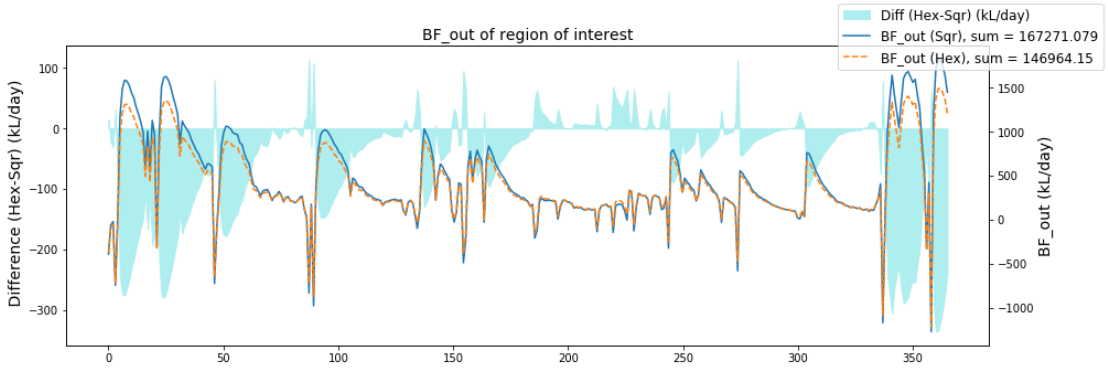


Figure 6 - 20. Outflow baseflow from the region of interest.

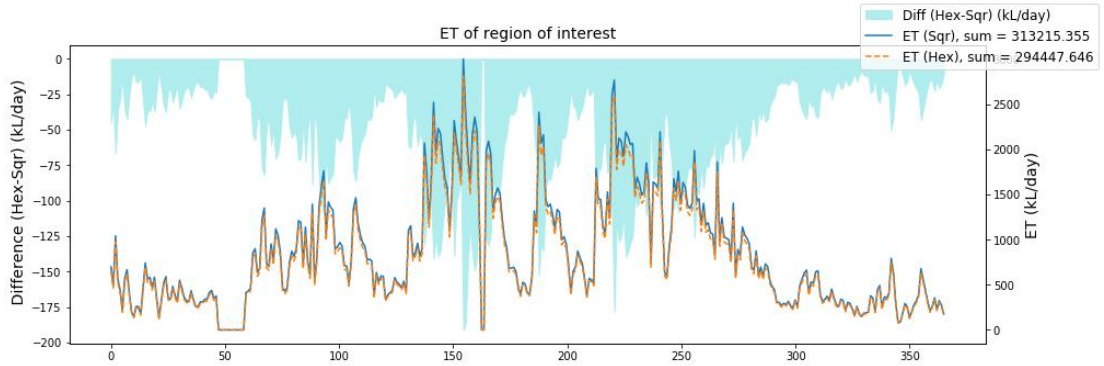


Figure 6 - 21. Outflow evapotranspiration from the region of interest.

The comparison of the model result of the region of interest with square and hexagon map demonstrates the effect of different spatial representation on total urban water cycle. The inflow from upstream to a region of interest differs in a certain amount because of the mismatched contributing area according to the flow path. The outflow is different because of the value of the parameters of the same location can be different when using the two grids. Overall, the components in the water balance cycle have the similar trend between hexagon and square map. We can determine which spatial representation provides better model performance with the same urban water cycle model (DUWCM) when the real observation data is available.

## 7. Discussion

DUWCM applies water balance approach to simulate the evolution of components in total urban water cycle with less calculation effort compared to hydrodynamic models. The application of 1-day time step in our model is acceptable for research of water resource, while this temporal resolution is too low for research about urban flooding. Applying daily time step in DUWCM, a model developed for sustainable water resource management, excludes the unnecessary complexity in the modeling process. The water transfer between blocks can be defined in a simple but reasonable assumption, that the process happens in one day from the upstream to downstream blocks.

As an improvement from Aquacycle (Mitchell et al., 2001), the combination of subsurface algorithms in DUWCM brings physical meaning to the simulation of evapotranspiration. Compared to Urbanwb model (Vergroesen & Brolsma, 2020), DUWCM integrates the flow interaction between urban hydrological process with the water supply-wastewater system, including the infiltration from groundwater to wastewater sewers and leakage from pressurized water supply mains. Moreover, the spatial explicit manner in DUWCM considers the local characteristics within the model domain, preserves the flow direction information, and allows locating the spatial-temporal peak of the outflows. Most integrated urban water cycle models use Urban Hydrological Element (UHE) as modeling unit to consider the different surface characteristics. Although UHE preserves the spatial information for the hydrological modeling compared to lumped model, the flow interaction between upstream and downstream is less reliable as the UHE can be composed of areas that are not spatially connected.

Previous research (Beven, 1993; Perrin et al., 2001) pointed out the challenge of determining parameters in spatially distributed models. Taking the concept of the method proposed by Tran et al. (2018), we first applied the same parameter sets for the blocks, and then adjust some values according to the various condition in the blocks. For example, the percentage of surface runoff inflow to sewer discharge should be close to zero for blocks having more than 99.95% pervious area. The adjustment of parameters according to local characteristics reflects the benefit of spatially detailed model to generate reliable simulation results for a certain location in the model domain.

The spatial detailed model results derived from DUWCM provide valuable information of the hot spot of annual outflows in the catchment. The peak flows in terms of space and time can be recognized when digging into the simulation result. From the two case

studies in this thesis, DUWCM is proven to be scalable – simulating an area in 2 blocks to over 400 blocks. Moreover, the adaptability of the model to UrbanBEATS allows the model to run areas anywhere between a few square kilometers to several thousands of square kilometers as how UrbanBEATS is capable of. This flexibility of model scale allows a wide range of application.

According to the model verification in section 5.1.2 and 5.1.3, the model result from DUWCM is in line with the hydrological process we are familiar with in a lumped model. The parameter sensitivity analysis provides deeper insight into the effect of changes in components on each other. Although observation data is absent for calibration in this research, we have been able to provide a general idea about the influence of the parameters to the simulation outputs from the parameter sensitivity analysis (section 5.1.4, 5.1.5 and 5.2.3). The infiltration capacity of paved area and pervious area are both important to the modelled stormwater runoff and wastewater sewer discharge. In addition, model results are sensitive to the head of deep groundwater when the deep seepage is estimated by the head difference between groundwater and deep groundwater. These analyses will support the parameter calibration when we have the observation data to work on.

The comparison of the model results using squared and hexagonal grids in chapter 6 demonstrated that the different spatial representation of the surface can generate different values and locations of peak flows. The advantage of hexagon grid is shown in the calculation efficiency. In this study, less number of blocks is needed to cover the entire catchment. In addition, less direction is applied for any calculation about flow path and neighbors. Finally, the execution time is shown in table 7-1.

Table 7 - 1. The calculation time of squared and hexagonal grids.

| | Length of side | Number of blocks | Area per block | Calculation time (+WB check) |
|---|---|---|---|---|
| Square | 300 m | 466 | 90000 $m^2$ | 144(+152) s |
| Hexagon | 200 m | 401 | 103923 $m^2$ | 127(+133) s |

It is proved in the research from de Sousa et al. (2006), hexagons perform better than squares to preserve the flow direction from higher resolution elevation data (Table. 7-2). Therefore, the model result of hexagon grids from our model can be expected to be superior to these of square grids, as the simulation is highly dependent on the flow path. However, observation data for calibration is required to support the point of view. In this thesis, parameters are determined by the background information of the study area because of the lack of observed data for calibration. The same parameter set is applied

in simulations using squared and hexagonal grids. A future work regarding the comparison of model performance in hexagon and square maps with different calibrated parameter sets is worth developing.

Table 7 - 2. Mean angular difference from the test grids to the resulting grids and the number of errors. Test grids refers to the original digital elevation map (DEM) data. (Source: de Sousa et al., 2006)

| Resolution (fraction of original) | Mean Angular difference (rad) | | Number of errors | |
|---|---|---|---|---|
| | Squares | Hexagons | Squares | Hexagons |
| 0.30 | 0.669 | 0.499 | 528047 | 462989 |
| 0.27 | 0.689 | 0.515 | 427355 | 374451 |
| 0.24 | 0.708 | 0.533 | 337665 | 296016 |
| 0.21 | 0.730 | 0.551 | 258183 | 225853 |
| 0.18 | 0.753 | 0.573 | 189320 | 165528 |
| 0.15 | 0.779 | 0.595 | 131376 | 114990 |
| 0.12 | 0.808 | 0.629 | 83791 | 73077 |
| 0.09 | 0.839 | 0.667 | 46897 | 41148 |
| 0.06 | 1.623 | 0.713 | 4726 | 18172 |

Although hexagonal grid is expected to perform well in total urban water cycle modeling, the weakness of it should be kept in mind. The composition and decomposition of hexagons is a challenge since it is not able to cover entirely the same area (Fig. 2-3). If the application of the total urban water cycle model requires changing the grid size, hexagonal grid is less suitable than traditional squared grid. And although UrbanBEATS is able to generate maps with different hexagonal grid size, the comparison between different resolution will become more complicated and less convincing.

The limitation in this research includes the geohydrology of the model domain and the lack of observation data. In Fehraltorf catchment, a great portion of area has no groundwater layer. In addition, the elevation in the catchment ranges more than 200 meters. Since the Urbanwb model is initially designed for low land areas such as the Netherlands, the simulation of subsurface fluxes and evapotranspiration is less reliable when implementing this model in hillslope areas without unconfined groundwater. Therefore, we made some assumptions when determining the parameters in such blocks to represent the catchment as good as possible. Ones should however be aware of the uncertainty in the simulation result of subsurface flows. For the future research work , we could consider coupling a geohydrological model that is capable to simulate mountainous and flat areas for more general application.

Another limitation is in the simulation of imported water demand in case Fehraltorf, we only considered the residential water demand and the irrigation demand for residential areas because of the lack of statistical data. We should be aware that the spatial

delineation result indicates a higher ratio of office and industrial land use than residential land use. The water demand and consumption from non-residential land use areas can be large as compared to the scale of precipitation inflow to the model domain. In this case, only the wastewater from houses dominates the wastewater sewer discharge. The effect of wastewater from non-residential areas should be investigated in future work.

The abundant spatial data input provided by UrbanBEATS allows the distributed urban water cycle model to simulate the Fehraltorf catchment with calibrated population and land use ratios of the blocks. Since the UrbanBEATS model is still under development, there are room for improvement in terms of the capability to capture the population and land use area better. However, the DUWCM works fine with the current output map from UrbanBEATS in both square and hexagon grids. It is good to see that the trend of the outflows are similar but small difference exist in the two spatial representations. Future work can consider distinguishing the total urban water cycle for different land use in a block in particular differentiate between pervious and impervious paved surfaces in each land use instead of integrating the various land use to only roof, pavement and pervious area like the current design.

## 8. Conclusion and Recommendation

This research project aims to investigate the potential of hexagonal grids as compared to square grids to represent the urban and regional water cycle. To this end a spatially distributed urban water balance model was developed for the total water cycle in urban areas. DUWCM is developed as a new integrated urban water cycle model that simulate the flux and water contents of total urban water cycle in a spatially explicit manner. It simulates the rainfall-runoff drainage system and the potable water supply-wastewater disposal system considering the local characteristics in each block. The simulation result was verified and seems reliable as it is similar to a widely applied hydrological model Aquacycle (shown in section 5.1.2).

The DUWCM simulation can run with hexagon grids, which generates similar results to simulation with squared grids. Nevertheless, a few differences in flows are obtained, which result from the differences in flow path, sampling of surface characteristics, and outlet block locations. Transfer of runoff between blocks is affected by the different spatial representations and its resulting flow path the most. Hexagonal grids seem to produce more realistic flow paths. The difference is apparent from the maps of annual stormwater runoff and wastewater sewer discharge in the case study Fehraltorf (Fig. 6-3, 6-4). The difference of annual stormwater runoff can be up to 500 $m^3/year$ at the same location between squared and hexagonal grids. On the other hand, annual wastewater sewer discharge shows more consistency between the two spatial representations. The comparison of square and hexagon model results demonstrates the potential of applying hexagon grids in hydrological modeling.

The methodology taken in this study brings us from adapting an existing urban water balance model into spatially distributed urban water cycle modelling to the comparison of model results in square and hexagon grids. The case studies and parameter sensitivity analyses showed that the urban hydrological model structure remains valid in either two or > 400 blocks catchment. The trend of the model results under changes in parameters shown in the section of parameter sensitivity analysis are explainable and consistent to the conceptual model. An experiment of applying local scale alternative water resource (rain tank) is carried out in the first case study and results in a significant reduction in the imported water demand as expected.

The case Fehraltorf unfortunately lacked sufficient data for model calibration. Hence, for further research, the priority is a case study along with calibration applying observation data to evaluate the performance of the model. The advantage of hexagonal

grids in urban water cycle modeling can be further explored and verified by comparison of model results with calibration to the results from squared grids.

In a next step, the effect of different block size for optimal simulation results and modeling efficiency is recommended to be investigated in both squared and hexagonal grids. Finally, the effect of different alternative water resources harvesting strategies on the system outflows can be explored with DUWCM.

## Appendix.

### 1. Important calculations

a. Infiltration from pavement to groundwater:

$$Inf_p = \max(0.0, \min(P + IR_p + Inflow_{rp} - (self.PIL - self.PSTpret), self.Infilc_p \times self.dt)$$

Inf_p happens only when the inflow is able to fulfill the initial loss (inflow + PSTpret> PIL). It is calculated as part of overflow from the interception.

b. Actual infiltration capacity of pervious area:

$$Infilc_{pera} = \min(self.dt \times self.Infilc_{per}, self.UZc - UZpret + \min(self.UZc - UZpret, self.dt \times self.UZKsat))$$

Actual infiltration capacity is limited by the predefined infiltration capacity and available space in unsaturated zone. The latter can be expanded by the percolation from unsaturated zone to groundwater.

c. Leakage from pressurized water supply main to groundwater zone

$$LD[mm] = ((IRtot + IWU) \times self.LR)/(1 - self.LR)/self.AGW$$

Leakage depth (LD) = [Leakage rate (LR) * total import water (IR+IWU+LD*AGW)] /AGW. Since LD appears in both sides of the equation, the equation is rearranged to derive LD.

d. Solve the ordinary differential equation to derive groundwater level

The unit of head of deep groundwater (H), groundwater (h(t)), and open water(OW) is meters below surface. Infiltration from groundwater to wastewater sewer (INFS).

(a) When seepage is defined by head difference:

$$\frac{dh(t)}{dt} = \frac{Inflow\ (In) - baseflow - deep\ seepage - INFS}{storage\ coefficient\ (\mu)}$$

$$\frac{d(-h(t))}{dt} = \frac{In - \frac{\left(-h(t) - (-H)\right)}{c} - \frac{\left(-h(t) - (-OW)\right)}{w} - (-h(t) - (-3)) \times IRC}{\mu}$$

$$= \frac{In - \frac{H - h(t)}{c} - \frac{OW - h(t)}{w} - \left(3 - h(t)\right) \times IRC}{\mu}$$

$$= \frac{w \times c \times In - \left(H - h(t)\right) \times w - \left(OW - h(t)\right) \times c - \left(3 - h(t)\right) \times IRC \times w \times c}{\mu \times w \times c}$$

$$= \frac{w \times c \times In - H \times w - OW \times c - 3 \times IRC \times w \times c}{\mu \times w \times c} + \frac{w + c + IRC \times w \times c}{\mu \times w \times c} \times h(t)$$

For a first order ODE in the form $\frac{d(-h(t))}{dt} = m + n \cdot h(t)$, solution can be written as:

$$h(t) = -\left[a \cdot e^{-nt} + \frac{-m}{-n}\right] = -[a \cdot e^{-nt} + \frac{m}{n}].$$

Initial condition (t=0), $h(t) = h_0 = a \times 1 + m/n$. Thus, $a = h_0 - m/n$

Here $m = \frac{w \times c \times In - H \times w - OW \times c - 3 \times IRC \times w \times c}{\mu \times w \times c}$, $n = \frac{w + c + -IRC \times w \times c}{\mu \times w \times c}$, and $\frac{m}{n} =$

$$\frac{w \times c \times In - H \times w - OW \times c - 3 \times IRC \times w \times c}{\mu \times w \times c} \times \frac{\mu \times w \times c}{w + c + IRC \times w \times c} = \frac{w \times c \times In - H \times w - OW \times c - 3 \times IRC \times w \times c}{w + c + IRC \times w \times c}.$$

$$h(t) = -[(h_0 - m/n) \times e^{-nt} + m/n]$$

$$h(t) = -\left[\left[h_0 - \frac{w \times c \times In - H \times w - OW \times c - 3 \times IRC \times w \times c}{w + c + IRC \times w \times c}\right] \times e^{-(\frac{w + c + IRC \times w \times c}{\mu w c}) \times t} + \frac{w \times c \times In - H \times w - OW \times c - 3 \times IRC \times w \times c}{w + c + IRC \times w \times c}\right]$$

The minus mark is added to make the unit [m-SL] (meters below surface). Total seepage over the time step is estimated as the head difference between deep groundwater and averaged groundwater level: (GWt0 = solution of h(t))

$$Q_{seep}[mm/d] = 1000 * \frac{H - 0.5 \times (GWt0 + self.GWpret + self.GWabpret)}{self.vc} \times self.dt$$

$$INFS[mm/d] = 1000 \times [3.0 - 0.5 \times (GWt0 + self.GWpret + self.GWabpret)] \times IRC \times self.dt$$

(b) When seepage is defined by predefined value $(q_s)$:

$$\frac{d(-h(t))}{dt} = \frac{In - q_s - \frac{\left(-h(t) - (-OW)\right)}{w} - (-h(t) - (-3)) \times IRC}{\mu}$$

$$= \frac{w \times In - q_s \times w - OW - 3 \times IRC \times w \times c}{\mu \times w} + \frac{1 + IRC \times w}{\mu \times w} \times h(t)$$

$$h(t) = -[(h_0 - m/n) \times e^{-nt} + m/n]$$

Here $\frac{m}{n} = \frac{w \times In - q_s \times w - OW - 3 \times IRC \times w \times c}{\mu \times w} \times \frac{\mu \times w}{1 + IRC \times w} = \frac{w \times In - q_s \times w - OW - 3 \times IRC \times w \times c}{1 + IRC \times w}$

$$h(t) = -\left[\left[h_0 - \frac{w \times In - q_s \times w - OW - 3 \times IRC \times w \times c}{1 + IRC \times w}\right] \times e^{-(\frac{1 + IRC \times w}{\mu \times w}) \times t} + \frac{w \times In - q_s \times w - OW - 3 \times IRC \times w \times c}{1 + IRC \times w})\right]$$

$$Q_{seep}[mm/d] = q_s * self.dt$$

$$INFS[mm/d] = 1000 \times [3.0 - 0.5 \times (GWt0 + self.GWpret + self.GWabpret)] \times IRC \times self.dt$$

e. From yearly irrigation to daily irrigation [mm/d]

To down scale the yearly irrigation to daily irrigation, we assume the yearly irrigation is distributed following the pattern of potential evaporation.

a. Ind = Ep,

b. Find the index of first days of the years

c. Calculate the yearly sum of index (Ep)

d. Daily irrigation of day t in year n is estimated as: IR * index (Ep) / the sum of index (Ep) of year n

## 2. List of soil type and crop type

Table A - 1. List of soil type

| | | |
|---|---|---|
| 1 | Veengrond met veraarde bovengrond | Peat soil with degenerate topsoil |
| 2 | Veengrond met veraarde bovengrond, zand | Peat soil with degraded topsoil:sand |
| 3 | Veengrond met kleidek | Peat soil with clay deck |
| 4 | Veengrond met kleidek op zand | Peat soil with clay deck on sand |
| 5 | Veengrond met zanddek op zand | Peat soil with sand cover on sand |
| 6 | Veengrond op ongerijpte klei | Peat soil on immature clay |
| 7 | Stuifzand | Blowing sand |
| 8 | Podzol (Leemarm, fijn zand) | Podzol (Loam poor: fine sand) |
| 9 | Podzol (zwak lemig, fijn zand) | Podzol (weakly loamy: fine sand) |
| 10 | Podzol (zwak lemig, fijn zand op grof zand) | Podzol (weakly loamy: fine sand on coarse sand)) |
| 11 | Podzol (lemig keileem) | Podzol (loamy boulder clay) |
| 12 | Enkeerd (zwak lemig, fijn zand) | Enkeerd (weak loamy: fine sand) |
| 13 | Beekeerd (lemig fijn zand) | Converted (loamy fine sand) |
| 14 | Podzol (grof zand) | Podzol (coarse sand) |
| 15 | Zavel | Sablon |
| 16 | Lichte klei | Light clay |
| 17 | Zware klei | Heavy clay |
| 18 | Klei op veen | Clay on peat |
| 19 | Klei op zand | Clay on sand |
| 20 | Klei op grof zand | Clay on coarse sand |
| 21 | Leem | Loam |

Table A - 2. List of crop type

| | | | |
|---|---|---|---|
| 1 | grass | 9 | orchard |
| 2 | corn | 10 | bulbous plants |
| 3 | potatoes | 11 | foliage forest |
| 4 | sugarbeet | 12 | pine forest |
| 5 | grain | 13 | nature |
| 6 | miscellaneous | 14 | fallow |
| 7 | non-arable land | 15 | vegetables |
| 8 | greenhouse area | 16 | flowers |

## 3. Parameter sensitivity (Case Curtin)

The parameter sensitivity analysis is done based on the calibrated parameter sets we derived in section 5.1.2. Eight parameters are analyzed: Infilc_p, Infilc_per, LR, IRC, w, vc, perI, and h_dgw. The change of the parameters to the six simulation results, including baseflow, deep seepage, Rs, Rw, total evapotranspiration, and import water are discussed. The hydrograph of the simulation results and box plot of standardized difference from the main simulation result are shown below.

3-a. Infiltration capacity of paved area (Infilc_p, mm/day):

Table A - 1. MSE list of different values of Infilc_p to the resulting flows.

| | MSE_BFout_all | MSE_Import_all | MSE_Qseep_all | MSE_Rs_out | MSE_Rw_out | MSE_totalE |
|---|---|---|---|---|---|---|
| **1.2** | 0.007854 | 0.0 | 0.000032 | 0.009028 | 0.000013 | 1.313950e-07 |
| **1.6** | 0.001942 | 0.0 | 0.000008 | 0.001914 | 0.000003 | 2.960208e-08 |
| **2.0** | 0.000000 | 0.0 | 0.000000 | 0.000000 | 0.000000 | 0.000000e+00 |
| **2.4** | 0.001553 | 0.0 | 0.000007 | 0.001004 | 0.000003 | 2.613560e-08 |
| **2.8** | 0.005753 | 0.0 | 0.000025 | 0.003414 | 0.000011 | 9.977650e-08 |

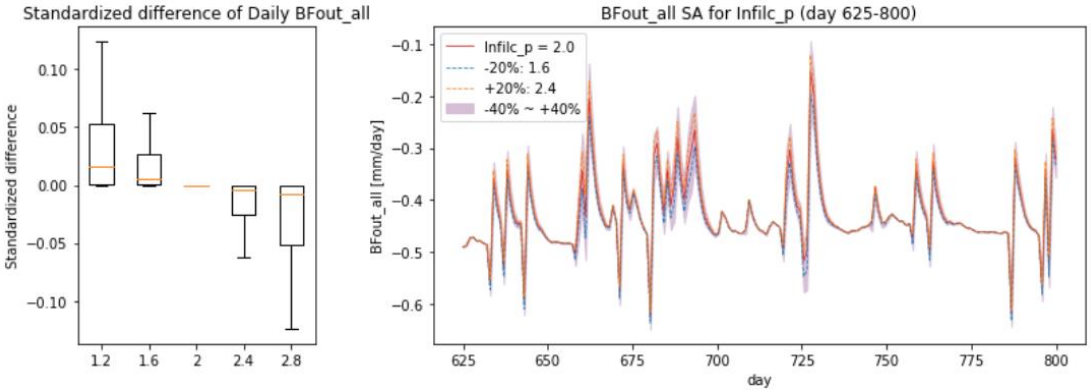


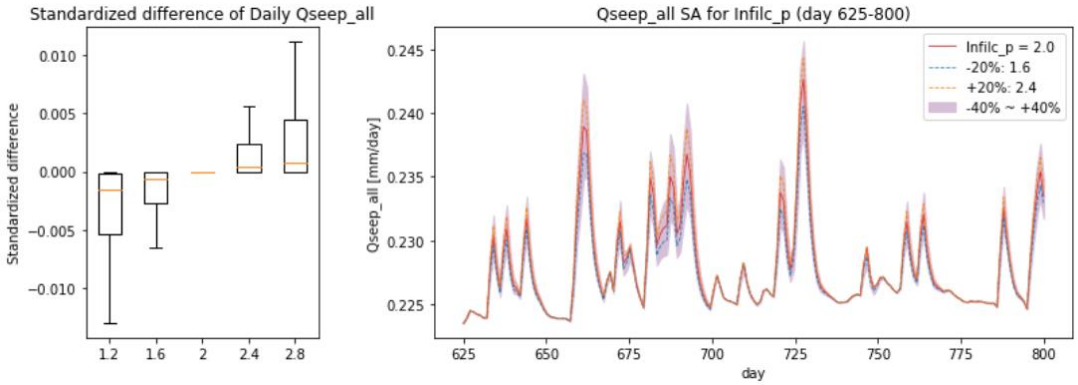

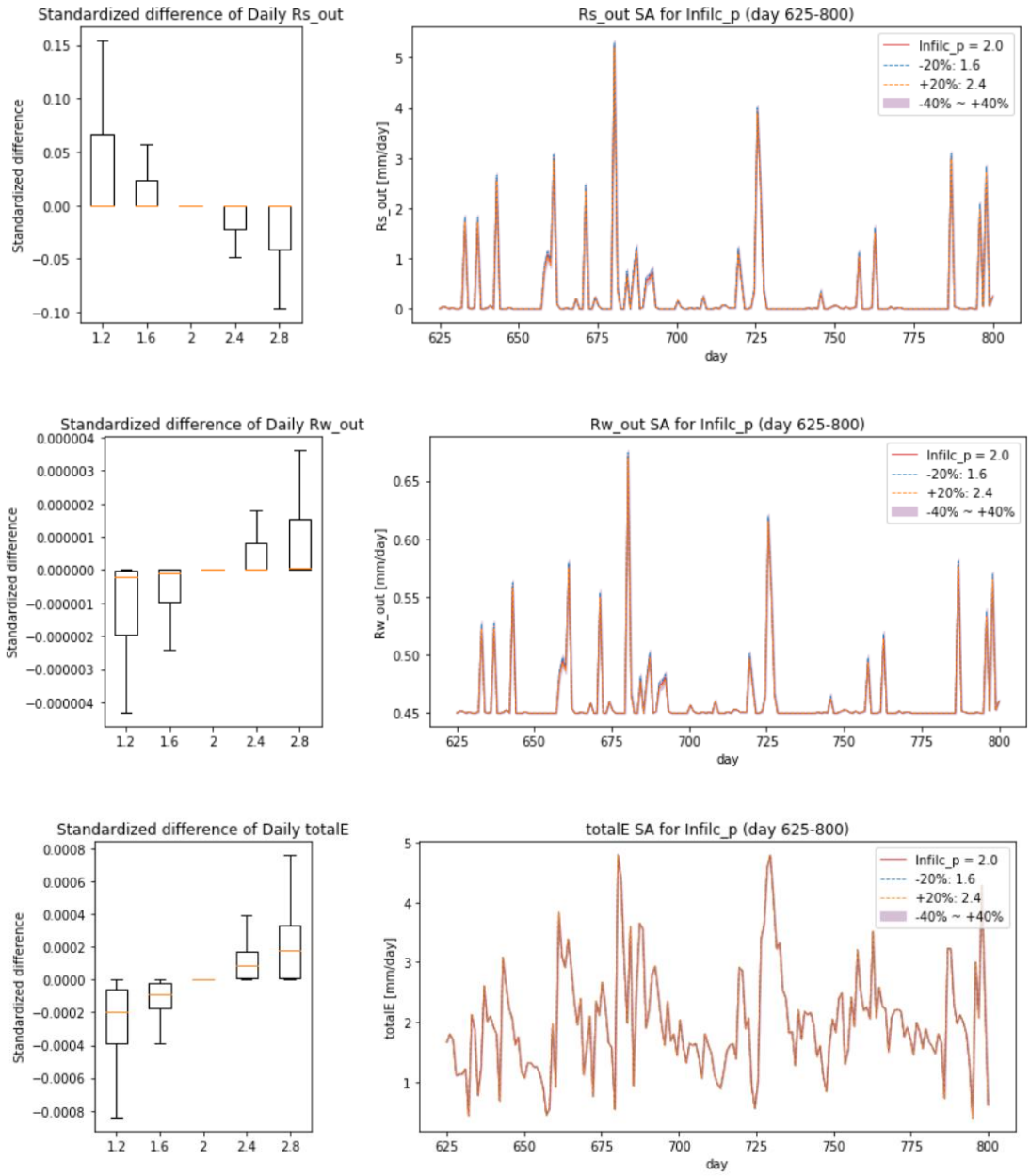


3-b. Infiltration capacity of pervious area (Infilc_per):

Table A - 2. MSE list of different values of Infilc_per to the resulting flows.

| | MSE_BFout_all | MSE_Import_all | MSE_Qseep_all | MSE_Rs_out | MSE_Rw_out | MSE_totalE |
|---|---|---|---|---|---|---|
| **48.0** | 0.0 | 0.0 | 0.0 | 0.025316 | 0.000000e+00 | 0.000440 |
| **64.0** | 0.0 | 0.0 | 0.0 | 0.025316 | 3.117737e-34 | 0.000059 |
| **80.0** | 0.0 | 0.0 | 0.0 | 0.000000 | 0.000000e+00 | 0.000000 |
| **96.0** | 0.0 | 0.0 | 0.0 | 0.012658 | 0.000000e+00 | 0.000006 |
| **112.0** | 0.0 | 0.0 | 0.0 | 0.012658 | 0.000000e+00 | 0.000006 |

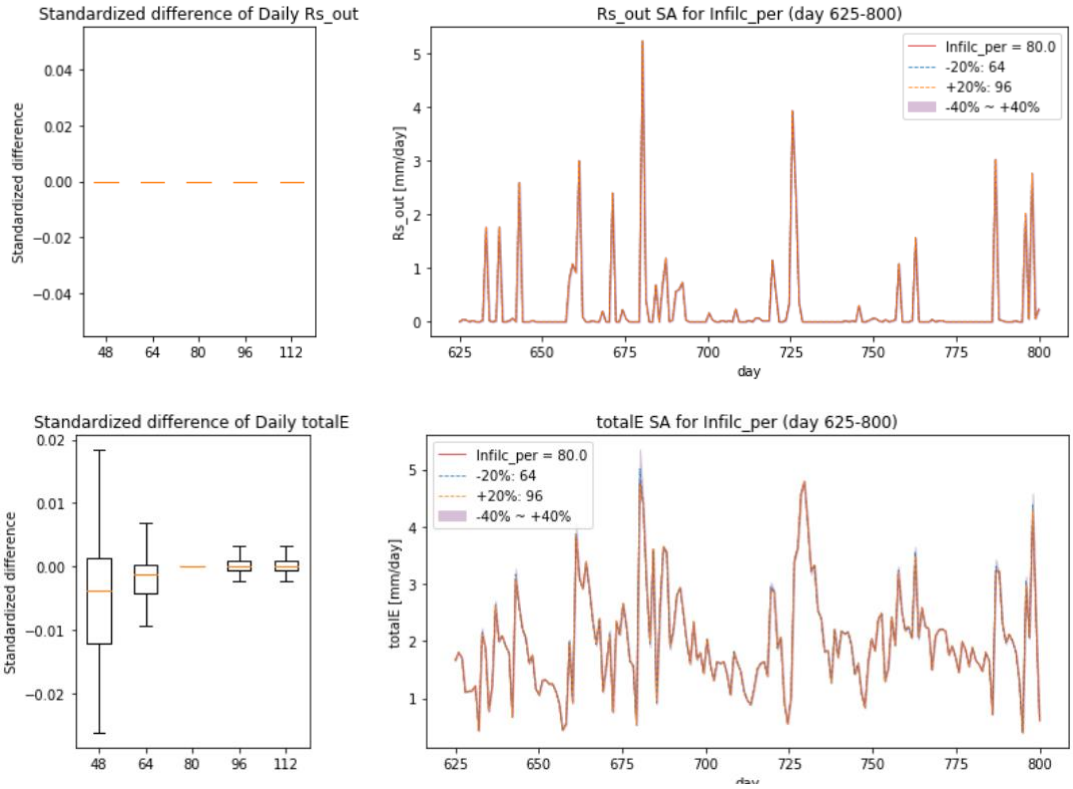


## 3-c. Leakage rate (LR):

Table A - 3. MSE list of different values of LR to the resulting flows.

| | MSE_BFout_all | MSE_Import_all | MSE_Qseep_all | MSE_Rs_out | MSE_Rw_out | MSE_totalE |
|---|---|---|---|---|---|---|
| **1.8** | 0.001594 | 0.000149 | 0.000013 | 4.171310e-32 | 7.435712e-12 | 9.627679e-08 |
| **2.4** | 0.000403 | 0.000038 | 0.000003 | 2.586260e-32 | 1.881857e-12 | 2.436607e-08 |
| **3.0** | 0.000000 | 0.000000 | 0.000000 | 0.000000e+00 | 0.000000e+00 | 0.000000e+00 |
| **3.6** | 0.000413 | 0.000039 | 0.000003 | 1.396390e-32 | 1.929007e-12 | 2.497653e-08 |
| **4.2** | 0.001675 | 0.000157 | 0.000014 | 2.345582e-32 | 7.812996e-12 | 1.011616e-07 |

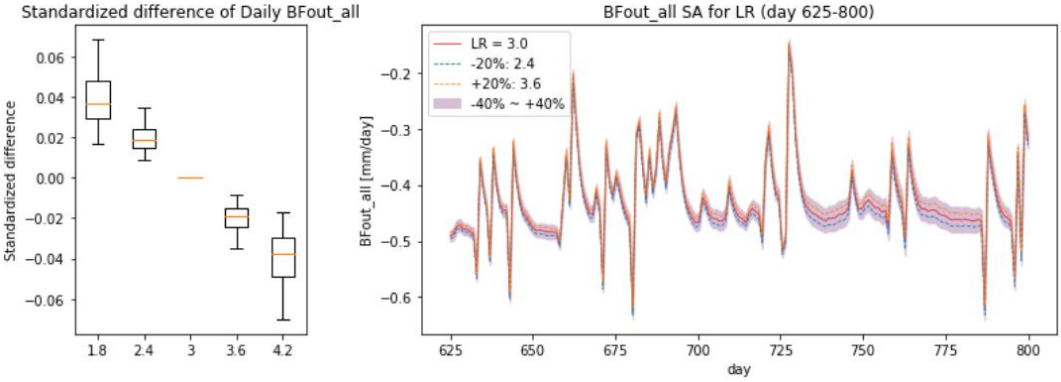

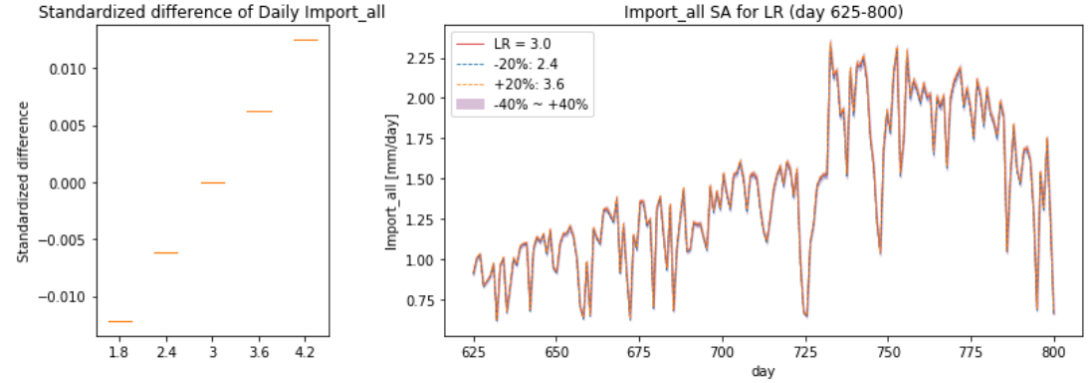


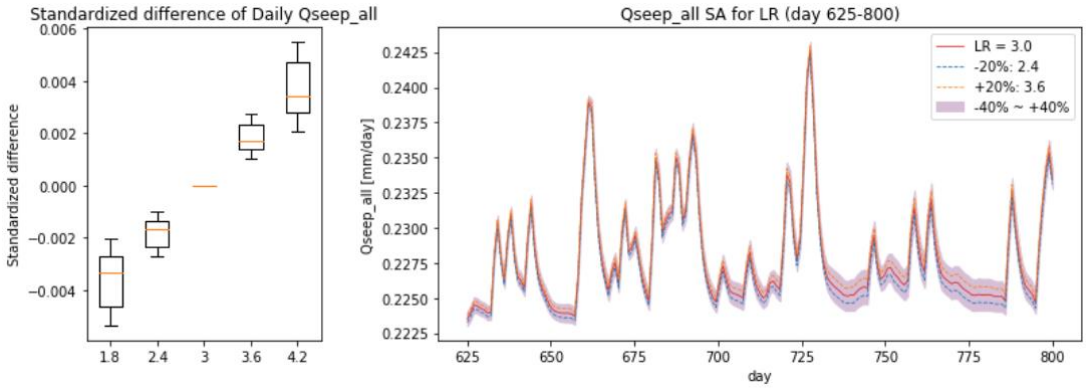


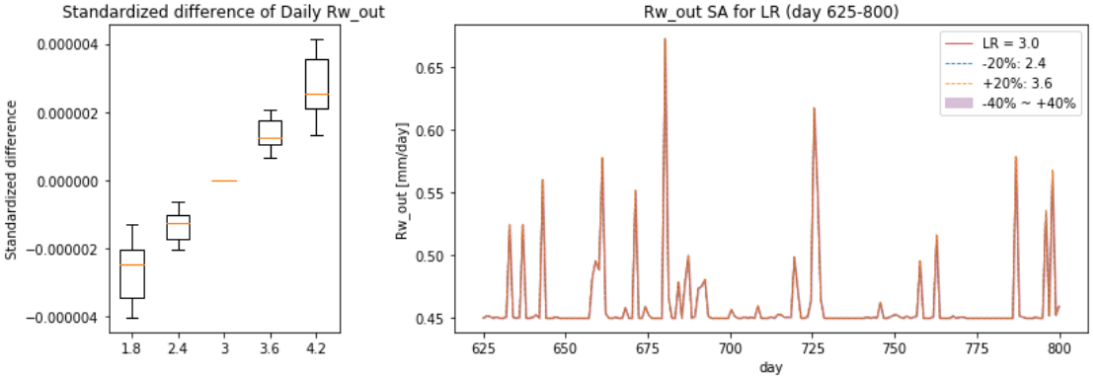


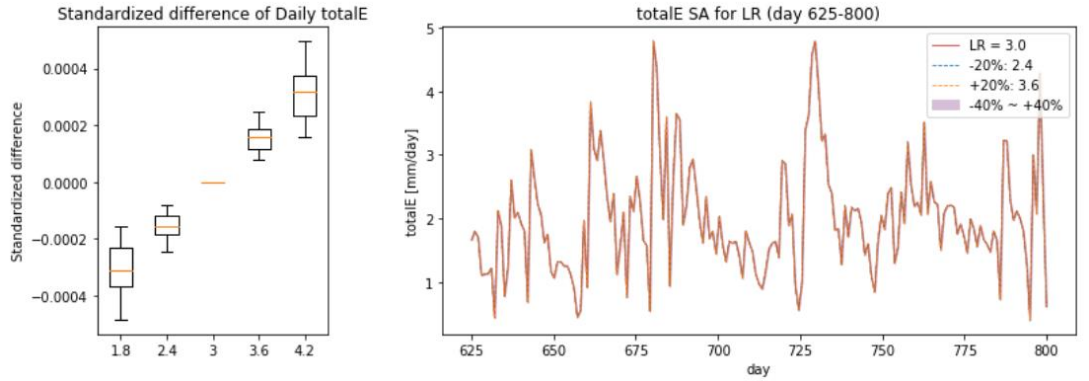


3-d. Infiltration recession rate (IRC):

Table A - 4. MSE list of different values of IRC to the resulting flows.

| | MSE_BFout_all | MSE_Import_all | MSE_Qseep_all | MSE_Rs_out | MSE_Rw_out | MSE_totalE |
|---|---|---|---|---|---|---|
| **9.000000e-07** | 0.000007 | 0.0 | 5.618742e-08 | 2.676609e-33 | 0.000006 | 5.423250e-10 |
| **1.200000e-06** | 0.000002 | 0.0 | 1.404646e-08 | 1.052623e-31 | 0.000002 | 1.355775e-10 |
| **1.500000e-06** | 0.000000 | 0.0 | 0.000000e+00 | 0.000000e+00 | 0.000000 | 0.000000e+00 |
| **1.800000e-06** | 0.000002 | 0.0 | 1.404569e-08 | 3.406196e-32 | 0.000002 | 1.355701e-10 |
| **2.100000e-06** | 0.000007 | 0.0 | 5.618119e-08 | 1.172791e-32 | 0.000006 | 5.422653e-10 |

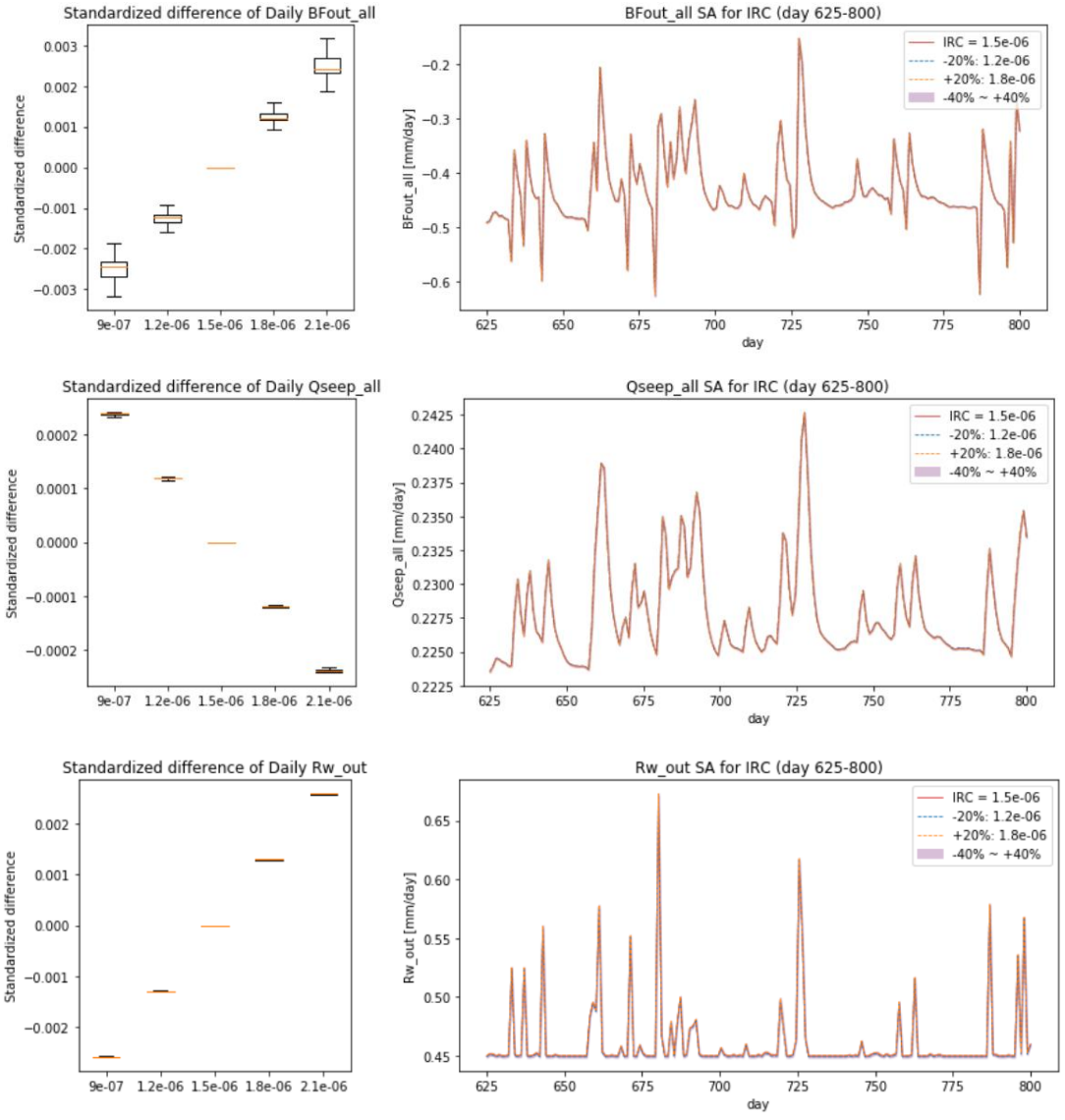

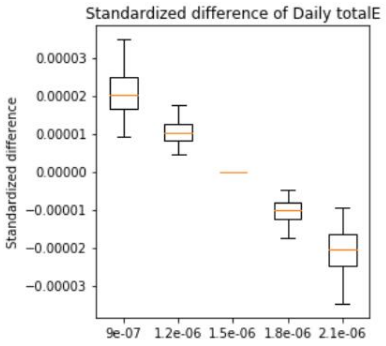


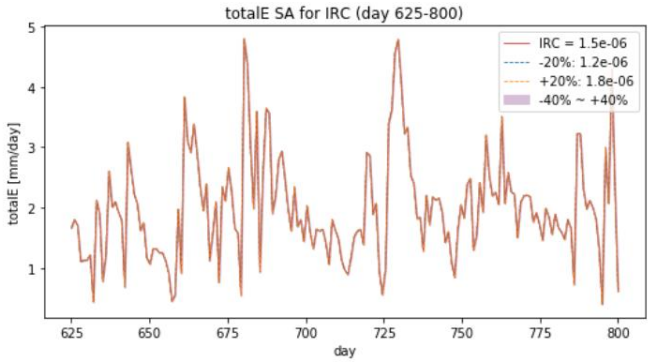


## 3-e. Drainage resistant of baseflow (w):

Table A - 5. MSE list of different values of w to the resulting flows.

| | MSE_BFout_all | MSE_Import_all | MSE_Qseep_all | MSE_Rs_out | MSE_Rw_out | MSE_totalE |
|---|---|---|---|---|---|---|
| **30.0** | 0.011601 | 0.0 | 0.001313 | 4.171310e-32 | 7.244171e-10 | 0.000009 |
| **40.0** | 0.001907 | 0.0 | 0.000318 | 1.440451e-32 | 1.755900e-10 | 0.000002 |
| **50.0** | 0.000000 | 0.0 | 0.000000 | 0.000000e+00 | 0.000000e+00 | 0.000000 |
| **60.0** | 0.001011 | 0.0 | 0.000299 | 4.596067e-32 | 1.652049e-10 | 0.000002 |
| **70.0** | 0.003173 | 0.0 | 0.001160 | 7.818184e-32 | 6.411837e-10 | 0.000008 |

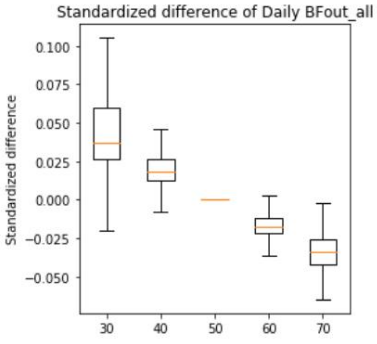


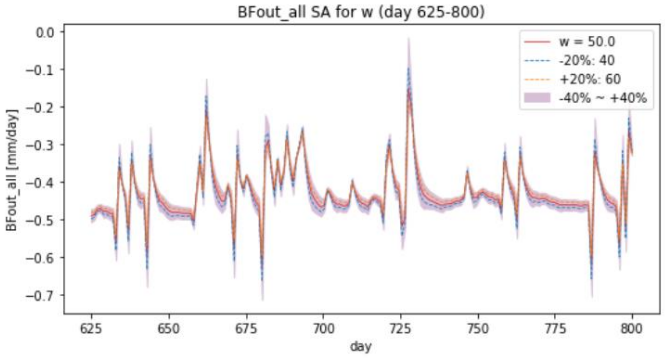


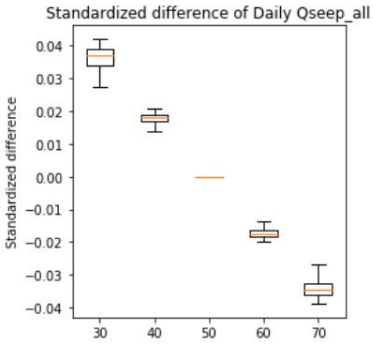


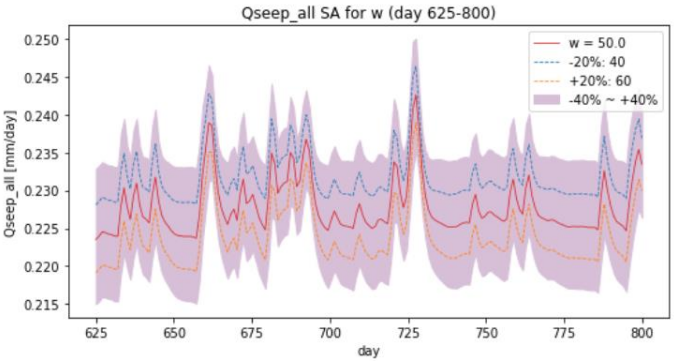

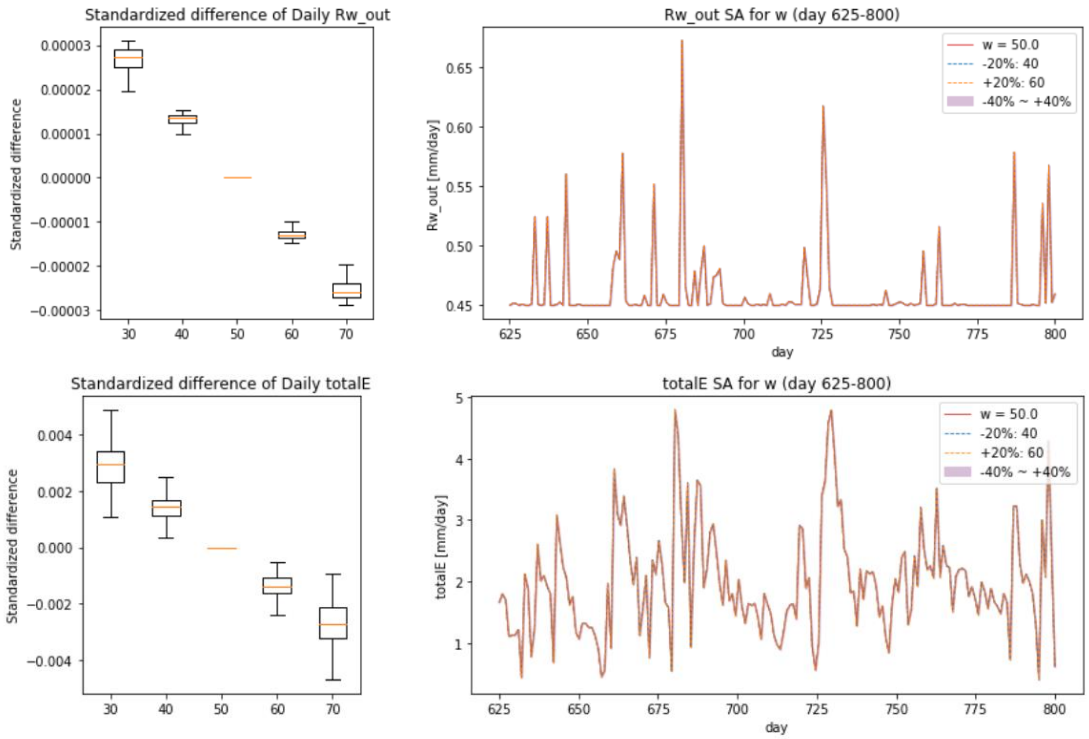


## 3-f. Drainage resistant of seepage (vc):

Table A - 6. MSE list of different values of vc to the resulting flows.

| | MSE_BFout_all | MSE_Import_all | MSE_Qseep_all | MSE_Rs_out | MSE_Rw_out | MSE_totalE |
|---|---|---|---|---|---|---|
| **600.0** | 0.115190 | 0.0 | 0.380532 | 4.394908e-32 | 4.959172e-10 | 9.003370e-06 |
| **800.0** | 0.016820 | 0.0 | 0.055568 | 1.396390e-32 | 7.241806e-11 | 1.315008e-06 |
| **1000.0** | 0.000000 | 0.0 | 0.000000 | 0.000000e+00 | 0.000000e+00 | 0.000000e+00 |
| **1200.0** | 0.007768 | 0.0 | 0.025664 | 1.440452e-32 | 3.344679e-11 | 6.071710e-07 |
| **1400.0** | 0.023082 | 0.0 | 0.076265 | 6.526676e-32 | 9.939142e-11 | 1.804170e-06 |

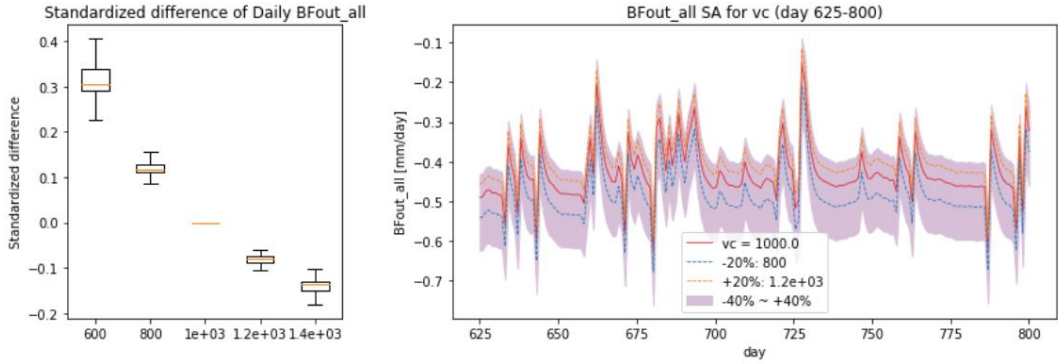

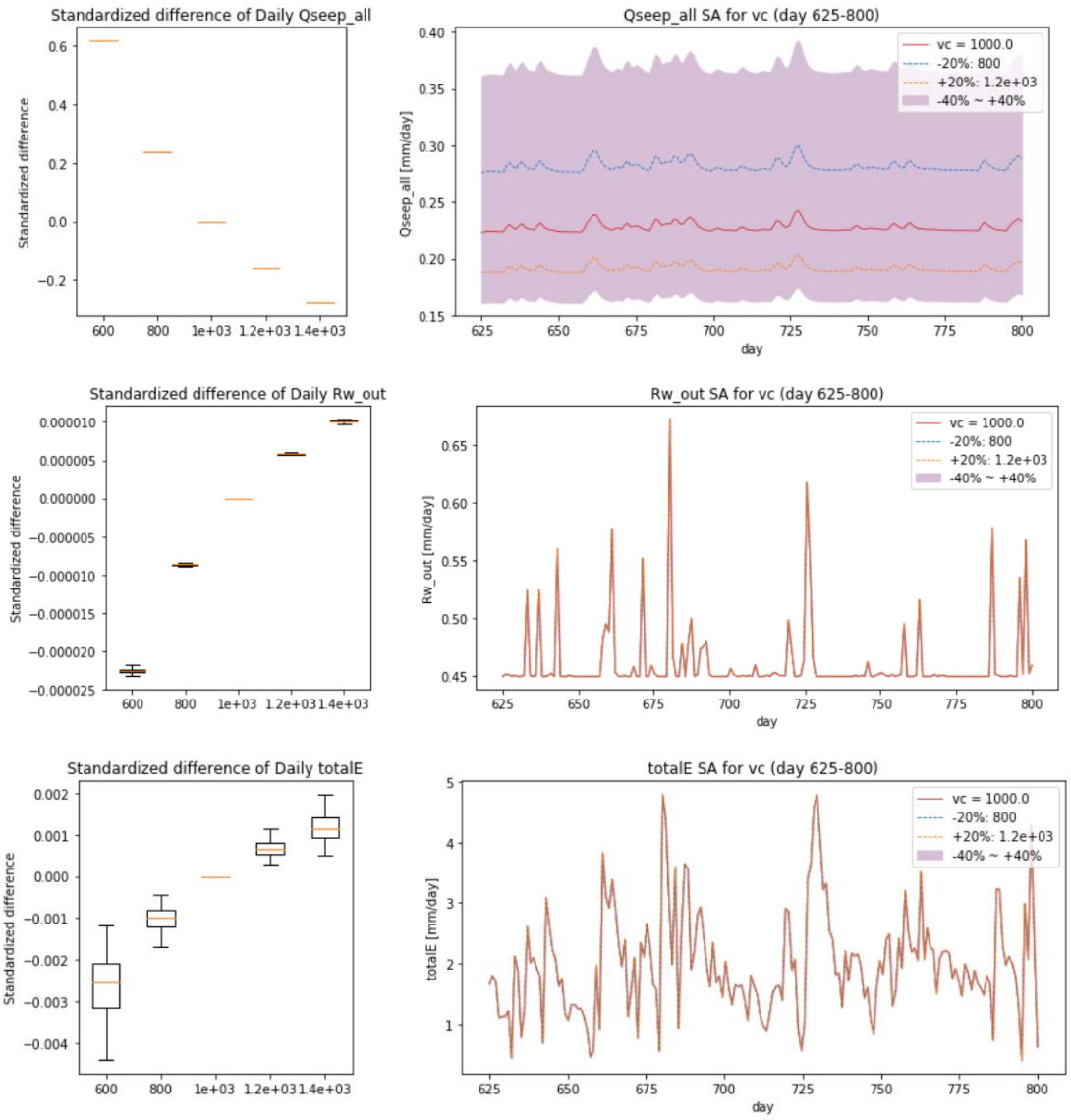


## 3-g. Drainage resistant of seepage (perI):

Table A - 7. MSE list of different values of perI to the resulting flows.

| | MSE_BFout_all | MSE_Import_all | MSE_Qseep_all | MSE_Rs_out | MSE_Rw_out | MSE_totalE |
|---|---|---|---|---|---|---|
| **1.8** | 0.0 | 0.0 | 0.0 | 0.000275 | 0.000531 | 0.0 |
| **2.4** | 0.0 | 0.0 | 0.0 | 0.000069 | 0.000132 | 0.0 |
| **3.0** | 0.0 | 0.0 | 0.0 | 0.000000 | 0.000000 | 0.0 |
| **3.6** | 0.0 | 0.0 | 0.0 | 0.000068 | 0.000131 | 0.0 |
| **4.2** | 0.0 | 0.0 | 0.0 | 0.000272 | 0.000524 | 0.0 |

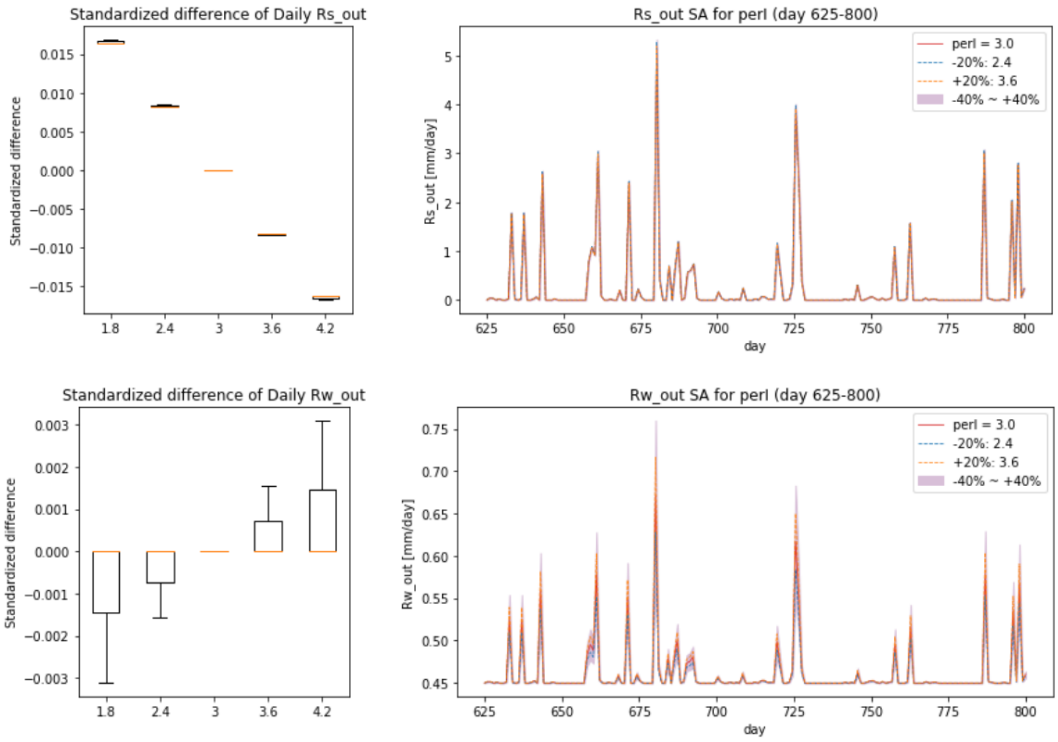


## 3-h. Head of deep groundwater (h_dgw):

Table A - 8. MSE list of different values of h_dgw to the resulting flows.

| | MSE_BFout_all | MSE_Import_all | MSE_Qseep_all | MSE_Rs_out | MSE_Rw_out | MSE_totalE |
|---|---|---|---|---|---|---|
| **0.768** | 1.375060 | 0.0 | 4.594233 | 1.396390e-32 | 5.989385e-09 | 0.000109 |
| **1.024** | 0.343766 | 0.0 | 1.148558 | 2.345582e-32 | 1.497348e-09 | 0.000027 |
| **1.280** | 0.000000 | 0.0 | 0.000000 | 0.000000e+00 | 0.000000e+00 | 0.000000 |
| **1.536** | 0.343768 | 0.0 | 1.148558 | 1.172791e-32 | 1.497350e-09 | 0.000026 |
| **1.792** | 1.375073 | 0.0 | 4.594233 | 2.235984e-33 | 5.989403e-09 | 0.000103 |

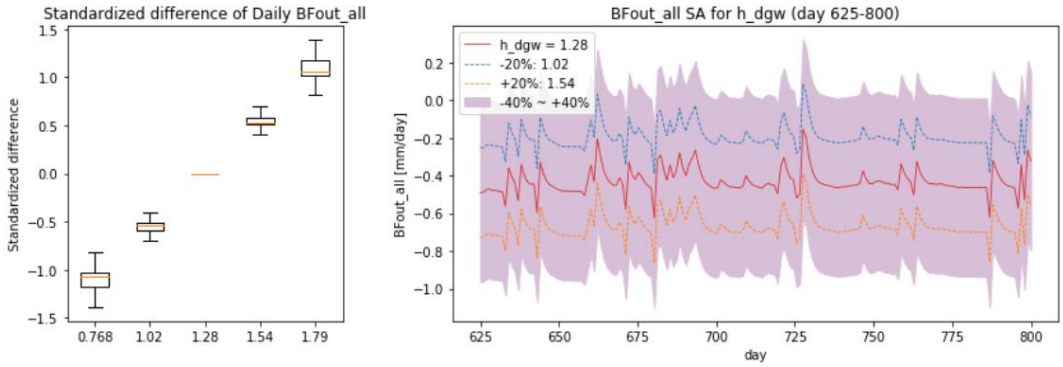

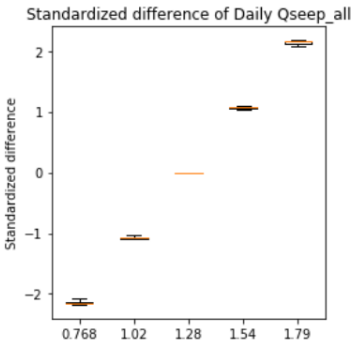
Standardized difference of Daily Qseep_all
Standardized difference
2
1
0
−1
−2
0.768
1.02
1.28
1.54
1.79

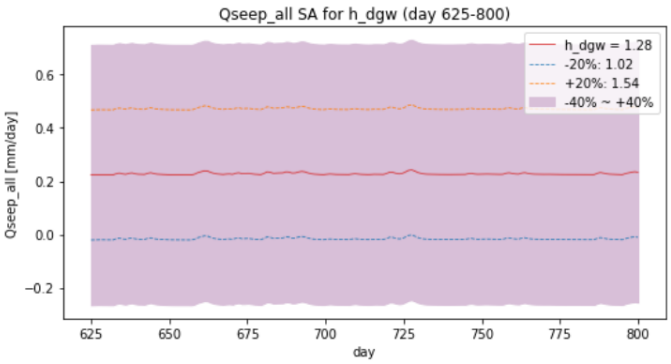
Qseep_all SA for h_dgw (day 625-800)
h_dgw = 1.28
-20%: 1.02
+20%: 1.54
-40% ~ +40%
Qseep_all [mm/day]
0.6
0.4
0.2
0.0
−0.2
625
650
675
700
725
750
775
800
day

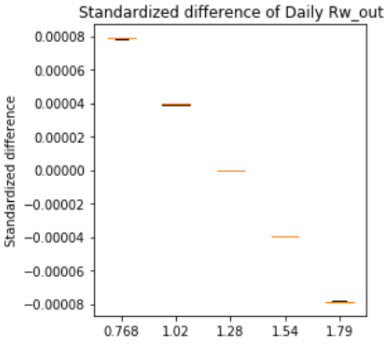
Standardized difference of Daily Rw_out
Standardized difference
0.00008
0.00006
0.00004
0.00002
0.00000
−0.00002
−0.00004
−0.00006
−0.00008
0.768
1.02
1.28
1.54
1.79

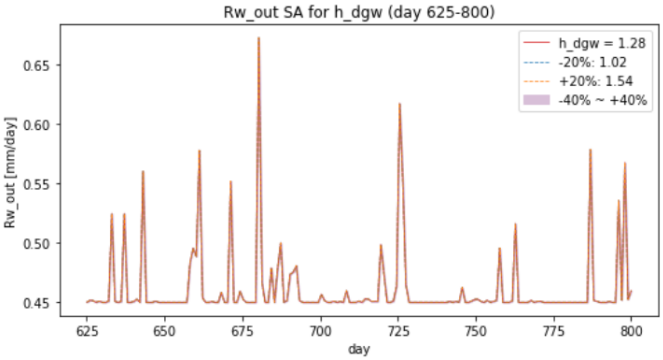
Rw_out SA for h_dgw (day 625-800)
h_dgw = 1.28
-20%: 1.02
+20%: 1.54
-40% ~ +40%
Rw_out [mm/day]
0.65
0.60
0.55
0.50
0.45
625
650
675
700
725
750
775
800
day

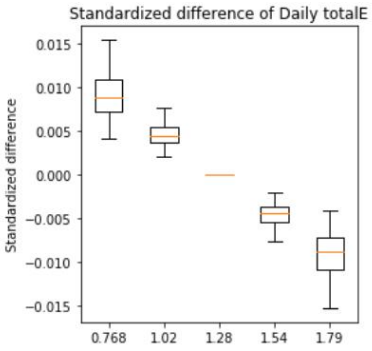
Standardized difference of Daily totalE
Standardized difference
0.015
0.010
0.005
0.000
−0.005
−0.010
−0.015
0.768
1.02
1.28
1.54
1.79

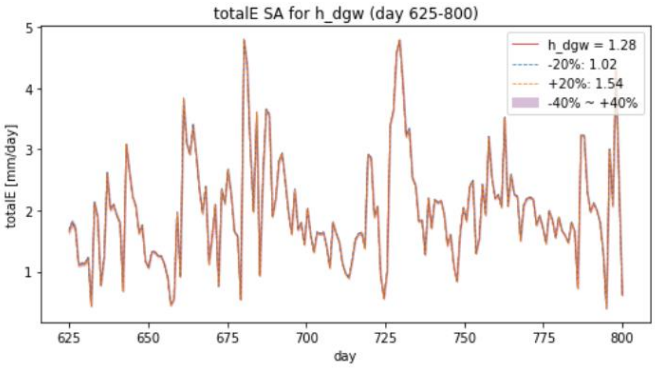
totalE SA for h_dgw (day 625-800)
h_dgw = 1.28
-20%: 1.02
+20%: 1.54
-40% ~ +40%
totalE [mm/day]
5
4
3
2
1
625
650
675
700
725
750
775
800
day

## 4. Land use sensitivity (Case Curtin):

The scenarios of the land use area changes are listed in Table A4-1, which is the same table as Table 5-6.

Table A - 3. The land use area of six urbanized scenarios

| Land use type | scenario | R | P | Pervious | Total | scenario | R | P | Pervious | total |
|---|---|---|---|---|---|---|---|---|---|---|
| Original | | 1800 | 2000 | 12700 | 16500 | | 1800 | 2000 | 12700 | 16500 |
| | | 3750 | 2700 | 11550 | 18000 | | 3750 | 2700 | 11550 | 18000 |
| | Change 10% of total area from pervious to Roof/ Paved area | | | | | Change 20% of total area from pervious to Roof/ Paved area | | | | |
| Roof (R) | LU1 | 3450 | 2000 | 11050 | 16500 | LU4 | 5100 | 2000 | 9400 | 16500 |
| | | 5500 | 2700 | 9750 | 18000 | | 7350 | 2700 | 7950 | 18000 |
| R+P | LU2 | 2625 | 2825 | 11050 | 16500 | LU5 | 3450 | 3650 | 9400 | 16500 |
| | | 4650 | 3600 | 9750 | 18000 | | 5550 | 4500 | 7950 | 18000 |
| Pavement (P) | LU3 | 1800 | 3650 | 11050 | 16500 | LU6 | 1800 | 5300 | 9400 | 16500 |
| | | 3750 | 4500 | 9750 | 18000 | | 3750 | 6300 | 7950 | 18000 |

| Case_name | MSE_BFout_all | MSE_Qseep_all | MSE_Rs_out | MSE_Rw_out | MSE_totalE | MSE_Import_all |
|---|---|---|---|---|---|---|
| **+10%,Roof** | 0.007813 | 0.000038 | 0.293698 | 0.000552 | 0.020096 | 0.008574 |
| **+5%R, +5%P** | 0.026598 | 0.000152 | 0.096672 | 0.000435 | 0.020017 | 0.008574 |
| **+10%Pavement** | 0.060422 | 0.000308 | 0.020342 | 0.000333 | 0.019938 | 0.008574 |
| **+20%Roof** | 0.030945 | 0.000239 | 1.210023 | 0.002254 | 0.080478 | 0.034296 |
| **+10%R, +10%P** | 0.107225 | 0.000614 | 0.386688 | 0.001739 | 0.080214 | 0.034296 |
| **+20%Pavement** | 0.243474 | 0.001242 | 0.081368 | 0.001333 | 0.079952 | 0.034296 |

4-a. Increase in Roof area (Scenario LU1 and LU4)

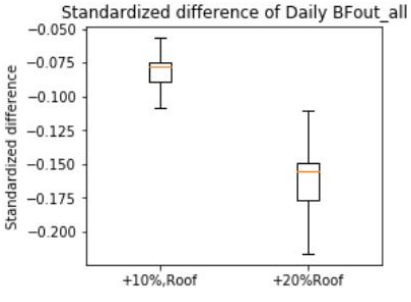


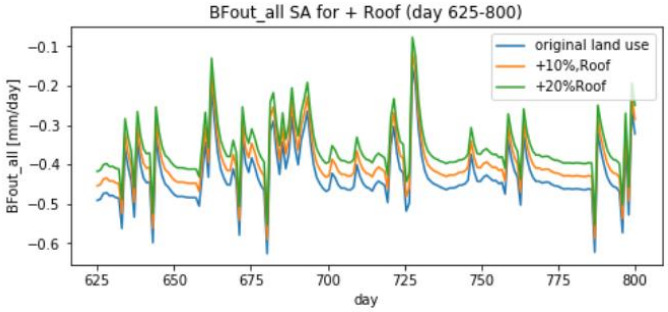

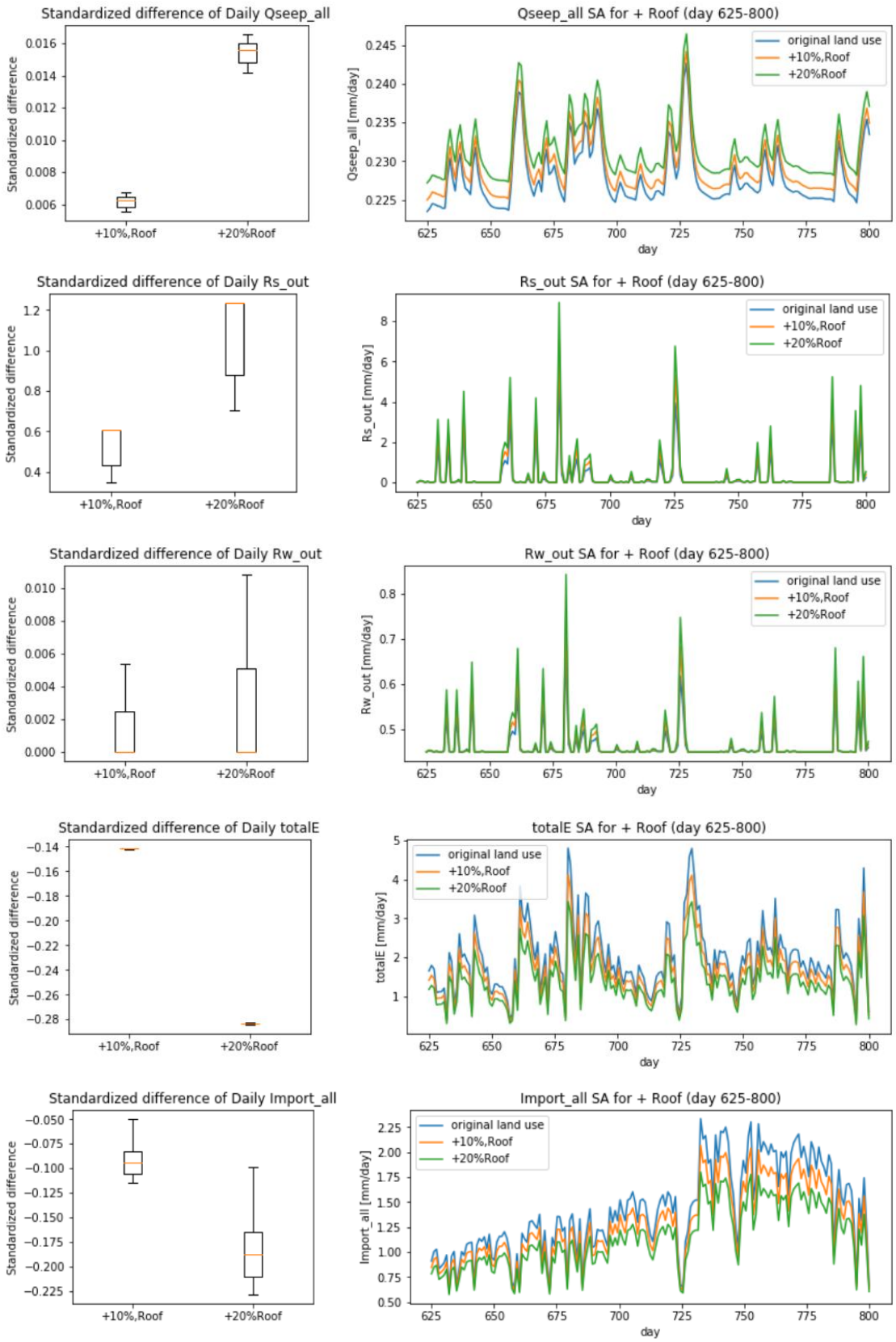


4-b. Increase in both roof and paved area (Scenario 2 and 5)

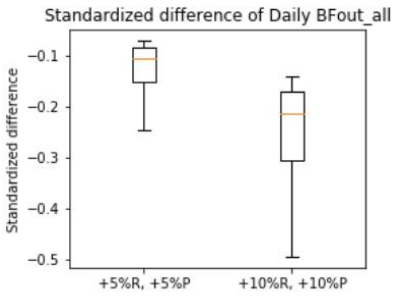
Standardized difference of Daily BFout_all
Standardized difference
−0.1
−0.2
−0.3
−0.4
−0.5
+5%R, +5%P
+10%R, +10%P

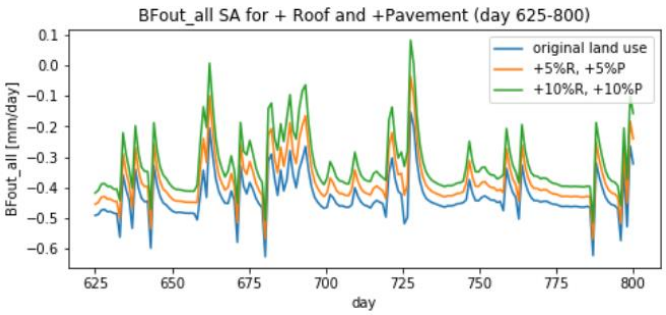
BFout_all SA for + Roof and +Pavement (day 625-800)
BFout_all [mm/day]
0.1
0.0
−0.1
−0.2
−0.3
−0.4
−0.5
−0.6
625
650
675
700
725
750
775
800
day
original land use
+5%R, +5%P
+10%R, +10%P

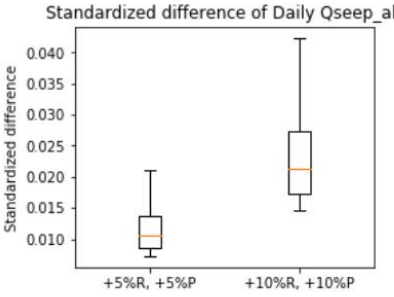
Standardized difference of Daily Qseep_all
Standardized difference
0.040
0.035
0.030
0.025
0.020
0.015
0.010
+5%R, +5%P
+10%R, +10%P

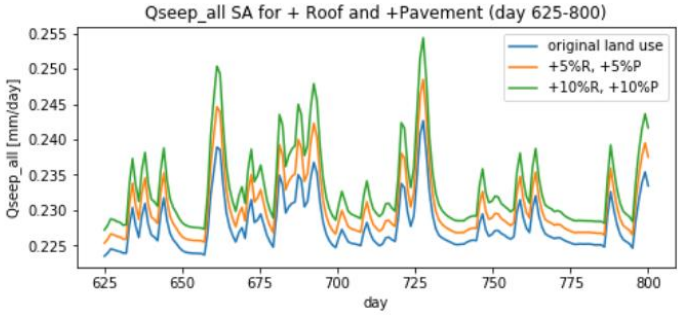
Qseep_all SA for + Roof and +Pavement (day 625-800)
Qseep_all [mm/day]
0.255
0.250
0.245
0.240
0.235
0.230
0.225
625
650
675
700
725
750
775
800
day
original land use
+5%R, +5%P
+10%R, +10%P

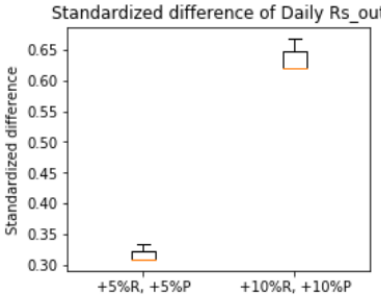
Standardized difference of Daily Rs_out
Standardized difference
0.65
0.60
0.55
0.50
0.45
0.40
0.35
0.30
+5%R, +5%P
+10%R, +10%P

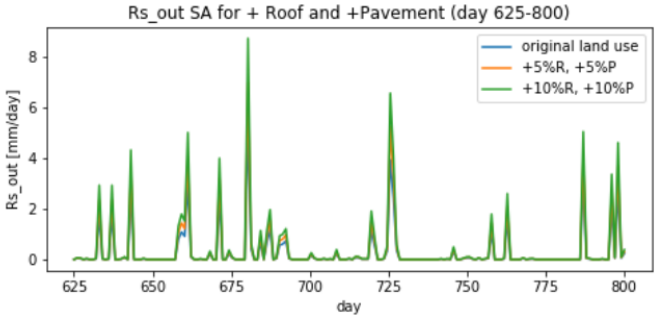
Rs_out SA for + Roof and +Pavement (day 625-800)
Rs_out [mm/day]
8
6
4
2
0
625
650
675
700
725
750
775
800
day
original land use
+5%R, +5%P
+10%R, +10%P

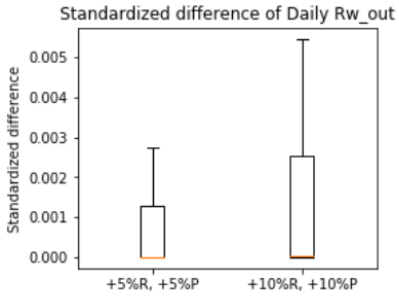
Standardized difference of Daily Rw_out
Standardized difference
0.005
0.004
0.003
0.002
0.001
0.000
+5%R, +5%P
+10%R, +10%P

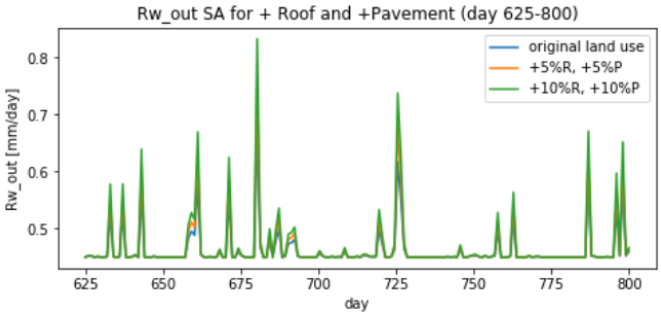
Rw_out SA for + Roof and +Pavement (day 625-800)
Rw_out [mm/day]
0.8
0.7
0.6
0.5
625
650
675
700
725
750
775
800
day
original land use
+5%R, +5%P
+10%R, +10%P

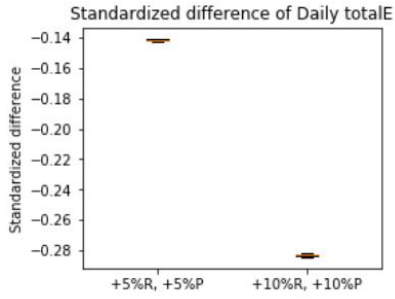
Standardized difference of Daily totalE
Standardized difference
−0.14
−0.16
−0.18
−0.20
−0.22
−0.24
−0.26
−0.28
+5%R, +5%P
+10%R, +10%P

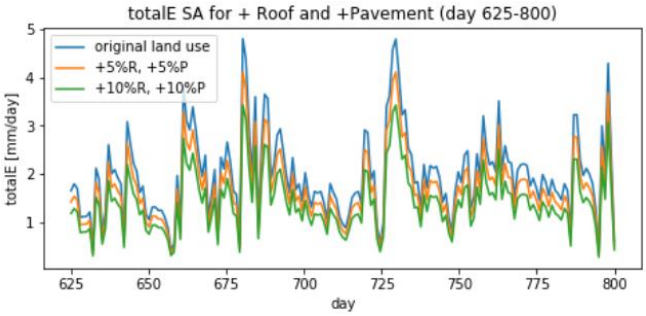
totalE SA for + Roof and +Pavement (day 625-800)
totalE [mm/day]
5
4
3
2
1
625
650
675
700
725
750
775
800
day
original land use
+5%R, +5%P
+10%R, +10%P

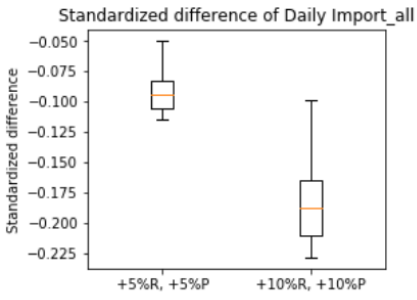


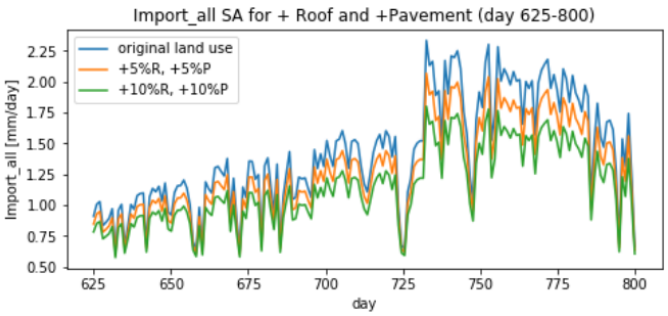


4-c. Increase in paved area (Scenario 3 and 6)

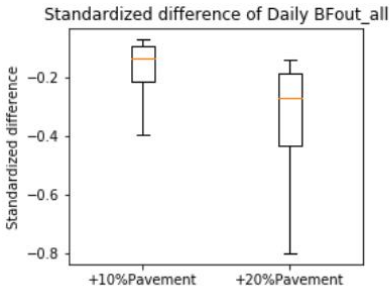


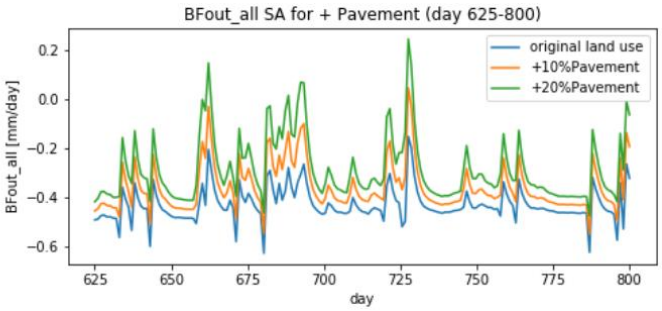


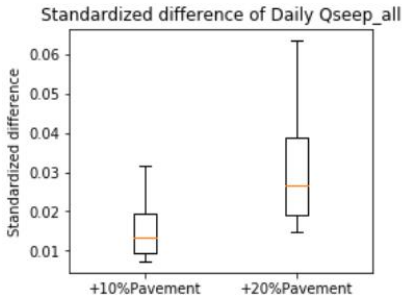


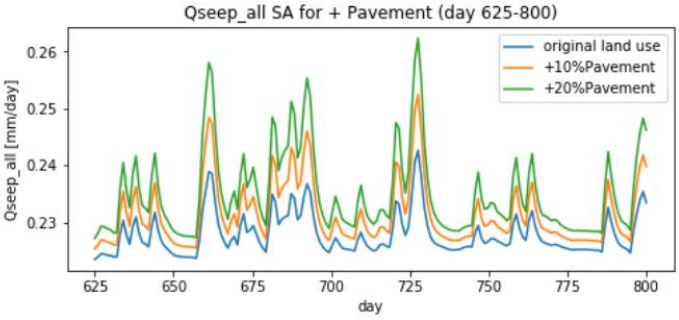


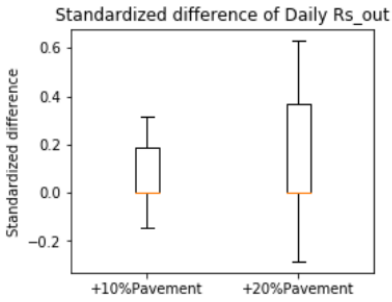


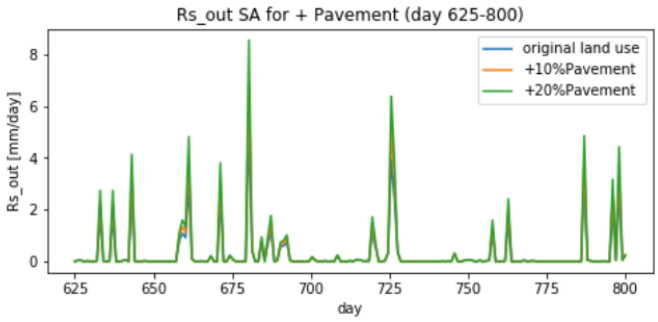


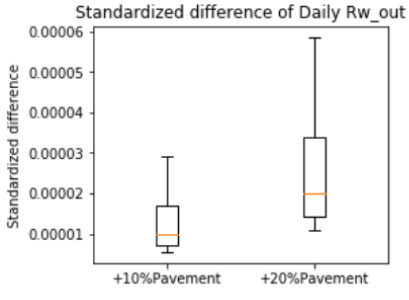


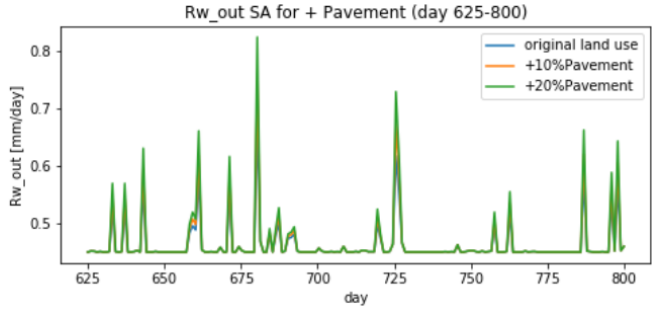

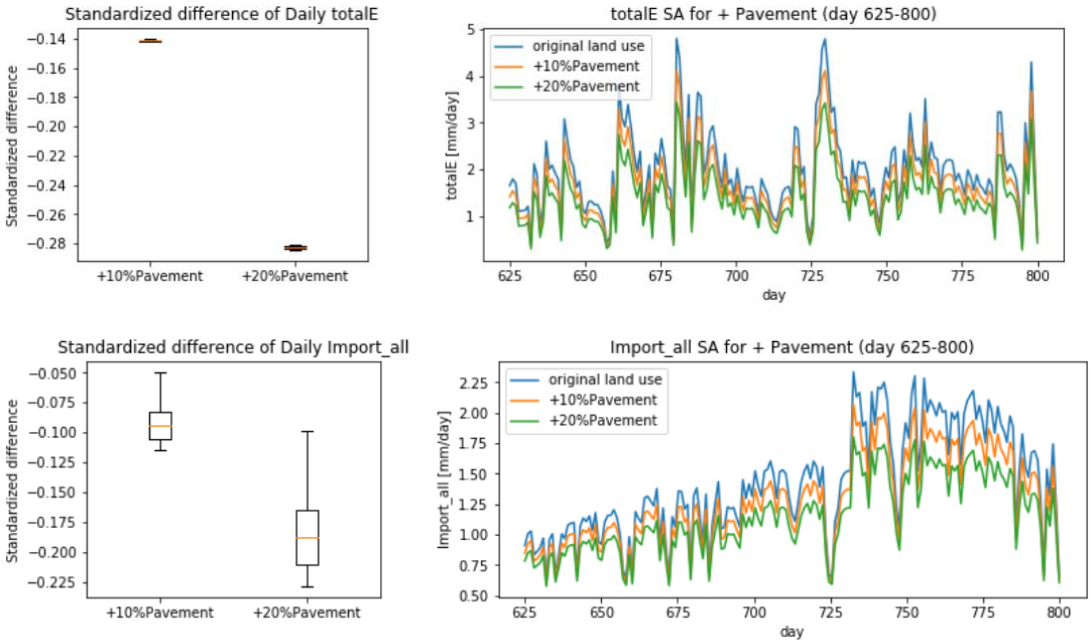


4-d. Change 10% of total area from pervious area to different impervious area (Scenario 1, 2, 3)

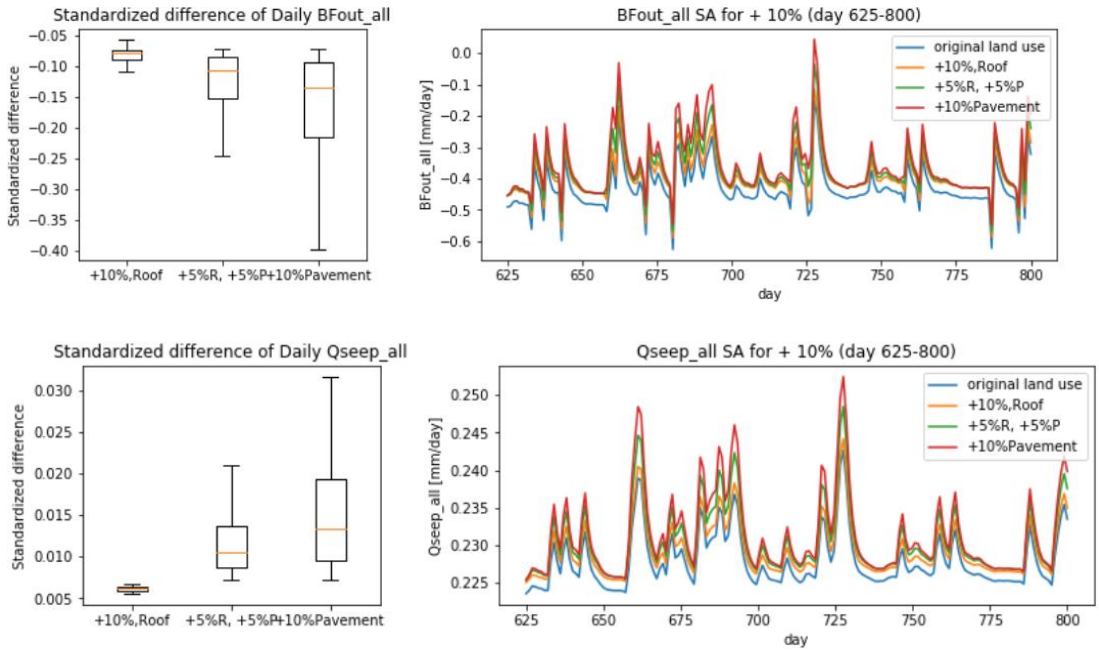

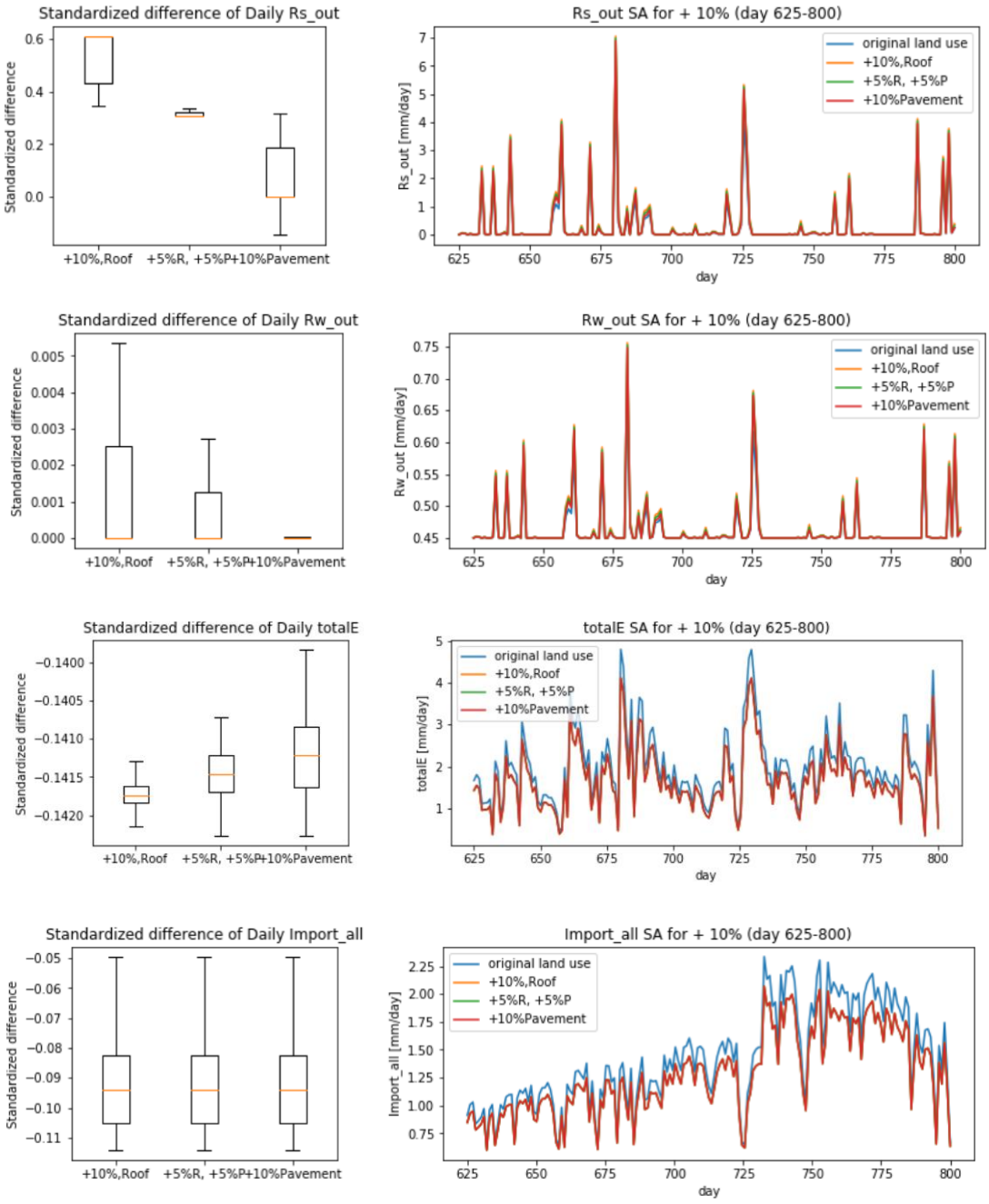


4-e. Change 20% of total area from pervious area to different impervious area (Scenario 4, 5, 6)

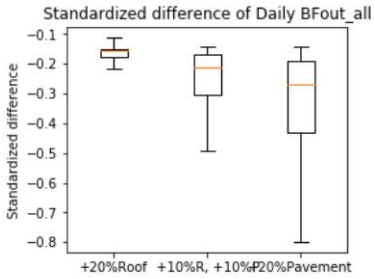
Standardized difference of Daily BFout_all
Standardized difference
+20%Roof
+10%R, +10%P
+20%Pavement

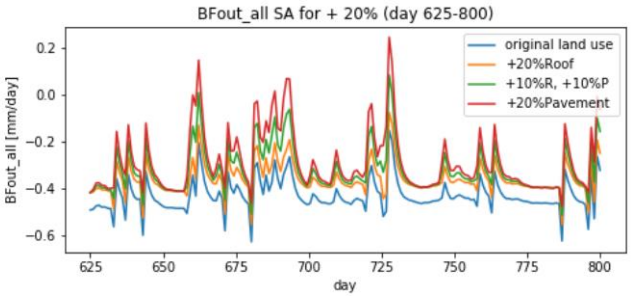
BFout_all SA for + 20% (day 625-800)
original land use
+20%Roof
+10%R, +10%P
+20%Pavement
BFout_all [mm/day]
day

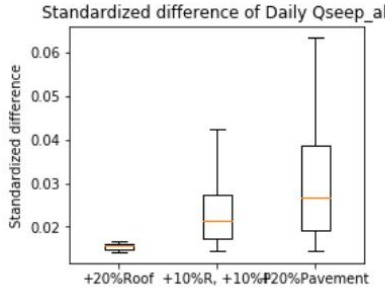
Standardized difference of Daily Qseep_all
Standardized difference
+20%Roof
+10%R, +10%P
+20%Pavement

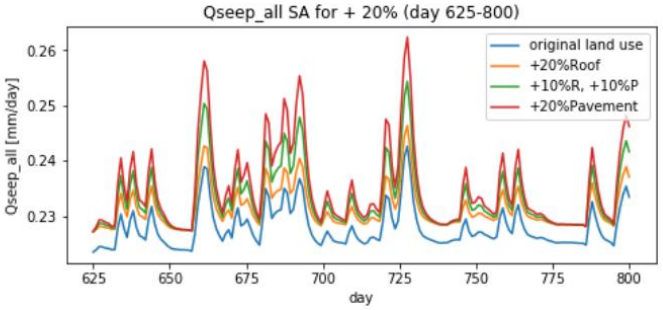
Qseep_all SA for + 20% (day 625-800)
original land use
+20%Roof
+10%R, +10%P
+20%Pavement
Qseep_all [mm/day]
day

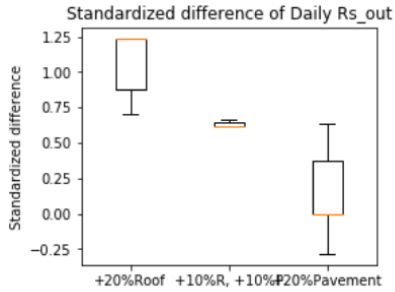
Standardized difference of Daily Rs_out
Standardized difference
+20%Roof
+10%R, +10%P
+20%Pavement

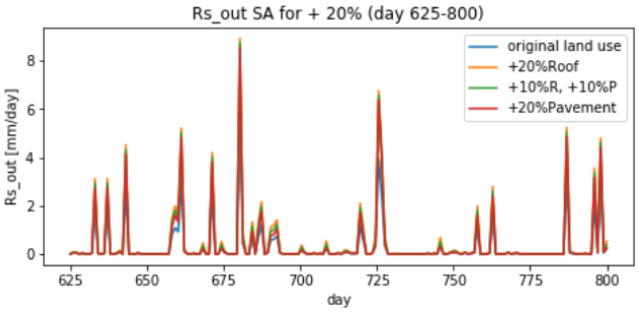
Rs_out SA for + 20% (day 625-800)
original land use
+20%Roof
+10%R, +10%P
+20%Pavement
Rs_out [mm/day]
day

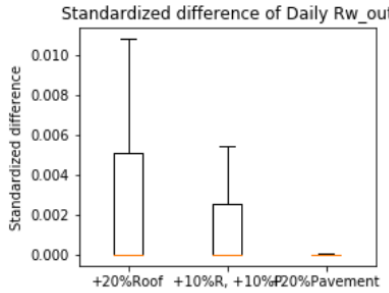
Standardized difference of Daily Rw_out
Standardized difference
+20%Roof
+10%R, +10%P
+20%Pavement

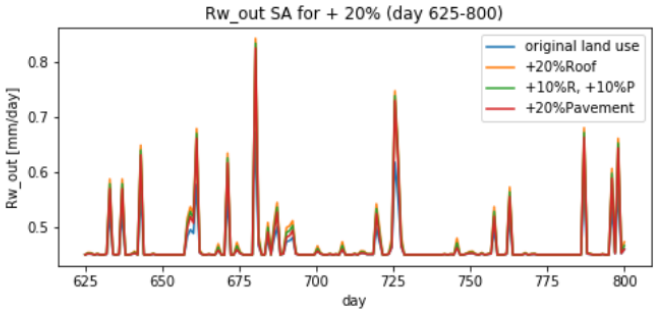
Rw_out SA for + 20% (day 625-800)
original land use
+20%Roof
+10%R, +10%P
+20%Pavement
Rw_out [mm/day]
day

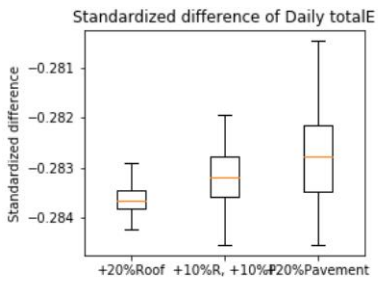
Standardized difference of Daily totalE
Standardized difference
+20%Roof
+10%R, +10%P
+20%Pavement

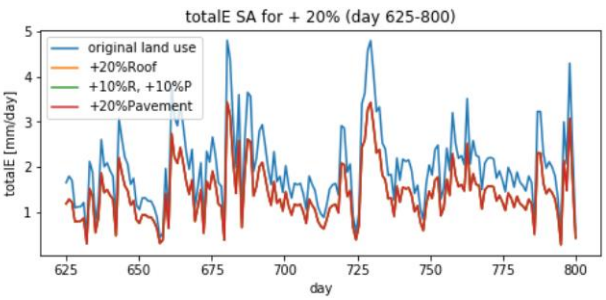
totalE SA for + 20% (day 625-800)
original land use
+20%Roof
+10%R, +10%P
+20%Pavement
totalE [mm/day]
day

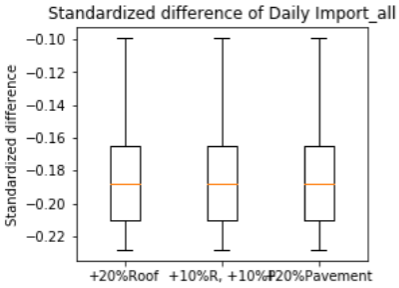
Standardized difference of Daily Import_all
Standardized difference
−0.10
−0.12
−0.14
−0.16
−0.18
−0.20
−0.22
+20%Roof
+10%R, +10%P
+20%Pavement

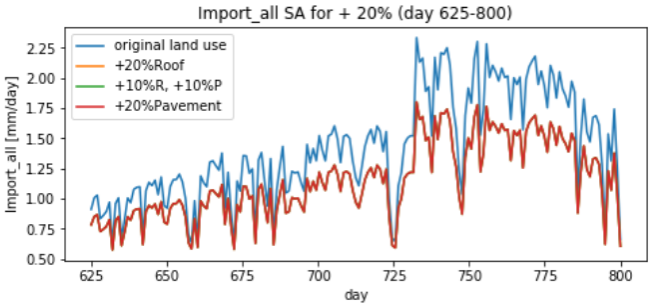
Import_all SA for + 20% (day 625-800)
original land use
+20%Roof
+10%R, +10%P
+20%Pavement
Import_all [mm/day]
2.25
2.00
1.75
1.50
1.25
1.00
0.75
0.50
625
650
675
700
725
750
775
800
day

## 5. Model result hydrograph of Case Fehraltorf.

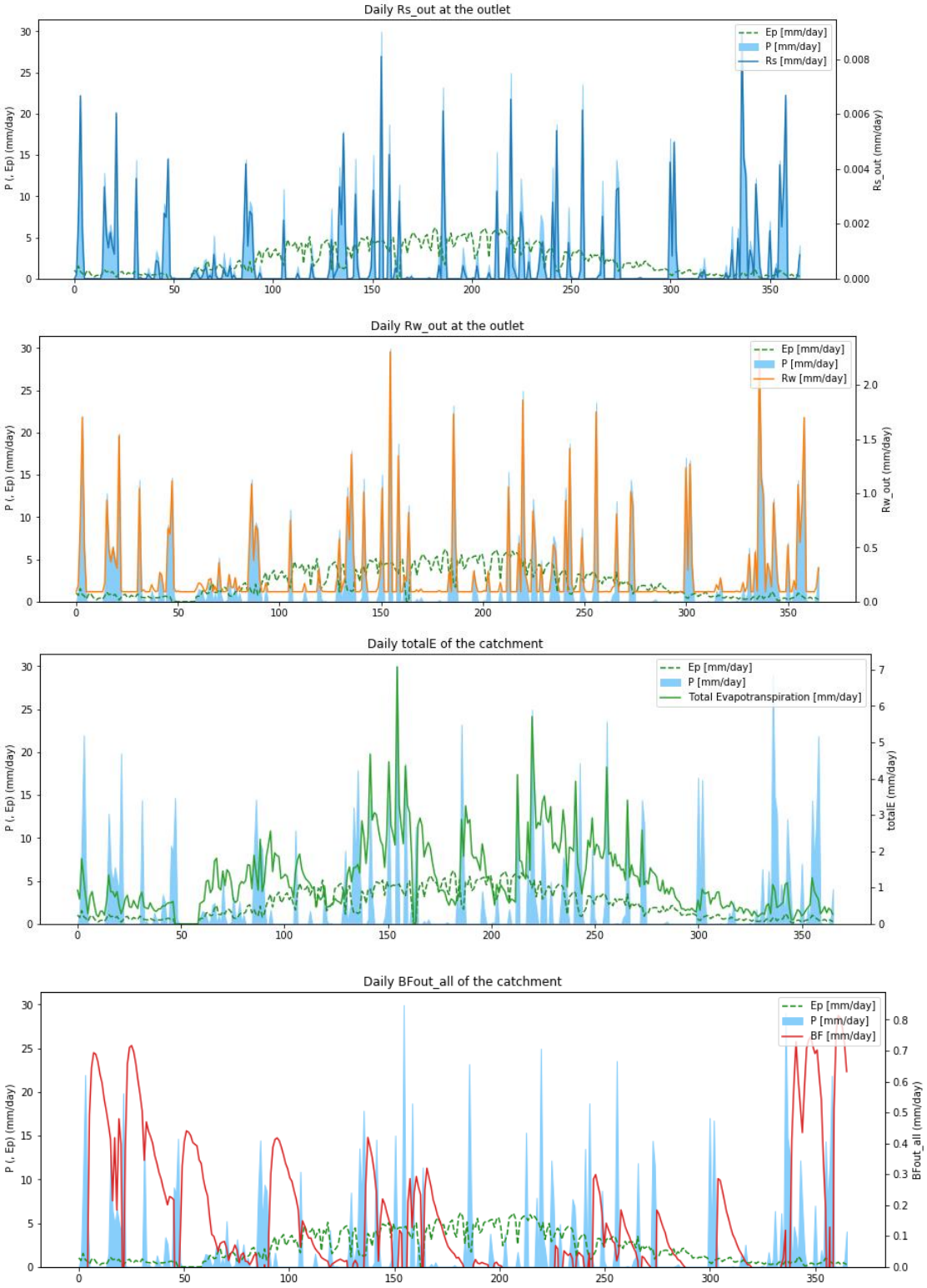

## 6. Parameter sensitivity analysis in Case Fehraltorf

### 6-a. Effective area of roof (ERA) [%]

Table A - 9. MSE list of different values of ERA to the resulting flows.

| | MSE_BFout_all | MSE_Qseep_all | MSE_Rs_out | MSE_Rw_out | MSE_totalE | MSE_Import_all |
|---|---|---|---|---|---|---|
| **60.0** | 0.103494 | 0.0 | 1.704195e+08 | 0.006459 | 0.000014 | 0.0 |
| **80.0** | 0.000000 | 0.0 | 0.000000e+00 | 0.000000 | 0.000000 | 0.0 |
| **100.0** | 0.132071 | 0.0 | 7.616992e+06 | 0.007075 | 0.000017 | 0.0 |

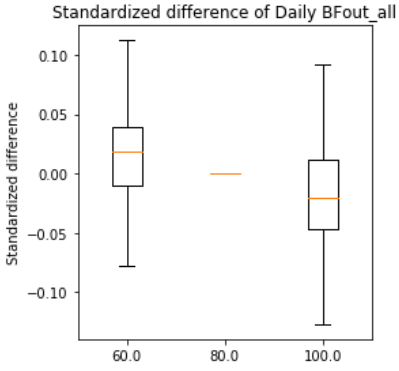


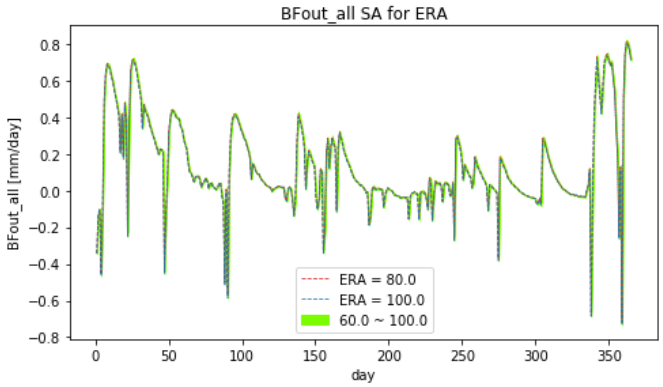


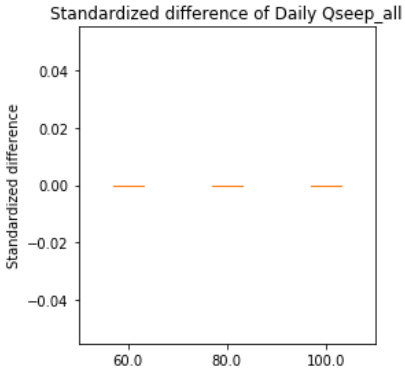


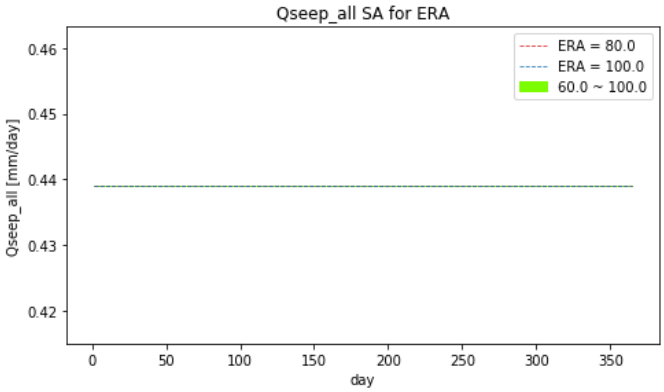


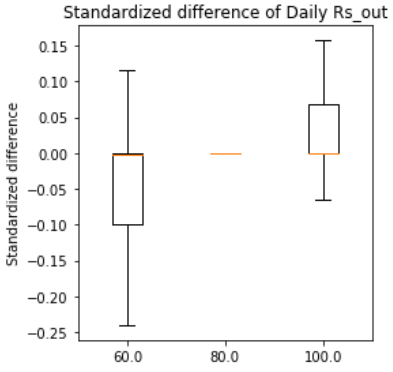


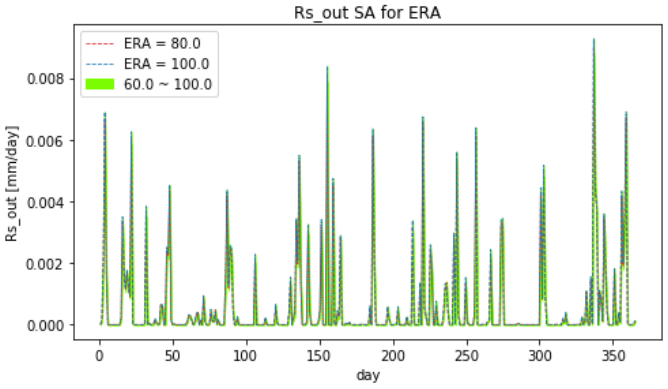

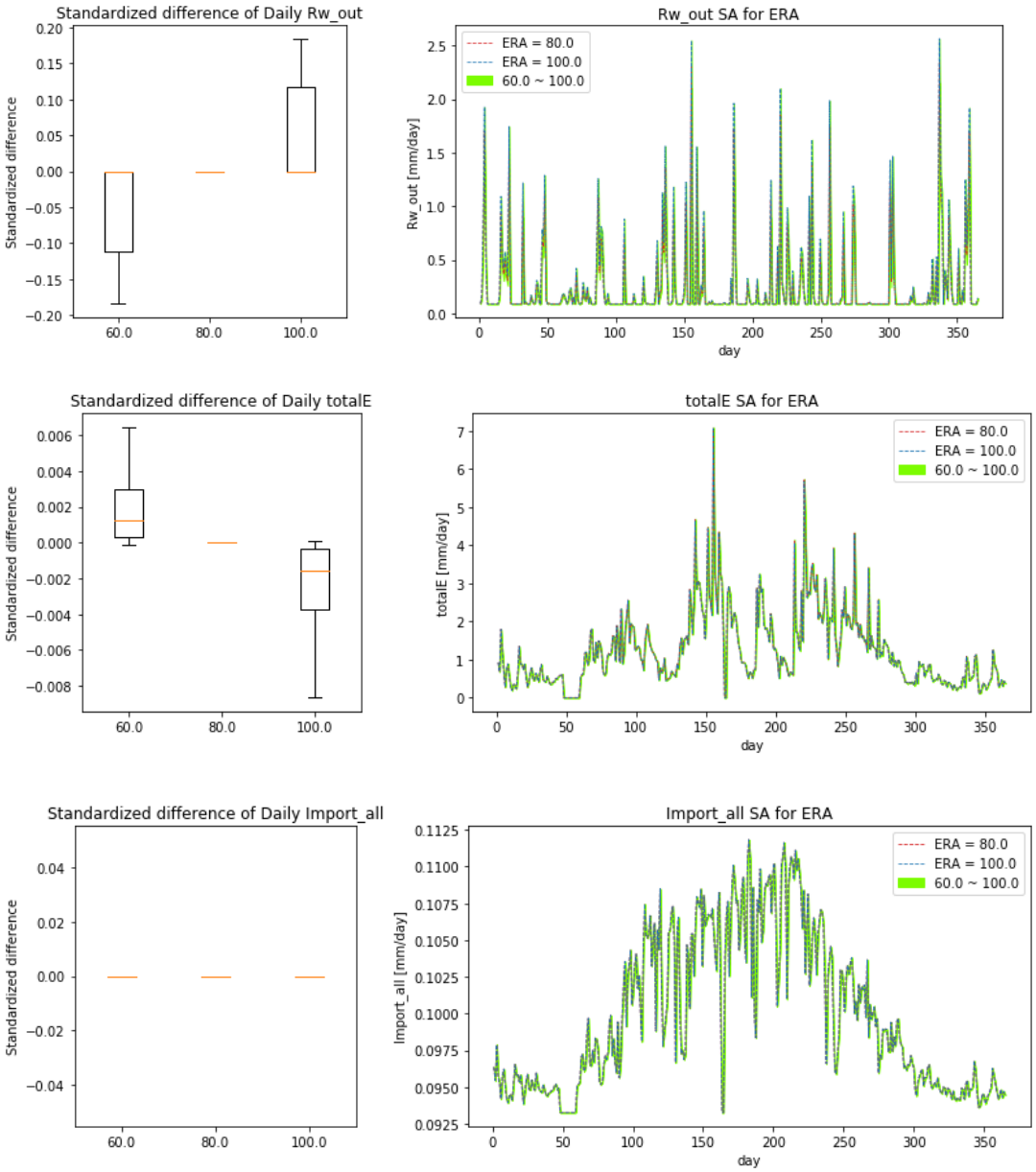


## 6-b. Effective area of pavement (EPA) [%]

Table A - 10. MSE list of different values of EPA to the resulting flows.

| | MSE_BFout_all | MSE_Qseep_all | MSE_Rs_out | MSE_Rw_out | MSE_totalE | MSE_Import_all |
|---|---|---|---|---|---|---|
| **30.0** | 0.007766 | 0.0 | 0.012624 | 0.000330 | 7.047743e-07 | 0.0 |
| **50.0** | 0.000000 | 0.0 | 0.000000 | 0.000000 | 0.000000e+00 | 0.0 |
| **70.0** | 0.007972 | 0.0 | 26.030100 | 0.000341 | 7.736670e-07 | 0.0 |

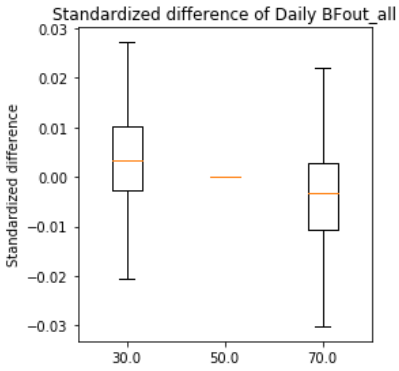
Standardized difference of Daily BFout_all
Standardized difference
0.03
0.02
0.01
0.00
−0.01
−0.02
−0.03
30.0
50.0
70.0

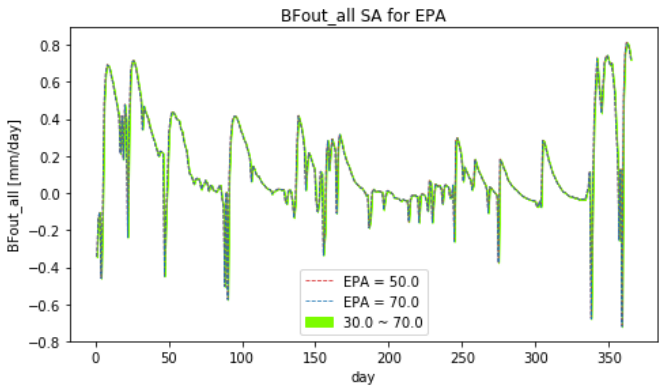
BFout_all SA for EPA
BFout_all [mm/day]
0.8
0.6
0.4
0.2
0.0
−0.2
−0.4
−0.6
−0.8
0
50
100
150
200
250
300
350
day
EPA = 50.0
EPA = 70.0
30.0 ~ 70.0

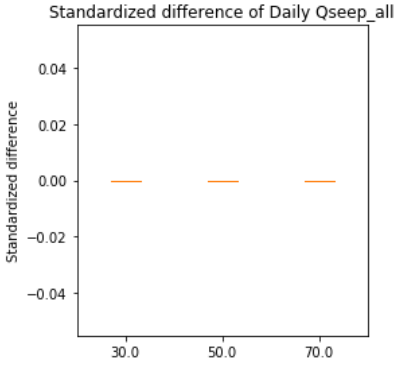
Standardized difference of Daily Qseep_all
Standardized difference
0.04
0.02
0.00
−0.02
−0.04
30.0
50.0
70.0

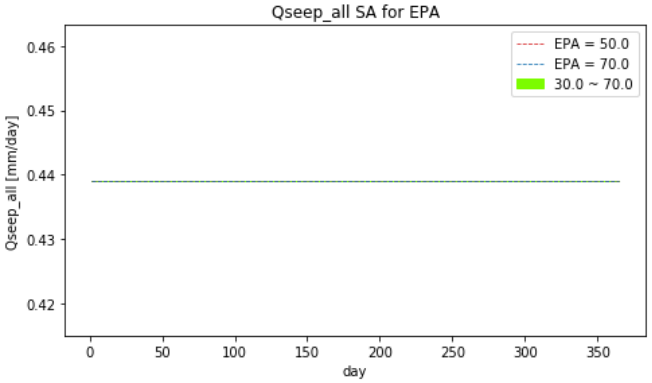
Qseep_all SA for EPA
Qseep_all [mm/day]
0.46
0.45
0.44
0.43
0.42
0
50
100
150
200
250
300
350
day
EPA = 50.0
EPA = 70.0
30.0 ~ 70.0

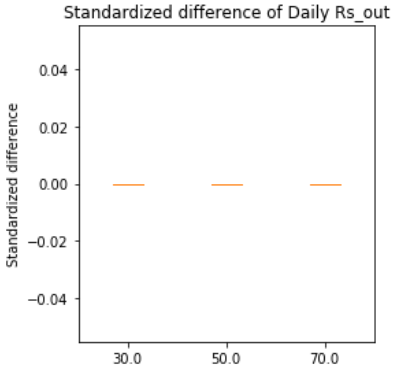
Standardized difference of Daily Rs_out
Standardized difference
0.04
0.02
0.00
−0.02
−0.04
30.0
50.0
70.0

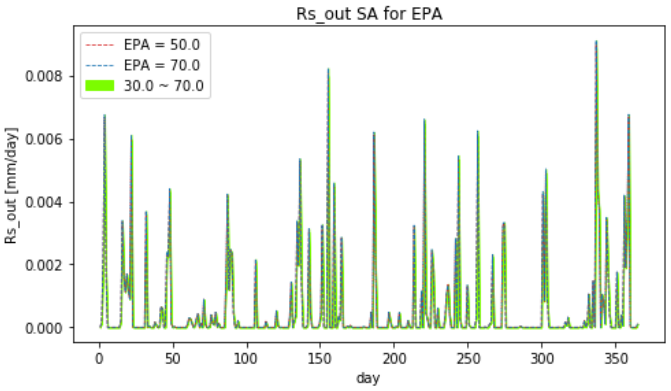
Rs_out SA for EPA
Rs_out [mm/day]
0.008
0.006
0.004
0.002
0.000
0
50
100
150
200
250
300
350
day
EPA = 50.0
EPA = 70.0
30.0 ~ 70.0

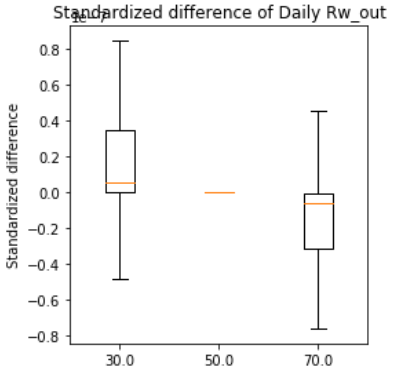
Standardized difference of Daily Rw_out
Standardized difference
0.8
0.6
0.4
0.2
0.0
−0.2
−0.4
−0.6
−0.8
30.0
50.0
70.0

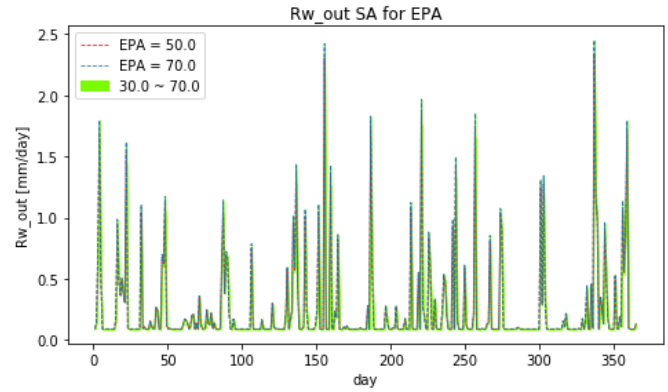
Rw_out SA for EPA
Rw_out [mm/day]
2.5
2.0
1.5
1.0
0.5
0.0
0
50
100
150
200
250
300
350
day
EPA = 50.0
EPA = 70.0
30.0 ~ 70.0

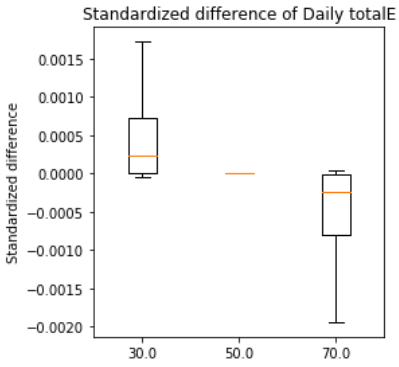


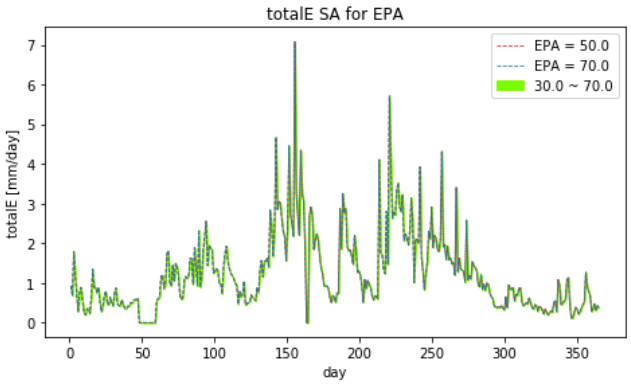


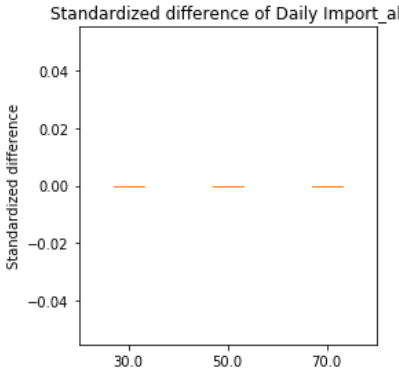


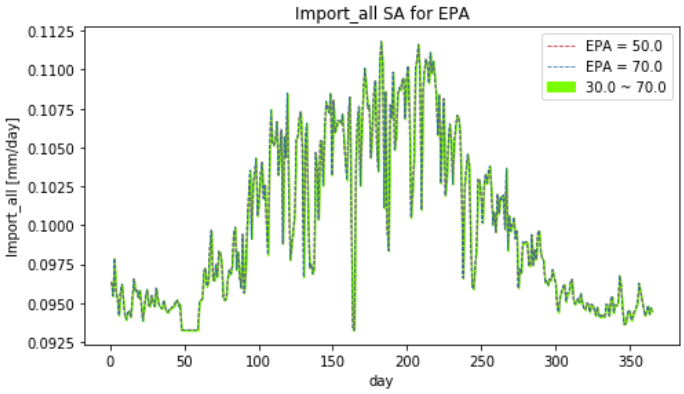


## 6-c. Pervious area initial loss (PerIL) [mm/day]

Table A - 11. MSE list of different values of PerIL to the resulting flows.

| | MSE_BFout_all | MSE_Qseep_all | MSE_Rs_out | MSE_Rw_out | MSE_totalE | MSE_Import_all |
|---|---|---|---|---|---|---|
| **5.0** | 0.000204 | 0.0 | 6.164396e+08 | 0.000050 | 0.000006 | 0.0 |
| **8.0** | 0.000000 | 0.0 | 0.000000e+00 | 0.000000 | 0.000000 | 0.0 |
| **11.0** | 0.000186 | 0.0 | 1.015942e+35 | 0.000027 | 0.000005 | 0.0 |

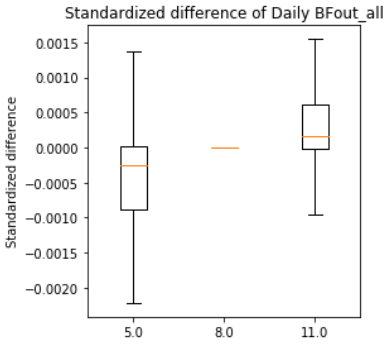


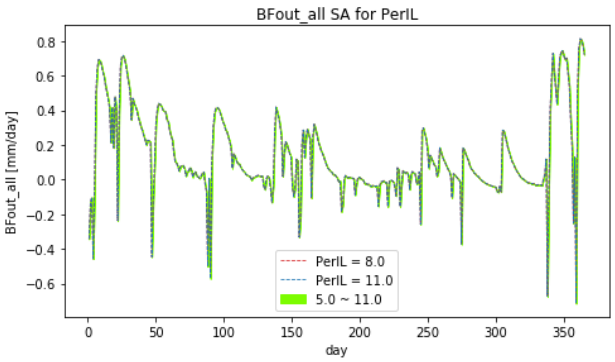

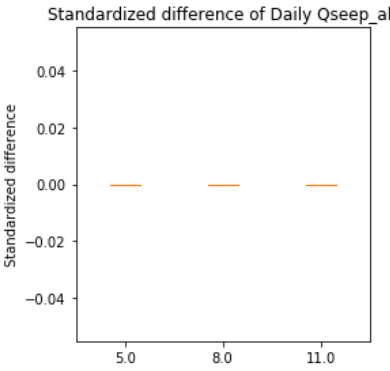
Standardized difference of Daily Qseep_all
Standardized difference
0.04
0.02
0.00
−0.02
−0.04
5.0
8.0
11.0

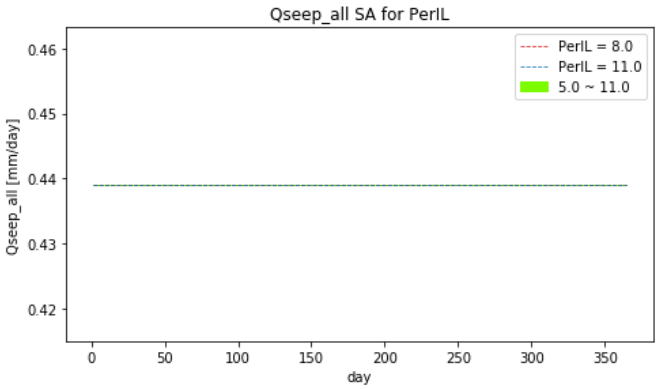
Qseep_all SA for PerIL
PerIL = 8.0
PerIL = 11.0
5.0 ~ 11.0
Qseep_all [mm/day]
0.46
0.45
0.44
0.43
0.42
0
50
100
150
200
250
300
350
day

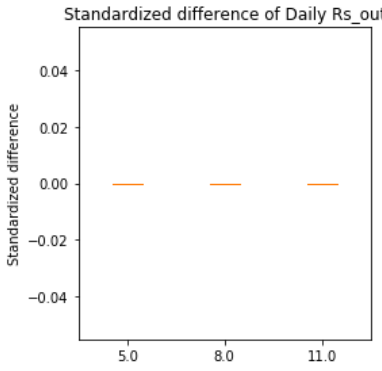
Standardized difference of Daily Rs_out
Standardized difference
0.04
0.02
0.00
−0.02
−0.04
5.0
8.0
11.0

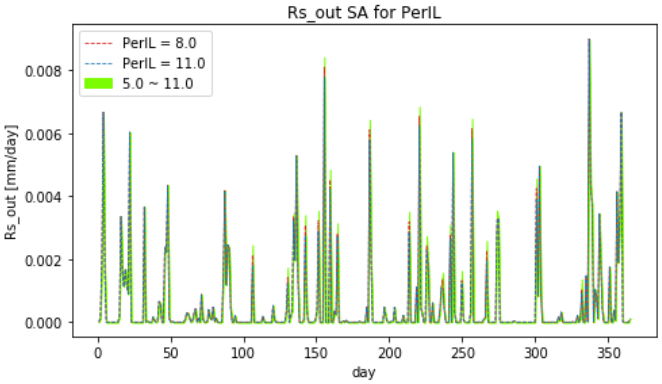
Rs_out SA for PerIL
PerIL = 8.0
PerIL = 11.0
5.0 ~ 11.0
Rs_out [mm/day]
0.008
0.006
0.004
0.002
0.000
0
50
100
150
200
250
300
350
day

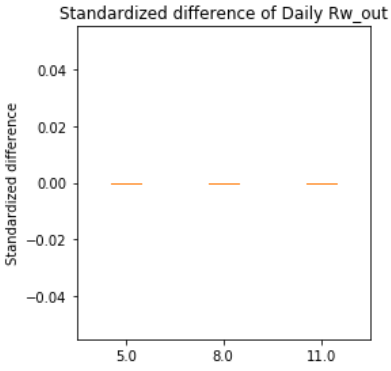
Standardized difference of Daily Rw_out
Standardized difference
0.04
0.02
0.00
−0.02
−0.04
5.0
8.0
11.0

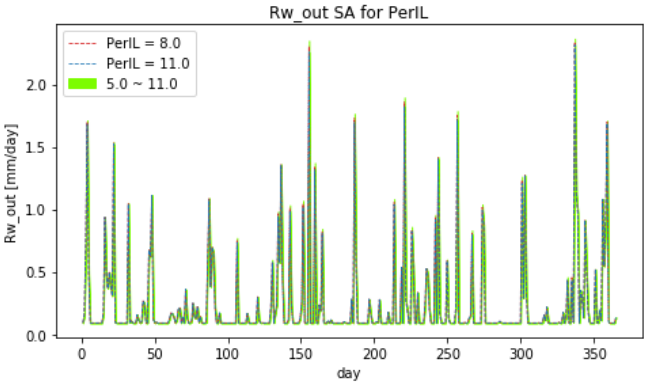
Rw_out SA for PerIL
PerIL = 8.0
PerIL = 11.0
5.0 ~ 11.0
Rw_out [mm/day]
2.0
1.5
1.0
0.5
0.0
0
50
100
150
200
250
300
350
day

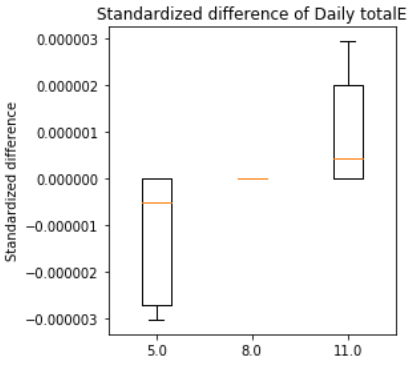
Standardized difference of Daily totalE
Standardized difference
0.000003
0.000002
0.000001
0.000000
−0.000001
−0.000002
−0.000003
5.0
8.0
11.0

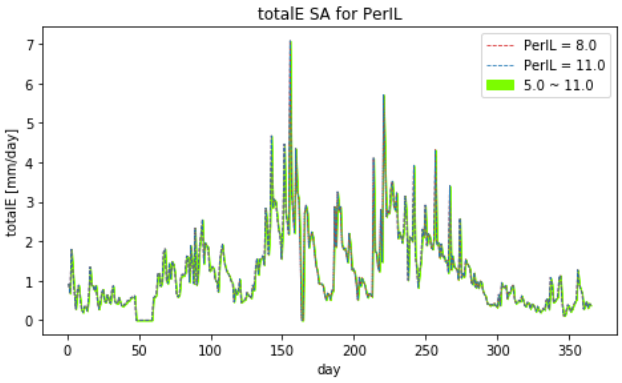
totalE SA for PerIL
PerIL = 8.0
PerIL = 11.0
5.0 ~ 11.0
totalE [mm/day]
7
6
5
4
3
2
1
0
0
50
100
150
200
250
300
350
day

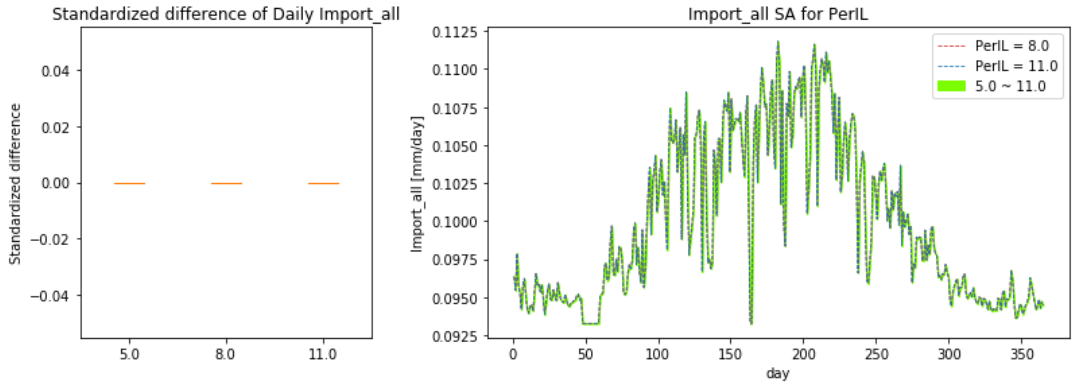


## 6-d. Infiltration capacity of paved area (Infilc_p) [mm/day]

Table A - 12. MSE list of different values of Infilc_p to the resulting flows.

| | MSE_BFout_all | MSE_Qseep_all | MSE_Rs_out | MSE_Rw_out | MSE_totalE | MSE_Import_all |
|---|---|---|---|---|---|---|
| **1.0** | 0.127783 | 0.0 | 0.404527 | 0.003640 | 0.000007 | 0.0 |
| **5.0** | 0.000000 | 0.0 | 0.000000 | 0.000000 | 0.000000 | 0.0 |
| **10.0** | 0.102928 | 0.0 | 17.095976 | 0.001056 | 0.000002 | 0.0 |

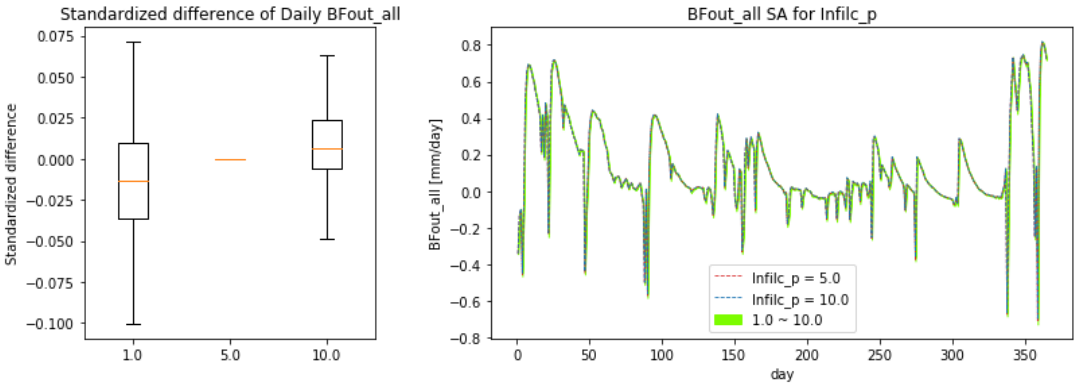


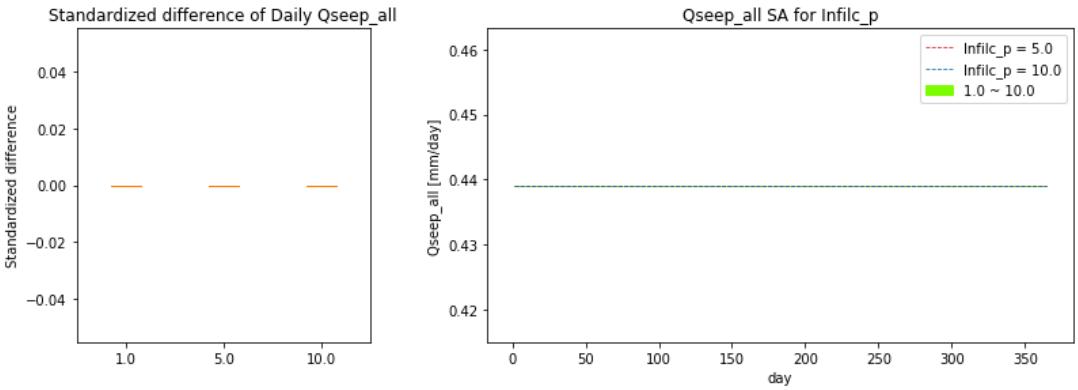

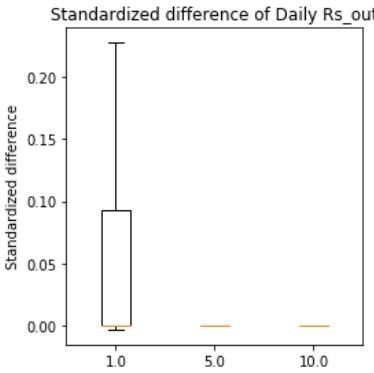
Standardized difference of Daily Rs_out
Standardized difference
0.20
0.15
0.10
0.05
0.00
1.0
5.0
10.0

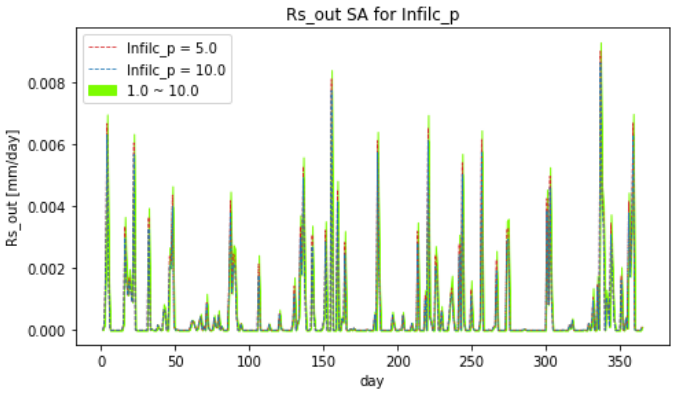
Rs_out SA for Infilc_p
Infilc_p = 5.0
Infilc_p = 10.0
1.0 ~ 10.0
Rs_out [mm/day]
0.008
0.006
0.004
0.002
0.000
0
50
100
150
200
250
300
350
day

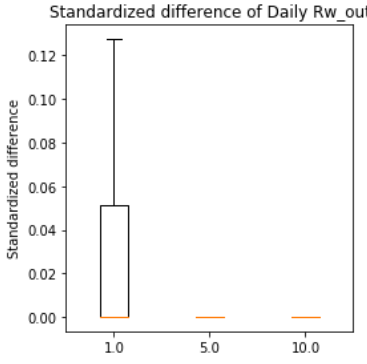
Standardized difference of Daily Rw_out
Standardized difference
0.12
0.10
0.08
0.06
0.04
0.02
0.00
1.0
5.0
10.0

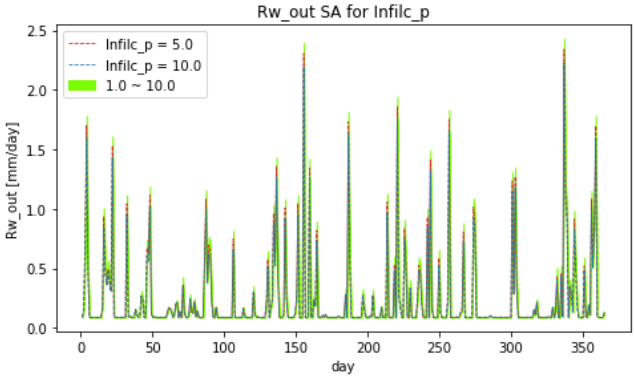
Rw_out SA for Infilc_p
Infilc_p = 5.0
Infilc_p = 10.0
1.0 ~ 10.0
Rw_out [mm/day]
2.5
2.0
1.5
1.0
0.5
0.0
0
50
100
150
200
250
300
350
day

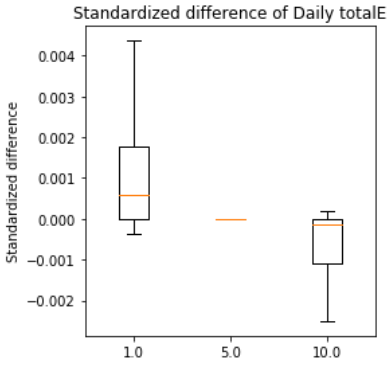
Standardized difference of Daily totalE
Standardized difference
0.004
0.003
0.002
0.001
0.000
−0.001
−0.002
1.0
5.0
10.0

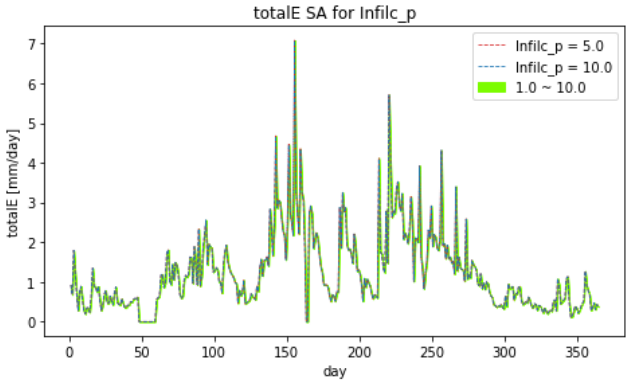
totalE SA for Infilc_p
Infilc_p = 5.0
Infilc_p = 10.0
1.0 ~ 10.0
totalE [mm/day]
7
6
5
4
3
2
1
0
0
50
100
150
200
250
300
350
day

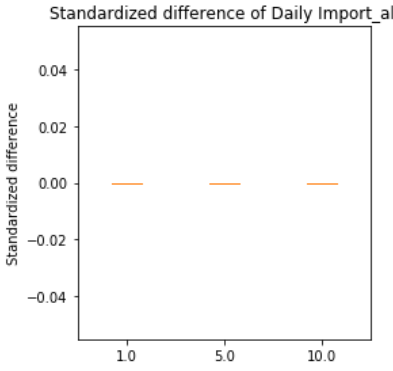
Standardized difference of Daily Import_all
Standardized difference
0.04
0.02
0.00
−0.02
−0.04
1.0
5.0
10.0

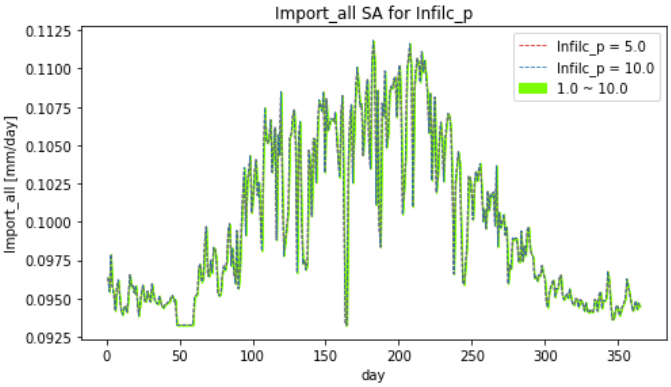
Import_all SA for Infilc_p
Infilc_p = 5.0
Infilc_p = 10.0
1.0 ~ 10.0
Import_all [mm/day]
0.1125
0.1100
0.1075
0.1050
0.1025
0.1000
0.0975
0.0950
0.0925
0
50
100
150
200
250
300
350
day

## 6-e. Infiltration capacity of pervious area (Infilc_per) [mm/day]

Table A - 13. MSE list of different values of Infilc_per to the resulting flows.

| | MSE_BFout_all | MSE_Qseep_all | MSE_Rs_out | MSE_Rw_out | MSE_totalE | MSE_Import_all |
|---|---|---|---|---|---|---|
| **20.0** | 1.003865 | 0.0 | 6.869788e+30 | 0.000614 | 0.006666 | 0.0 |
| **35.0** | 0.000000 | 0.0 | 0.000000e+00 | 0.000000 | 0.000000 | 0.0 |
| **50.0** | 0.200586 | 0.0 | 5.116511e+31 | 0.000016 | 0.001123 | 0.0 |

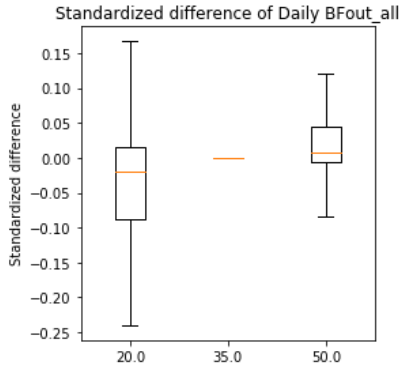


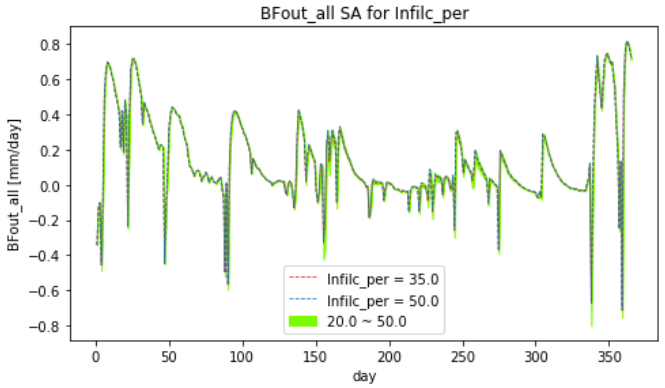


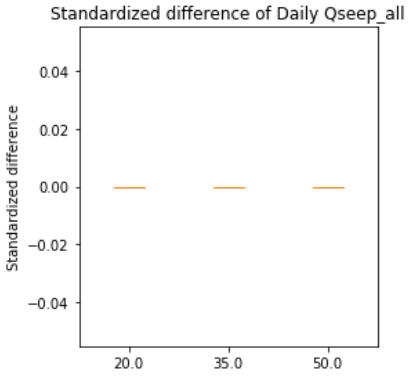


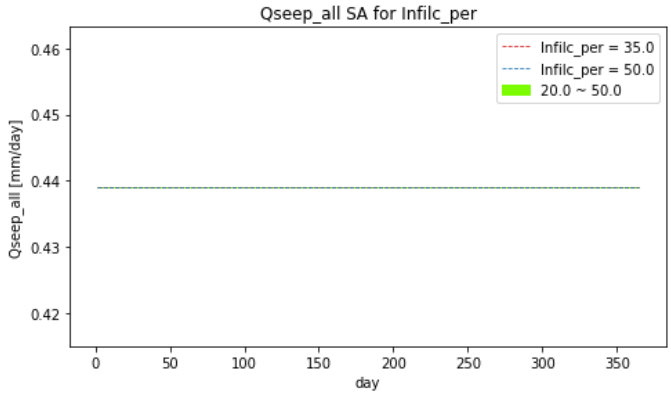


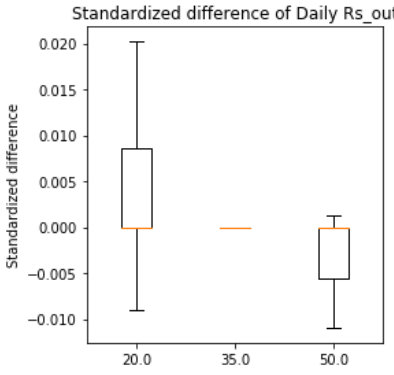


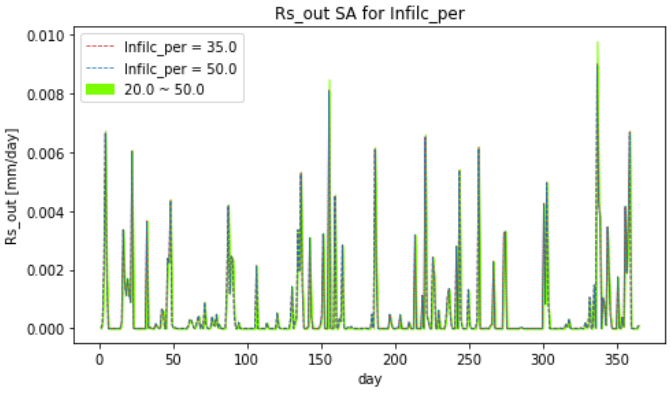

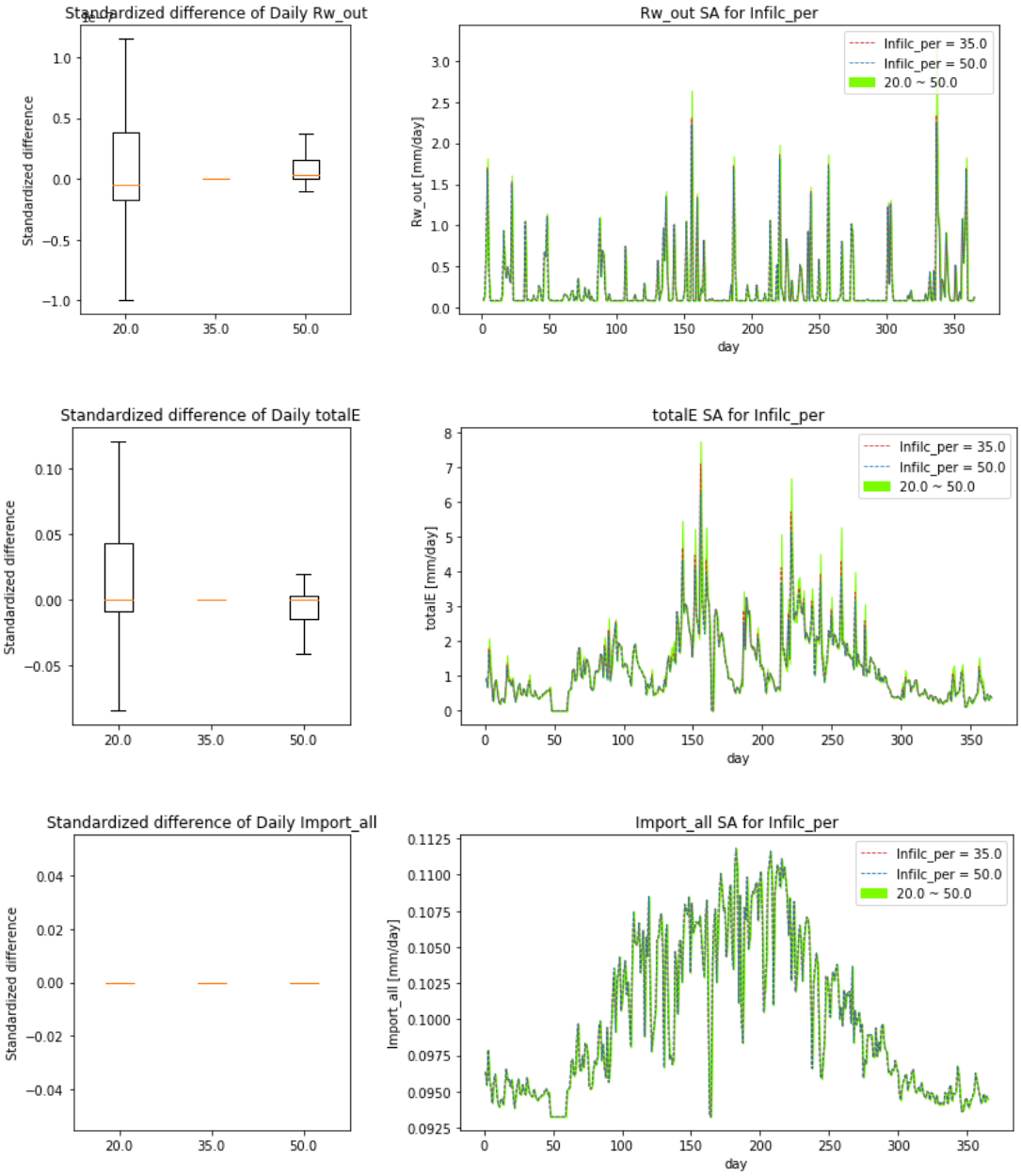


## 6-f. Leakage rate (LR) [%]

Table A - 14. MSE list of different values of LR to the resulting flows.

| | MSE_BFout_all | MSE_Qseep_all | MSE_Rs_out | MSE_Rw_out | MSE_totalE | MSE_Import_all |
|---|---|---|---|---|---|---|
| **0.5** | 0.004991 | 0.0 | 0.0 | 5.188149e-18 | 9.930370e-11 | 0.000404 |
| **2.5** | 0.000000 | 0.0 | 0.0 | 0.000000e+00 | 0.000000e+00 | 0.000000 |
| **4.5** | 0.005418 | 0.0 | 0.0 | 5.632086e-18 | 1.063662e-10 | 0.000439 |

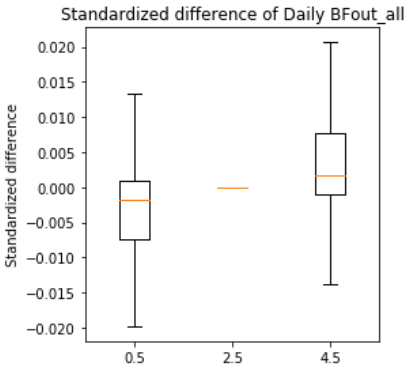
Standardized difference of Daily BFout_all
Standardized difference
0.020
0.015
0.010
0.005
0.000
−0.005
−0.010
−0.015
−0.020
0.5
2.5
4.5

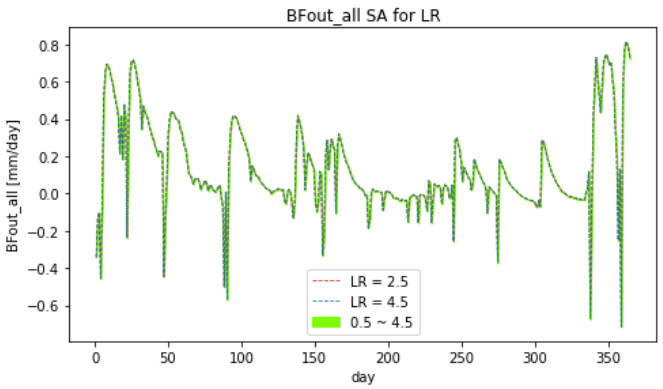
BFout_all SA for LR
BFout_all [mm/day]
0.8
0.6
0.4
0.2
0.0
−0.2
−0.4
−0.6
LR = 2.5
LR = 4.5
0.5 ~ 4.5
0
50
100
150
200
250
300
350
day

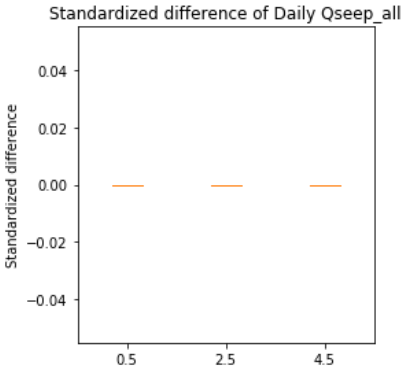
Standardized difference of Daily Qseep_all
Standardized difference
0.04
0.02
0.00
−0.02
−0.04
0.5
2.5
4.5

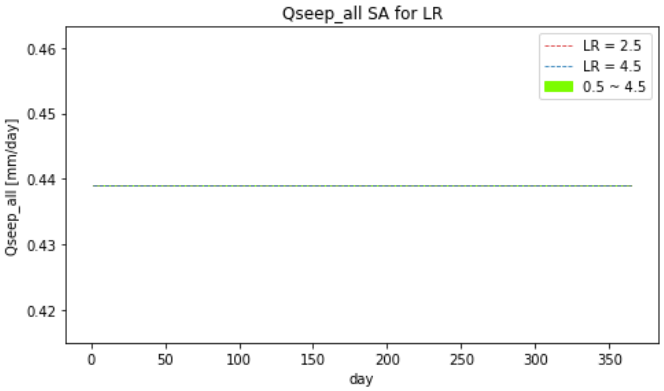
Qseep_all SA for LR
Qseep_all [mm/day]
0.46
0.45
0.44
0.43
0.42
LR = 2.5
LR = 4.5
0.5 ~ 4.5
0
50
100
150
200
250
300
350
day

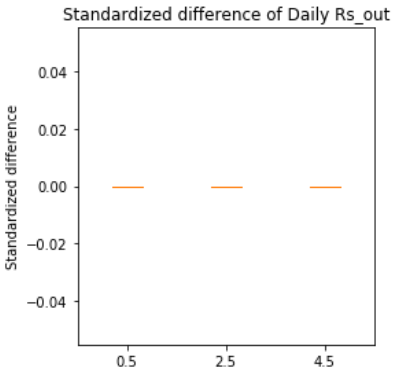
Standardized difference of Daily Rs_out
Standardized difference
0.04
0.02
0.00
−0.02
−0.04
0.5
2.5
4.5

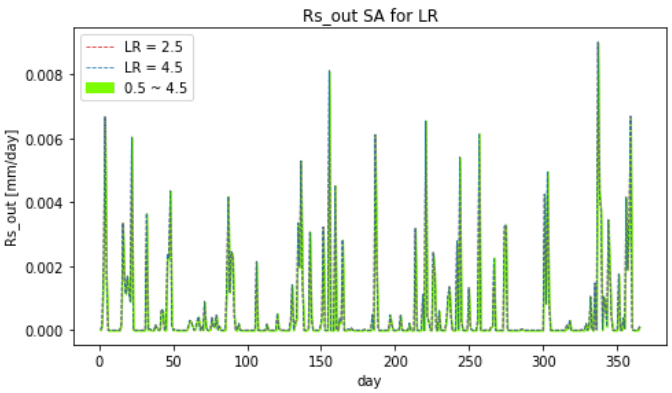
Rs_out SA for LR
Rs_out [mm/day]
0.008
0.006
0.004
0.002
0.000
LR = 2.5
LR = 4.5
0.5 ~ 4.5
0
50
100
150
200
250
300
350
day

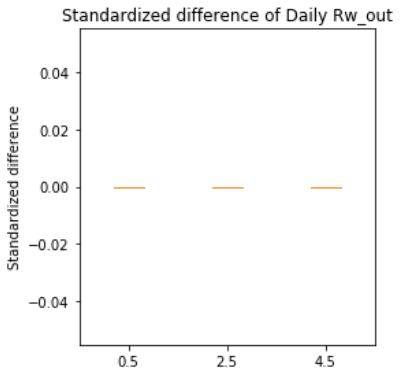
Standardized difference of Daily Rw_out
Standardized difference
0.04
0.02
0.00
−0.02
−0.04
0.5
2.5
4.5

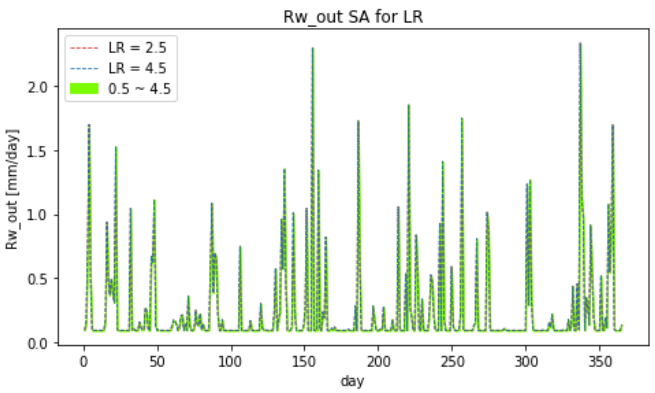
Rw_out SA for LR
Rw_out [mm/day]
2.0
1.5
1.0
0.5
0.0
LR = 2.5
LR = 4.5
0.5 ~ 4.5
0
50
100
150
200
250
300
350
day

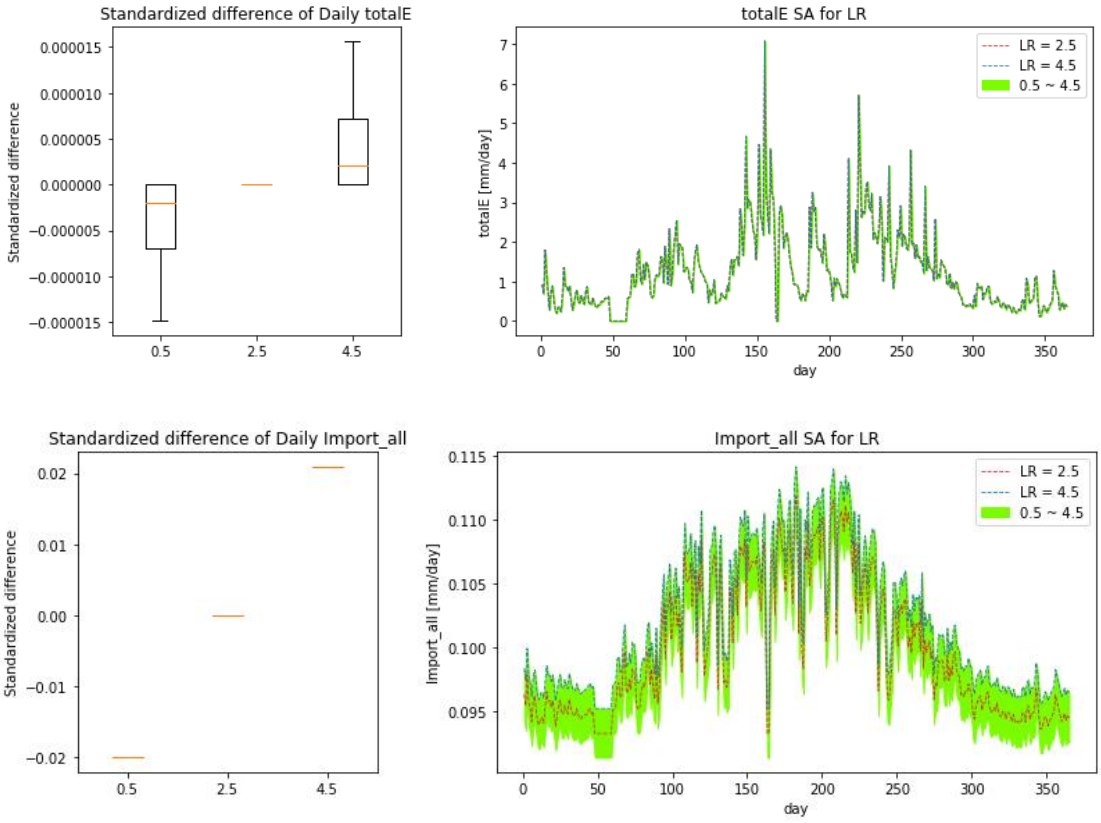


6-g. Parallel drainage resistance (w) [day]

Table A - 15. MSE list of different values of w to the resulting flow.

| | MSE_BFout_all | MSE_Qseep_all | MSE_Rs_out | MSE_Rw_out | MSE_totalE | MSE_Import_all |
|---|---|---|---|---|---|---|
| **10.0** | 17.674677 | 0.0 | 0.0 | 2.862994e-12 | 1.361452e-07 | 0.0 |
| **25.0** | 0.000000 | 0.0 | 0.0 | 0.000000e+00 | 0.000000e+00 | 0.0 |
| **50.0** | 14.100877 | 0.0 | 0.0 | 7.774207e-12 | 2.335596e-07 | 0.0 |

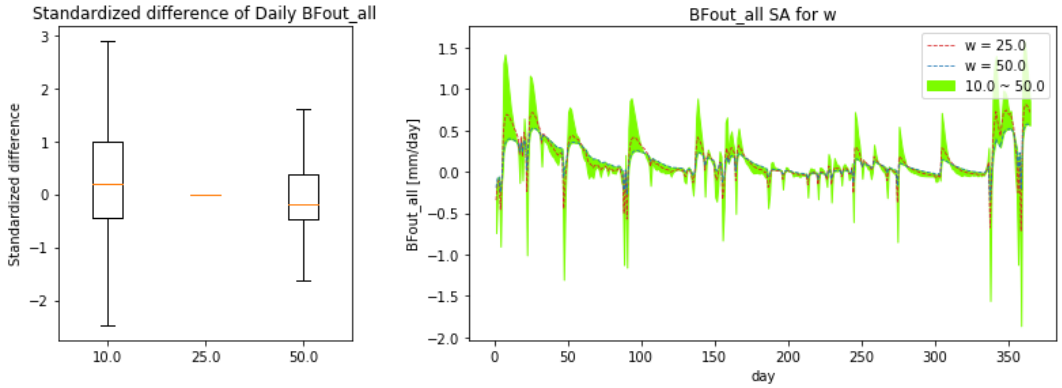

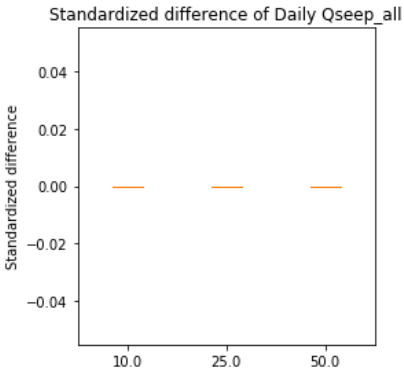
Standardized difference of Daily Qseep_all
Standardized difference
0.04
0.02
0.00
−0.02
−0.04
10.0
25.0
50.0

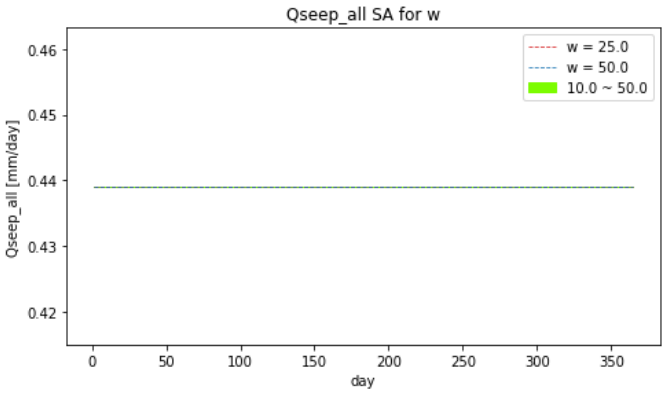
Qseep_all SA for w
w = 25.0
w = 50.0
10.0 ~ 50.0
Qseep_all [mm/day]
0.46
0.45
0.44
0.43
0.42
0
50
100
150
200
250
300
350
day

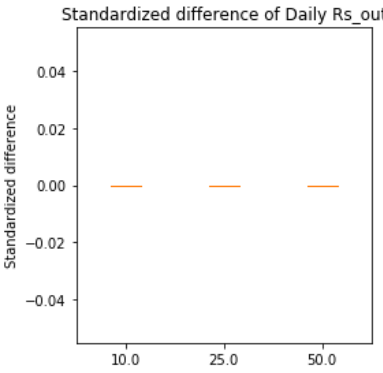
Standardized difference of Daily Rs_out
Standardized difference
0.04
0.02
0.00
−0.02
−0.04
10.0
25.0
50.0

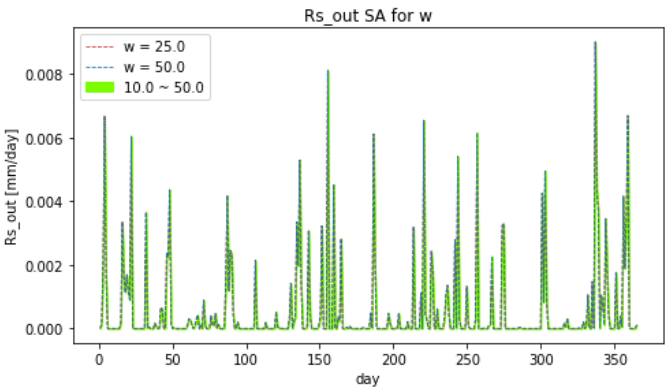
Rs_out SA for w
w = 25.0
w = 50.0
10.0 ~ 50.0
Rs_out [mm/day]
0.008
0.006
0.004
0.002
0.000
0
50
100
150
200
250
300
350
day

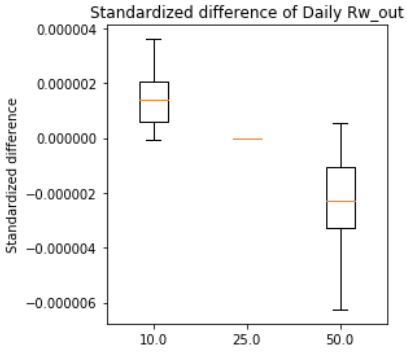
Standardized difference of Daily Rw_out
Standardized difference
0.000004
0.000002
0.000000
−0.000002
−0.000004
−0.000006
10.0
25.0
50.0

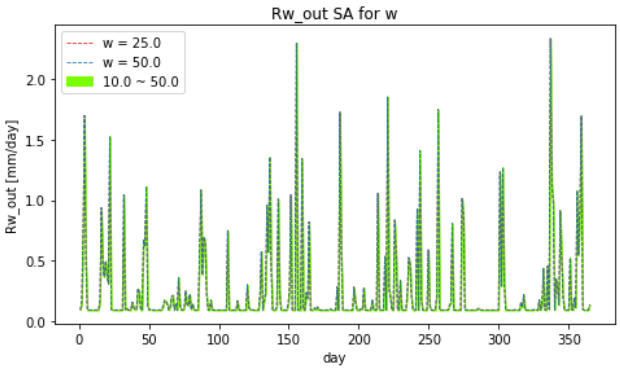
Rw_out SA for w
w = 25.0
w = 50.0
10.0 ~ 50.0
Rw_out [mm/day]
2.0
1.5
1.0
0.5
0.0
0
50
100
150
200
250
300
350
day

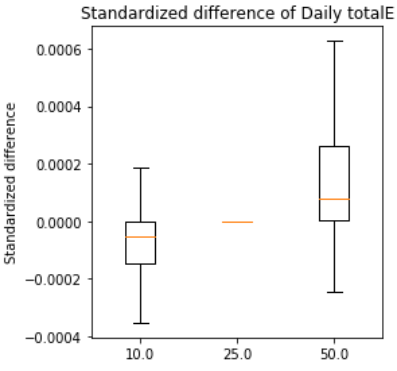
Standardized difference of Daily totalE
Standardized difference
0.0006
0.0004
0.0002
0.0000
−0.0002
−0.0004
10.0
25.0
50.0

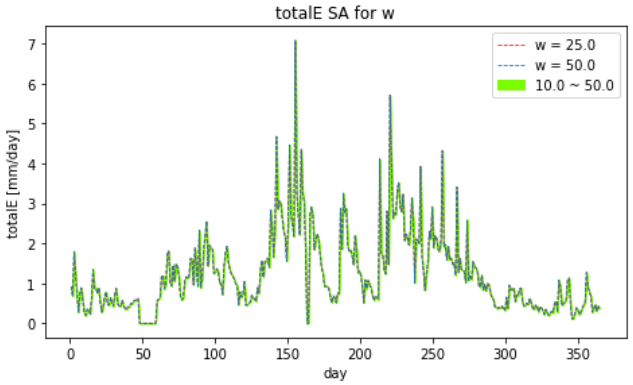
totalE SA for w
w = 25.0
w = 50.0
10.0 ~ 50.0
totalE [mm/day]
7
6
5
4
3
2
1
0
0
50
100
150
200
250
300
350
day

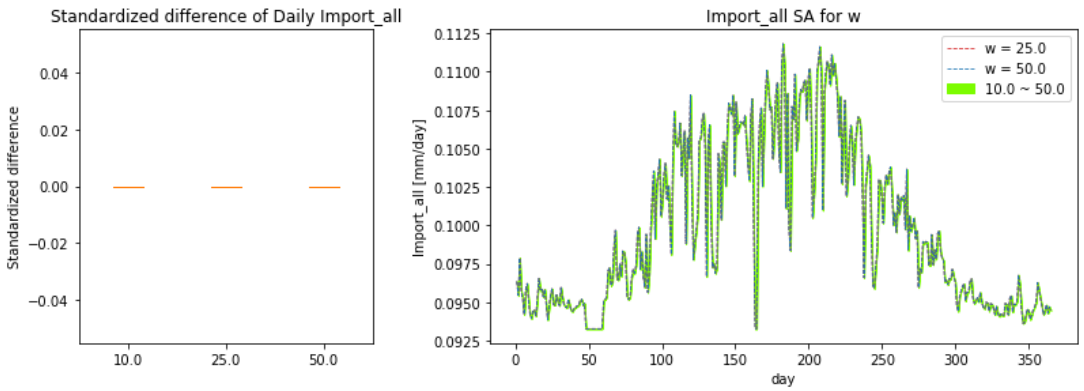


## 6-h. Constant deep seeapage (down_seep) [mm/day]

Table A - 16. MSE list of different values of down_seep to the resulting flows.

| | MSE_BFout_all | MSE_Qseep_all | MSE_Rs_out | MSE_Rw_out | MSE_totalE | MSE_Import_all |
|---|---|---|---|---|---|---|
| **0.5** | 60.848288 | 0.413265 | 0.0 | 9.105509e-11 | 0.000024 | 0.0 |
| **1.4** | 0.000000 | 0.000000 | 0.0 | 0.000000e+00 | 0.000000 | 0.0 |
| **2.5** | 91.025782 | 0.617347 | 0.0 | 6.355536e-12 | 0.000024 | 0.0 |

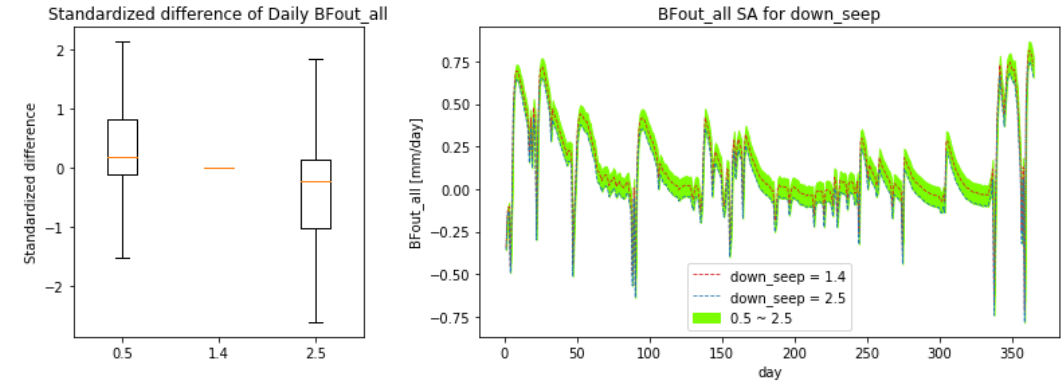


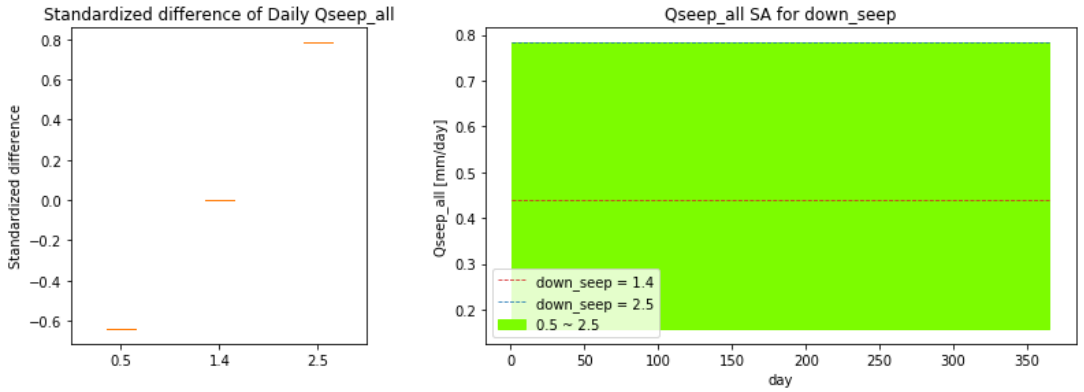

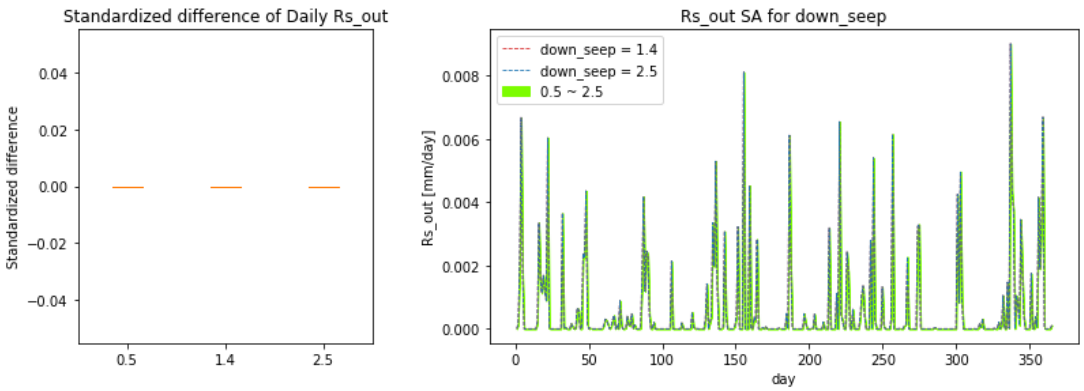
Standardized difference of Daily Rs_out
Standardized difference
0.04
0.02
0.00
−0.02
−0.04
0.5
1.4
2.5


Rs_out SA for down_seep
down_seep = 1.4
down_seep = 2.5
0.5 ~ 2.5
Rs_out [mm/day]
0.008
0.006
0.004
0.002
0.000
0
50
100
150
200
250
300
350
day

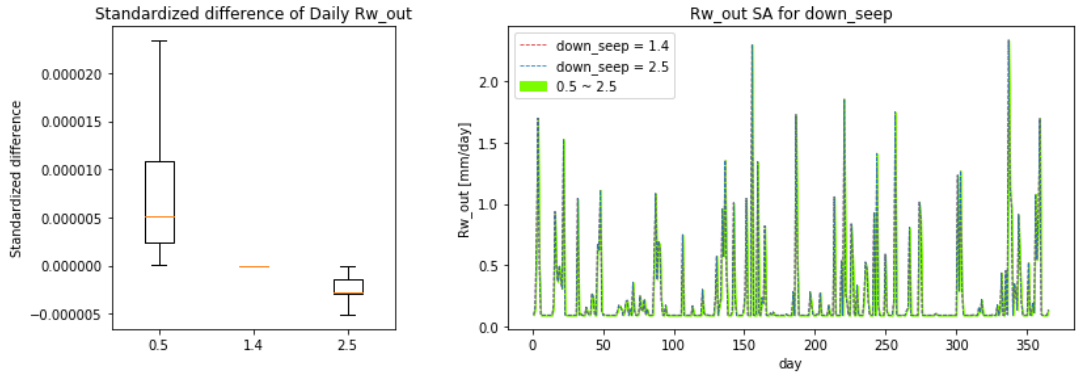
Standardized difference of Daily Rw_out
Standardized difference
0.000020
0.000015
0.000010
0.000005
0.000000
−0.000005
0.5
1.4
2.5


Rw_out SA for down_seep
down_seep = 1.4
down_seep = 2.5
0.5 ~ 2.5
Rw_out [mm/day]
2.0
1.5
1.0
0.5
0.0
0
50
100
150
200
250
300
350
day

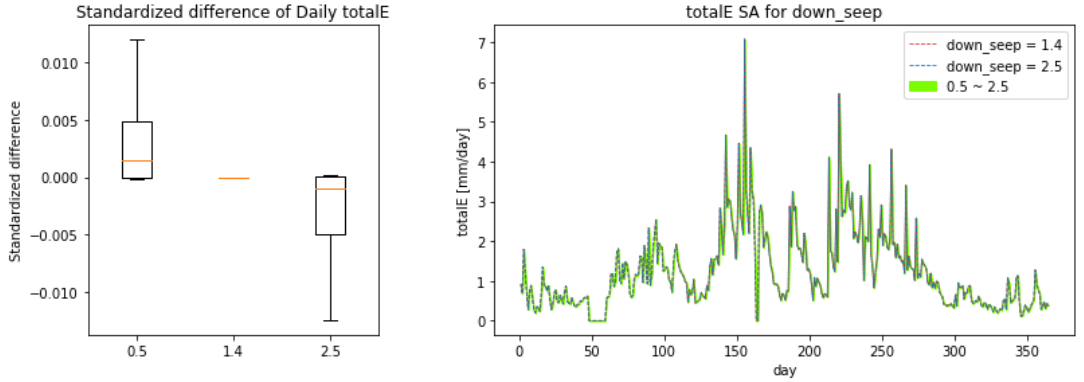
Standardized difference of Daily totalE
Standardized difference
0.010
0.005
0.000
−0.005
−0.010
0.5
1.4
2.5


totalE SA for down_seep
down_seep = 1.4
down_seep = 2.5
0.5 ~ 2.5
totalE [mm/day]
7
6
5
4
3
2
1
0
0
50
100
150
200
250
300
350
day

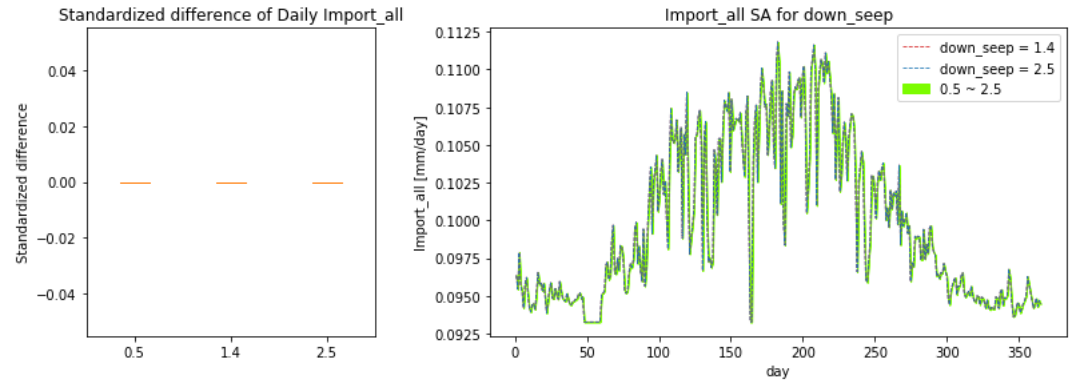
Standardized difference of Daily Import_all
Standardized difference
0.04
0.02
0.00
−0.02
−0.04
0.5
1.4
2.5


Import_all SA for down_seep
down_seep = 1.4
down_seep = 2.5
0.5 ~ 2.5
Import_all [mm/day]
0.1125
0.1100
0.1075
0.1050
0.1025
0.1000
0.0975
0.0950
0.0925
0
50
100
150
200
250
300
350
day

## 6-i. Percentage of surface runoff inflow sewer pipes (perI) [-]

Table A - 17. MSE list of different values of perI to the resulting flows.

| | MSE_BFout_all | MSE_Qseep_all | MSE_Rs_out | MSE_Rw_out | MSE_totalE | MSE_Import_all |
|---|---|---|---|---|---|---|
| **80.0** | 0.0 | 0.0 | 2.173082e+09 | 0.000006 | 0.0 | 0.0 |
| **90.0** | 0.0 | 0.0 | 0.000000e+00 | 0.000000 | 0.0 | 0.0 |
| **100.0** | 0.0 | 0.0 | 1.000000e+00 | 0.000002 | 0.0 | 0.0 |

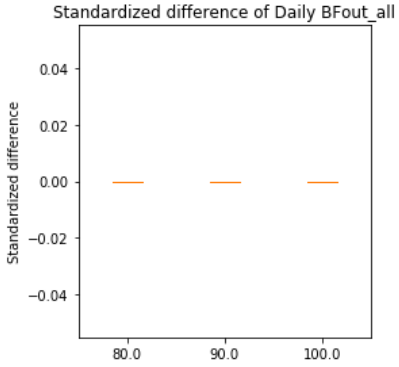


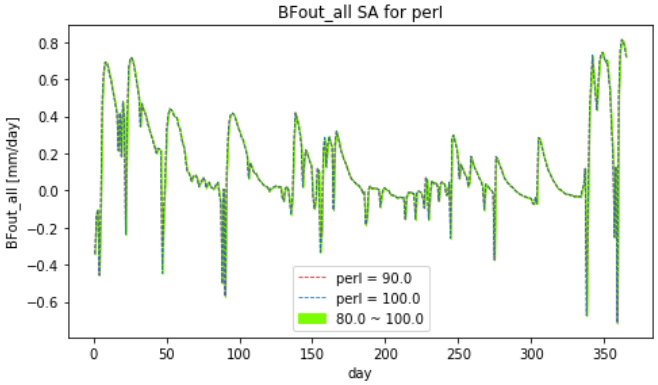


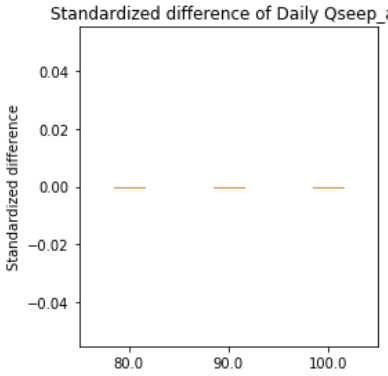


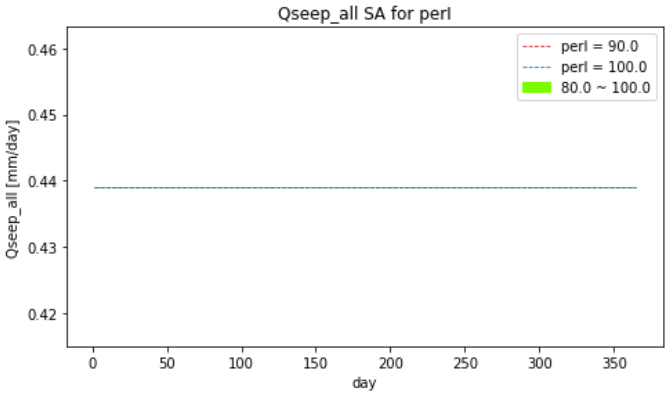


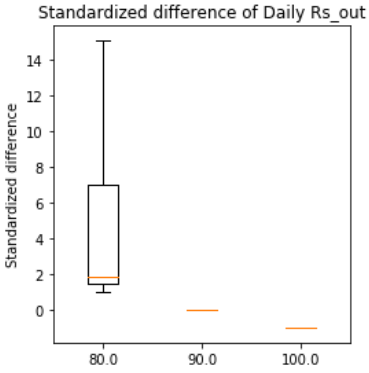


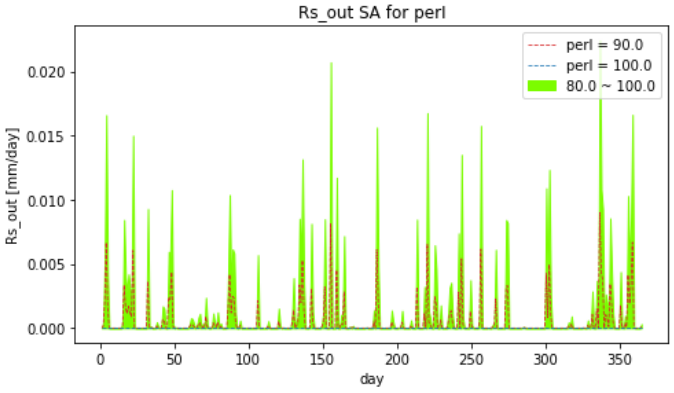

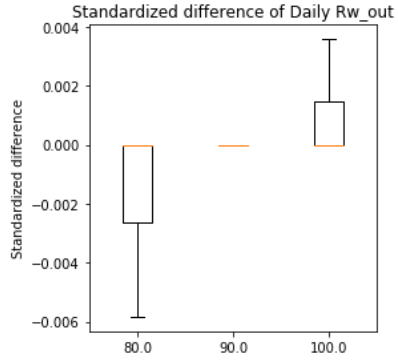
Standardized difference of Daily Rw_out
Standardized difference
0.004
0.002
0.000
−0.002
−0.004
−0.006
80.0
90.0
100.0

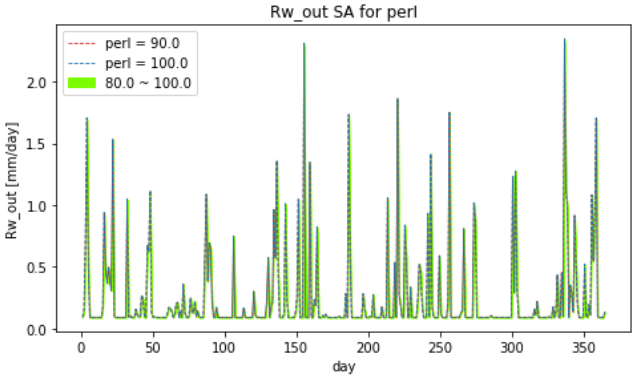
Rw_out SA for perl
perl = 90.0
perl = 100.0
80.0 ~ 100.0
Rw_out [mm/day]
day

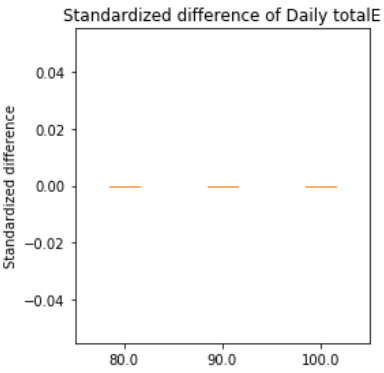
Standardized difference of Daily totalE
Standardized difference
0.04
0.02
0.00
−0.02
−0.04
80.0
90.0
100.0

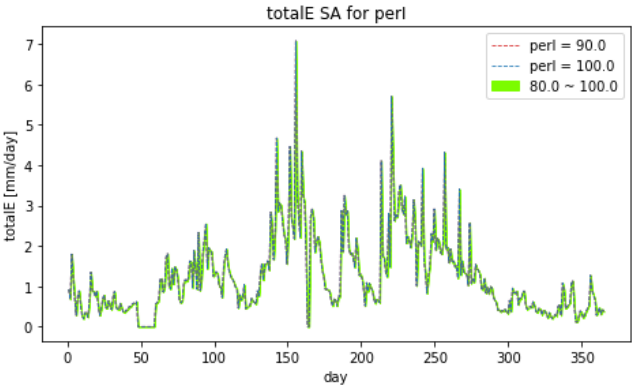
totalE SA for perl
perl = 90.0
perl = 100.0
80.0 ~ 100.0
totalE [mm/day]
day

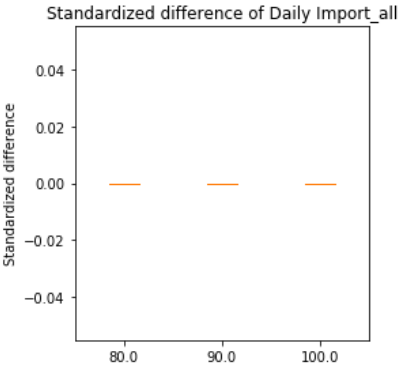
Standardized difference of Daily Import_all
Standardized difference
0.04
0.02
0.00
−0.02
−0.04
80.0
90.0
100.0

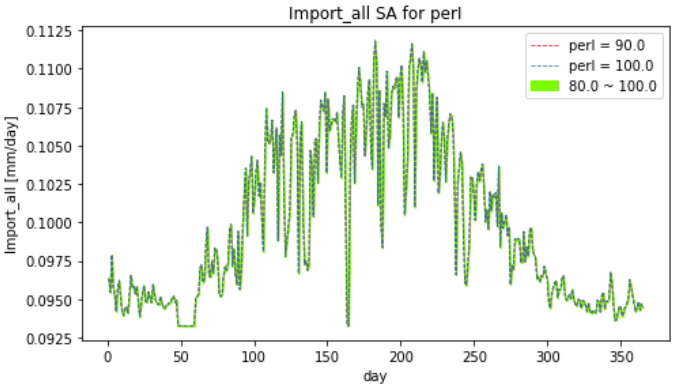
Import_all SA for perl
perl = 90.0
perl = 100.0
80.0 ~ 100.0
Import_all [mm/day]
day

**Reference:**


Allen, R. G., Pereira, L. S., Raise, D. and Smith, M., 1998. Crop evapotranspiration: Guidelines for computing crop water requirements. FAO Irrigation and Drainage Paper No. 56, United Nations, FAO, Rome, Italy.

Bach, P.M., Rauch,W., Mikkelsen, P.S., McCarthy, D.T., Deletic, A., 2014. A critical review of integrated urban water modelling—Urban drainage and beyond. *Environ. Model.* Softw. 54, 88–107.

Bach, P.M., McCarthy, D.T., Deletic, A., 2015a. Can we model the implementation of Water Sensitive Urban Design in evolving cities? *Water Sci.* Technol. 71 (1), 149e156

Bach, P.M., Staalesen, S., McCarthy, D.T. and Deletic, A., 2015b. Revisiting land use classification and spatial aggregation for modelling integrated urban water systems. *Landscape and Urban Planning, 143*, pp.43-55.

Bach, P. M., Deletic, A., Urich, C., & Mccarthy, D. T., 2018. Modelling characteristics of the urban form to support water systems planning. *Environmental Modelling & Software*, 104, 249–269. doi: 10.1016/j.envsoft.2018.02.012

Bach, P. M., Kuller, M., McCarthy, D. T., & Deletic, A. (2020). A spatial planning-support system for generating decentralised urban stormwater management schemes. *Science of The Total Environment*, 726, 138282. doi:10.1016/j.scitotenv.2020.138282

Beven, K., 1993. Prophecy, reality and uncertainty in distributed hydrological modelling. *Advances in Water Resources, 16(1)*, 41–51. https://doi-org.tudelft.idm.oclc.org/10.1016/0309-1708(93)90028-E

Birch, C. P., Oom, S. P., & Beecham, J. A., 2007. Rectangular and hexagonal grids used for observation, experiment and simulation in ecology. *Ecological Modelling*, 206(3-4), 347–359. doi: 10.1016/j.ecolmodel.2007.03.041

Brodsky, I., 2017. H3: Uber's Hexagonal Hierarchical Spatial Index. Retrieved from https://eng.uber.com/h3/.

Christaller W., 1966. Central Places in Southern Germany. C. Baskin, trans. Englewood Cliffs, NJ: Prentice Hall.

de Jong van Lier, Q., et al, 2008. Macroscopic root water uptake distribution using a matric flux potential approach. Vadose Zone Journal, 2008, 7.3: 1065-1078.

de Sousa, L. M., Nery, F., Sousa, R., & Matos, J., 2006. Assessing the accuracy of hexagonal versus square tiled grids in preserving DEM surface flow directions. Proceedings of the Seventh International Symposium on Spatial Accuracy Assessment in Natural Resources and Environmental Sciences. Lisbon, Portugal.

de Sousa, L. M., Chen, A.S., Gibson, M.J., Savic, D.A., & Leitão, J.P., 2017. Exploring the advantages of hexagonal raster for flood modelling using cellular automata. 14th ICUD: International Conference on Urban Drainage.

de Sousa, L. M., & Leitão, J. P., 2017. Hex-utils: A tool set supporting HexASCII hexagonal rasters. Proceedings of the Third International Conference on Geographical Information Systems Theory, Applications and Management. Porto, Portugal.

de Sousa, L. M., Leitão, J.P., 2018. HexASCII: a file format for cartographical hexagonal grids. Transactions in GIS, 22(1), 217-232. doi: 10.1111/tgis.12304

Dunnigan, J.F., 1992. The Complete Wargames Handbook, 2nd ed. Quill, New York.

Elga S., Jan B., Okke B., 2015. Hydrological modeling of urbanized catchments: A review and future directions. *Journal of Hydrology* 52.

Engelen, G., Lavalle, C., Barredo, J. I., Meulen, M. van der, & White, R., 2007. The MOLAND modelling framework for urban and regional land-use dynamics. Modelling Land-Use Change (pp. 297–320). Springer.

Feddes, R.A., Kowalik, P.J. and Zaradny, H., 1978. Simulation of field water use and crop yield. Pudoc, Wageningen. Simulation Monographs.

Freer, J. E., McMillan, H., McDonnell, J.J. and Beven, K.J., 2004. Constraining dynamic TOPMODEL responses for imprecise water table information using fuzzy rule based performance measures. *Journal of Hydrology*, 291(3-4): 254-277

Frisch, U., Hasslacher, B., & Pomeu, Y., 1986. Lattice-gas automata for the Navier–Stokes equation. *Physical Review Letters, 56(14),* 1505–1508.

Hardy, MJ., Kuczera, G., & Coombes, P.J., 2005. Integrated urban water cycle management: the UrbanCycle model. *Water Science & Technology, 52 (9)*

Hennessy, K. J., Gregory, J. M., & Mitchell , J. F. B., 1997. Changes in daily precipitation under enhanced greenhouse conditions. *Climate Dyn.*, *13*, 667-680.

Islam, M., & Aktar, S., 2011. Measuring Physical Accessibility to Health Facilities – A Case Study on Khulna City. *World Health & Population*, 12(3). doi: 10.12927/whp.2011.22195

Kenway, S., Gregory, A., & McMahon, J., 2011. *Journal of Industrial Ecology*. Vol 15, No. 5.

Khatami, S., C. Peel, M., J. Peterson, T., W. Western, A., 2019. Equifinality and Flux Mapping: A New Approach to Model Evaluation and Process Representation Under Uncertainty. *Water Resources Research*. Volume 55, Issue 11

Konrad, C.P., 2003. Effects of urban development on floods. Fact Sheet 076-03 . Reston, VA: US Geological Survey , 4 pp.

Kothavala, Z., 1997: Extreme precipitation events and the applicability of global climate models to study floods and droughts. *Math. Comput. Simul*., 43, 261-268.

Mackay, R., Last, E., 2010. SWITCH city water balance: a scoping model for integrated urban water management. *Environ Sci Biotechnol*, 9:291–296

Makropoulos, C.K., Natsis, K., Liu, S., Mittas, K., Butler, D., 2008. Decision support for sustainable option selection in integrated urban water management. Environmental Modelling and Software 23 (12), 1448e1460.

Mersereau, R., 1979. The processing of hexagonally sampled two-dimensional signals. Proceedings of the IEEE, 67, 930–949.

Mitchell, V.G., Mein, R.G., McMahon, T.A., 2001. Modelling the urban water cycle. *Environ. Model*. Softw., 16, 615–629.

Mitchell, V. G., 2005. Aquacycle User Guide. Retrieved from: https://toolkit.ewater.org.au/Tools/Aquacycle/documentation.

Mitchell, V.G., Diaper, C., 2006. UVQ: A tool for assessing the water and contaminant balance impacts of urban development scenarios. *Water Science & Technology*. 52 (12)

Mitchell, V.G., 2006. Applying Integrated Urban Water Management Concepts: A Review of Australian Experience. *Environmental Management* Vol. 37, No. 5.

O'Callaghan, J.F. and Mark, D.M., 1984. The extraction of drainage networks from digital elevation data. *Computer vision, graphics, and image processing, 28(3)*, pp.323-344.

Palmer, N., 1977. The Comprehensive Guide to Board Wargaming. Weidenfeld, London, 223 pp.

Paul, R., Kenway, S., McIntosh, B., Mukheibir, P., 2018. *Journal of Industrial Ecology*. Vol 22, No. 6.

Peña-Guzmán, C. A, Melgarejo, J., Prats, D., Torres, A., and Martínez, S., 2017. Urban Water Cycle Simulation/Management Models: A Review. *Water*, 9 (4).

Perrin, C., Michel, C., & Andréassian, V., 2001. Does a large number of parameters enhance model performance? Comparative assessment of common catchment model structures on 429 catchments. *Journal of Hydrology, 242(3-4)*, 275–301. https://doi-org.tudelft.idm.oclc.org/10.1016/S0022-1694(00)00393-0

Racsko, P., Szeidl, L., & Semenov, M., 1991. A serial approach to local stochastic weather models. Ecological modelling, 57(1), 27– 41.

Rittel, H.W. & Webber, M.M., 1973. Dilemmas in a general theory of planning. Policy sciences, 4(2), pp.155-169.

Rozos, E. & Makropoulos, C., 2012. Assessing the combined benefits of water recycling technologies by modeling the total urban water cycle, Urban Water Journal, 9:1, 1-10, DOI: 10.1080/1573062X.2011.630096

Rozos, E. & Makropoulos, C., 2013. Source to tap urban water cycle modelling. *Environmental Modelling & Software*, 41

Sapkota, M., Arora, M., Malano, H., Moglia, M., Sharma, A., George, B., & Pamminger, F., 2016. An Integrated Framework for Assessment of Hybrid Water Supply Systems. *Water*, 8,4

Semenov, M. A., & Barrow, E. M., 1997. Use of a stochastic weather generator in the development of climate change scenarios. Climatic change, 35(4), 397–414

Shahumyan, H., White, R., Twumasi, B. O., Convery, S., Williams, B., Critchley, M., Carty, J., 2009. The MOLAND Model Calibration and Validation for the Greater Dublin Region

Dublin Region. Dublin. Retrieved from http://www.uep.ie/downloads/index.php?area=document&category=35

Shuster, W. D., Bonta, J., Thurston, H., Warnemuende, E. & Smith, D. R., 2005. Impacts of impervious surface on watershed hydrology: A review. *Urban Water Journal, 2:4*, 263-275, DOI: 10.1080/15730620500386529

Tholen, C., Nolle, L., Zielinski, O., 2017. On the effect of neighborhood schemes and cell shape on the behaviour of cellular automata applied to the simulation of submarine groundwater discharge. In: 31th European Conference on Modelling and Simulation ECMS 2017, pp. 255–261

Tran, Q. Q., Niel, J. D., & Willems, P., 2018. Spatially Distributed Conceptual Hydrological Model Building: A Generic Top-Down Approach Starting From Lumped Models. *Water Resources Research, 54*(10), 8064-8085. doi:10.1029/2018wr023566

Vergroesen, T., Brolsma, R., AST 2.0 Documentation - Urban Water Balance Model. Retrieved from https://publicwiki.deltares.nl/display/AST/Urban+Water+balance+model.

Wang, J., & Kwan, M.-P. (2018). Hexagon-Based Adaptive Crystal Growth Voronoi Diagrams Based on Weighted Planes for Service Area Delimitation. ISPRS International Journal of Geo-Information, 7(7), 257. doi: 10.3390/ijgi7070257

Willuweit, L., O;Sullivan, J.J., Shahumyan, H., 2013. Modeling the effects of Urban Growth Scenarios on Water Demand and Runoff Patterns in Dublin, Ireland. In Proceedings of the 20th International Congress on Modelling and Simulation, Adelaide, Australia, 10–13 November 2013; pp. 3162–3168

Zhu, X., Liu, S., & Yeow, M.-C. (2006). Accessibility analysis for housing development in Singapore with GIS and multi-criteria analysis methods. *Applied GIS, 2(2).* doi: 10.2104/ag060013